



## Taxonomic novelties of saprobic Pleosporales from selected dicotyledons and grasses

Brahmanage RS<sup>1,2,3</sup>, Dayarathne MC<sup>6</sup>, Wanasinghe DN<sup>4,5</sup>, Thambugala KM<sup>7</sup>, Jeewon R<sup>8</sup>, Chethana KWT<sup>1,3</sup>, Samarakoon MC<sup>1</sup>, Tennakoon DS<sup>1,4,5</sup>, De Silva NI<sup>1,4,5</sup>, Camporesi E<sup>9,10,11</sup>, Raza M<sup>13</sup>, Yan JY<sup>2</sup> and Hyde KD<sup>1,3,5,12</sup>

<sup>1</sup>Center of Excellence in Fungal Research, Mae Fah Luang University, Chiang Rai, 57100, Thailand

<sup>2</sup>Institute of Plant and Environment Protection, Beijing Academy of Agriculture and Forestry Sciences, Beijing 100097, People's Republic of China

<sup>3</sup>School of Science, Mae Fah Luang University, Chiang Rai, Chiang Rai, 57100, Thailand

<sup>4</sup>World Agro forestry Centre East and Central Asia Office, 132 Lanhei Road, Kunming 650201, People's Republic of China

<sup>5</sup>CAS Key Laboratory for Plant Biodiversity and Biogeography of East Asia (KLPB), Kunming Institute of Botany, Chinese Academy of Science, Kunming 650201, Yunnan, People's Republic of China

<sup>6</sup>Department of Plant Pathology, Agriculture College, Guizhou University, Guiyang, Guizhou Province, 550025, People's Republic of China

<sup>7</sup>Genetics and Molecular Biology Unit, Faculty of Applied Sciences, University of Sri Jayawardenepura, Gangodawila, Nugegoda, Sri Lanka

<sup>8</sup>Department of Health Sciences, Faculty of Medicine and Health Sciences, University of Mauritius, Reduit, Mauritius.

<sup>9</sup>A.M.B. Circolo Micologico "Giovanni Carini", C.P. 314, Brescia, Italy

<sup>10</sup>A.M.B. Gruppo, Micologico Forlivese "Antonio Cicognani", Via Roma 18, Forlì, Italy

<sup>11</sup>Società per gli Studi Naturalistici della Romagna, C.P. 143, Bagnacavallo, RA, Italy

<sup>12</sup>Institute of Plant Health, Zhongkai University of Agriculture and Engineering, Haizhu District, Guangzhou 510225, People's Republic of China

<sup>13</sup>State Key Laboratory of Mycology, Institute of Microbiology, Chinese Academy of Sciences, Beijing, 100101, People's Republic of China

Brahmanage RS, Dayarathne MC, Wanasinghe DN, Thambugala KM, Jeewon R, Chethana KWT, Samarakoon MC, Tennakoon DS, De Silva NI, Camporesi E, Raza M, Yan JY, Hyde KD 2020 – Taxonomic novelties of saprobic Pleosporales from selected dicotyledons and grasses. *Mycosphere* 11(1), 2481–2541, Doi 10.5943/mycosphere/11/1/15

### Abstract

Pleosporales is the largest order in the class Dothideomycetes, comprising a quarter of all species of Dothideomycetes. This paper provides comprehensive illustrations and descriptions of newly collected saprobic pleosporalean taxa from dicotyledons and grasses in China, Italy, Russia and Thailand. These species are accommodated in 8 families in Pleosporales. The taxa described here include 14 new species, a new geographical record and three new host records of known species. New species are *Alternaria rumicis*, *Bambusicola ficuum*, *Comoclathris flammulae*, *C. europaeae*, *C. loniceriae*, *Ophiobolus lathyri*, *Paraophiobolus torilicola*, *Parastagonospora dactylidicola*, *P. hieracioidis*, *Pseudopaucispora hyalinospora*, *Stagonospora poaceicola*, *Stemphylium artemisiae* and *Subplenodomus meldolanus*. All species descriptions presented herein are based on morphological comparisons coupled with multi-gene phylogenetic analyses.

**Key words** – 14 new species – Dothideomycetes – microfungi – phylogeny – taxonomy

## Table of contents

The pleosporalean taxa are organized as in the “Outline of fungi and fungus-like taxa” (Wijayawardene et al. 2020).

### Ascomycota R.H. Whittaker

#### Pleosporomycetidae C.L. Schoch, Spatafora, Crous & Shoemaker

#### Pleosporales Luttr. ex M.E. Barr

#### Bambusicolaceae D.Q. Dai & K.D. Hyde

1. *Bambusicola ficuum* N.I. de Silva & K.D. Hyde, sp. nov.

#### Lentitheciaceae

2. *Keissleriella italica* Brahmanage, Camporesi & K.D. Hyde, sp. nov.
3. *Pseudomurilentithecium clematidis* Brahmanage, Camporesi & K.D. Hyde, sp. nov.

#### Leptosphaeriaceae

4. *Plenodomus biglobosus* (Shoemaker & H. Brun) Gruyter, Aveskamp & Verkley, new host record
5. *Plenodomus enteroleucus* (Sacc.) Gruyter, Aveskamp & Verkley, new host record
6. *Subplenodomus meldolanus* Brahmanage & K.D. Hyde, sp. nov.

#### Lophiostomataceae

7. *Pseudopaucispora hyalinospora* Samarak. & K.D. Hyde, sp. nov.

#### Massarinaceae

8. *Stagonospora poaceicola* Tennakoon, Phookamsak R & K.D. Hyde, sp. nov.

#### Morosphaeriaceae

9. *Helicascus chiangraiensis* Z.L. Luo, J.K Liu, H.Y. Su & K.D. Hyde, new geographical record

#### Phaeosphaeriaceae

10. *Ophiobolus lathyri* Brahmanage, Camporesi & K.D. Hyde, sp. nov.
11. *Paraophiobolus torilicola* Brahmanage, Camporesi & K.D. Hyde, sp. nov.
12. *Parastagonospora dactylidicola* Brahmanage, Camporesi & K.D. Hyde, sp. nov.

#### Pleosporaceae

13. *Alternaria rumicis* Brahmanage, Camporesi & K.D. Hyde, sp. nov.
14. *Comoclathris europaeae* Brahmanage, Camporesi & K.D. Hyde, sp. nov.
15. *Comoclathris flammulae* Brahmanage, Camporesi & K.D. Hyde, sp. nov.
16. *Comoclathris lonicerae* Brahmanage, Camporesi & K.D. Hyde, sp. nov.
17. *Stemphylium artemisiae* Brahmanage, Camporesi & K.D. Hyde, sp. nov.
18. *Stemphylium vesicarium* (Wallr.) E.G. Simmons, new host record

## Introduction

Luttrell (1955) invalidly introduced Pleosporales, but it was subsequently validated by Barr (1987a) with Pleosporaceae as an important family and *Pleospora* Rabenh. ex Ces. & De Not., as the type genus (currently synonymized under *Stemphylium* Wallr), (Wijayawardene et al 2017). The type species of *Pleospora* is *P. herbarum* (Barr 1987b). Previous studies indicated that the order comprises 20 families (Kodsueb et al. 2006, Boehm et al. 2009a, b, Mugambi & Huhndorf 2009, Schoch et al. 2009, Shearer et al. 2009, Suetrong et al. 2009, Tanaka et al. 2009, Zhang et al. 2009) and later, Zhang et al. (2012) accepted 25 families in Pleosporales. Subsequent studies by

Hyde et al. (2013), Wijayawardene et al. (2017, 2020) accepted 41, 75 and 87 families, respectively. In a recent treatment, Hongsanan et al. (2020) accepted 91 families. These pleosporalean species comprises pseudothecial ascomata with papilla and a peridium comprising several layers of cells (Zhang et al. 2008, 2009, 2012, Hyde et al. 2013, Jaklitsch & Voglmayr 2016, Jaklitsch et al. 2018). Their asci are bitunicate, fissitunicate and exist within a persistent hamathecium with or without pseudoparaphyses (Ariyawansa et al. 2014, 2015a, b, c, Hyde et al. 2013). Ascospores are septate with differences in color and shape and with or without a gelatinous sheath (Zhang et al. 2009, 2012, Hyde et al. 2013, Jaklitsch & Voglmayr 2016, Jaklitsch et al. 2018). Members of Pleosporales can be found in different habitats, as epiphytes, endophytes, saprobes, parasites, hyperparasites on fungi or insects and as lichenized fungi (Ramesh 2003, Jeewon et al. 2013, 2017, Kruys et al. 2006, Pinnoi et al. 2007, Zhang et al. 2012, Ariyawansa et al. 2014, Li et al. 2017, Hyde et al. 2018, Jayasiri et al. 2019). Asexual morphs of Pleosporales can be either coelomycetes or hyphomycetes (Heidari et al. 2018, Li et al. 2020). Camarosporium-like, coniothyrium-like, phaeosphaeria-like, phoma-like, pyrenochaeta-like, and septoria-like asexual morphs are the most common forms of coelomycetes in Pleosporales. These taxa are polyphyletic within the order (Wijayawardene et al. 2016, Li et al. 2020).

Many new pleosporalean lineages from freshwater (Brahmanage et al. 2017, Luo et al. 2018), marine (Devadatha et al. 2018, Jones et al. 2019, Dayarathne et al. 2020) and terrestrial habitats (Tanaka et al. 2009, Wanasinghe et al. 2017a, 2018a, Zhang et al. 2019) have been recently documented. Phylogenetic analyses have shown that the placement of a large number of taxa is still unresolved, and there is a need to reconsider their classification (Wang et al. 2007, Pem et al. 2019). For example, Kruys et al. (2006) and Zhang et al. (2012) documented that Venturiaceae have a set of morphological and ecological characters, which are dissimilar to other Pleosporales members. Phylogenetic results of Schoch et al. (2009) indicated that members of Venturiaceae form a well-supported clade distant from the core members of Pleosporales, and excluded it from Pleosporomycetidae and Dothideomycetidae. Zhang et al. (2012) therefore introduced the new order, Venturiales. Other families, such as Zopfiaceae (as Testudinaceae) have also been shown to be unrelated to Pleosporales based on rDNA sequence data (Kodsueb et al. 2006). Tanaka et al. (2015) revised their taxonomy based on DNA sequence data from protein-coding regions for the suborder Massarineae. Given that the Pleosporales is highly diverse with many more new species awaiting to be discovered in the tropics (Hyde et al. 2018), there is a need to revise their taxonomy (especially with regards to the nomenclature of old species) with fresh collections (Dayarathne et al. 2016, Pem et al. 2019).

### **Economic significance of pleosporalean taxa**

*Phoma* is an example of a coelomycetous genus, which are associated with a wide range of terrestrial plants, causing stem and leaf spots (Aveskamp et al. 2008, Zhang et al. 2009). At least 50% of the *Phoma* taxa re-described by Boerema et al. (2004) have been recognized as phytopathogenic species with plant quarantine issues (Boerema et al. 2004, Aveskamp et al. 2008, Chen et al. 2015). Although most of the taxa exist in the environment as saprobic soil organisms, many species can switch to a pathogenic lifestyle once the favourable conditions received (Aveskamp et al. 2008, Promputtha et al. 2007, Jayawardena et al. 2019b). Some *Phoma* species are pathogens of humans and other vertebrates, such as cattle (Costa et al. 1993, De Hoog et al. 2000) and fish (Voronin, 1989, Faisal et al. 2007). Furthermore, *Phoma* spp. can indirectly affect animal health by producing toxic secondary metabolites (Rabie et al. 1975, Bennett 1983, Pedras & Biesenthal 2000, Rai et al. 2009, Sørensen et al. 2011). One of the most unexplored habitats for *Phoma* species is the marine environment (Kohlmeyer & Volkmann-Kohlmeyer 1991, Osterhage et al. 2000, Yarden et al. 2007) and several species have been listed from mangroves which need reexamining (Dayarathne et al. 2020).

*Stemphylium* species are saprobes (Han et al. 2019), but also occur on crops such as alfalfa (*Medicago sativa* L.), red clover (*Trifolium pratense* L.), potato (*Solanum tuberosum* L.), tomato (*Solanum lycopersicum* L.) (Ellis & Gibson 1975, Irwin 1984, Johnson & Lunden 1986, Simmons

et al. 1990, Aveling & Snyman 1993), sugar beet (Hanse 2013), asparagus, garlic, onion (Gálvez et al. 2016), bird's-foot trefoil (*Lotus corniculatus*) (Seaney 1973), lentil, lucerne, pear, parsley (*Medicago sativa*) and a variety of other horticultural crops (Miller et al. 1978, Lamprecht et al. 1984, Falloon et al. 1987, Llorente & Montesinos 2006, Reis et al. 2011, Nasehi et al. 2013, Vakalounakis & Markakis 2013, Subedi et al. 2014). *Stemphylium vesicarium* causes leaf spots in onion and garlic and purple spots in asparagus (Gálvez et al. 2016). *Stemphylium solani* is responsible for grey leaf spot on tomato and potato (Ellis & Gibson 1975, Irwin 1984, Johnson & Lunden 1986, Simmons et al. 1990, Aveling & Snyman 1993). *Stemphylium loti* has been reported as the causative agent of the bird's-foot trefoil foliar disease (Seaney 1973). *Stemphylium* pathogens have been found from several vegetables and flowers, including aster, Chinese chives, sweet pepper, tomato, Welsh onion, and white lace flower (Enjoji 1931, Suzui 1973, Ichikawa & Sato 1994, Tomioka et al. 1997, Shibata et al. 2000, Misawa 2009, Tomioka & Sato 2011, Kurose et al. 2015, Brahmanage et al. 2019). Species of *Alternaria* are serious plant pathogens that trigger diseases on an extensive variety of crops, and some are important as postharvest pathogens, human pathogens which causes phaeohyphomycosis in immuno-compromised patients or act as airborne allergens (Woudenberg et al. 2013, 2015). Pleosporales also comprises species and varieties that are recognized as fungicolous, lichenicolous and endophytes (Xianshu et al. 1994, Hawksworth 2004, Schoch et al. 2009, Sun et al. 2019).

Recognition of plant-associated fungi is often hindered by the lack of morphological characters described or illustrated in the original publications and the endophytic or inconspicuous nature of pleosporalean taxa. DNA sequence data provide reliable information for diagnostic purposes of pathogens (Hyde et al. 2013, Jayawardena et al. 2019a, b).

### **Aim of the paper**

This paper reports on the taxonomy of saprobic pleosporalean taxa on dicotyledons and identifies the species using morphology and multi-locus phylogenies. We also establish possible links between the asexual and sexual morphs. This study is a continuity of our studies on bitunicate fungi (Wanasinghe et al. 2017, Jayasiri et al. 2019, Pem et al. 2019, Hyde et al. 2020) and is an additional taxonomic contribution, where we recover novel saprobic pleosporalean taxa associated with dicotyledons.

### **Materials and Methods**

#### **Sample collections**

Plant samples with pleosporalean taxa were collected from selected dicotyledons and grasses in China, Italy, Russia and Thailand from 2017 to 2019. Materials were labeled and brought to the laboratory in plastic Ziplock bags. These substrata were branches, fruits, roots, twigs and small parts cut from tree stems that are variable in size, length, color, texture and at different stages of decomposition.

#### **Incubation and specimen examination**

Samples were incubated in plastic containers with moistened sterilized tissue at 16–25°C for one week and then the fruiting bodies were examined using a dissecting microscope. Squash mounts and sections of the fruiting structures were mounted in water and stained with Melzer's reagent, Indian ink or Congo red, when necessary for microscopic studies and photomicrography. Morphological characteristics of fungi were examined using a Nikon ECLIPSE 80i compound microscope and photographed by a Canon EOS 550D digital camera fitted to the microscope or Nikon, NIS-Elements F3.0. Measurements such as the diameter of ascomata, length and width of asci and ascospores and width of pseudoparaphyses were made with the Tarosoft Image Frame Work program and images use for figures were processed with Adobe Photoshop CS3 Extended version 10.0 software (Adobe Systems Inc., US).

#### **Isolation of pleosporalean fungi**

For single spore isolation, a modified method of Chomnunti et al. (2014) was followed. Contents of the sectioned fruiting body were transferred to a drop of sterile water on a flame-sterilized slide. Drops of the spore suspension were pipetted and spread on a Petri-dish containing 2% water agar (WA). Then the plates were incubated at 10–30°C overnight. Germinated ascospores or conidia were transferred to potato dextrose agar (PDA) or malt extract agar (MEA).

### **Cultures and herbarium specimens**

Cultures and herbarium specimens of isolated fungi were deposited in the Mae Fah Luang University culture collection (MFLUCC) and Mae Fah Luang University Herbarium (Herb. MFLU), Thailand respectively. Their duplicates were deposited at the Beijing Academy of Agricultural and Forestry Sciences (JZB), China and the Herbarium of Cryptogams Kunming Institute of Botany Academia Sinica (KUNHKAS), China. Facesoffungi numbers (FoF) and Index Fungorum (IF) numbers were obtained as explained by Jayasiri et al. (2015) and Index Fungorum (2020). New species are established based on the recommendations by Jeewon & Hyde (2016).

### **DNA extraction, Polymerase chain reactions (PCR) and sequencing**

Mycelia (approximately 50 mg) were harvested from the fungal cultures grown on PDA, MEA or seawater PDA and extracted genomic DNA using EZ gene TM fungal gDNA kit (GD2416). When fungi failed to grow in culture, DNA was extracted directly from fruiting bodies following the method described by Zeng et al. (2018) and Wanasinghe et al. (2018b) using E.Z.N.A.® Forensic DNA kit (D3591-01, Omega Bio-Tek) according to manufacturer instructions. DNA amplifications were performed by polymerase chain reaction (PCR). Six loci were amplified including rDNA ITS (White et al. 1990), LSU, SSU (Vilgalys & Hester 1990), RPB2 (Liu et al. 1999), TEF1 (Carbone & Kohn 1999), GAPDH (White et al. 1990) and TUB2 (O'Donnell & Cigelnik 1997). The primers and PCR protocols are listed in Table 1. Amplifications were performed in 25 µl of PCR mixtures, containing 9.5 µl of ddH<sub>2</sub>O, 12.5 µl of PCR Master Mix, 1 µl of DNA template, and 1 µl of each primer (10 pM). The PCR products were visualized under UV light on 1% agarose electrophoresis gels stained with 4S green stain or ethidium bromide using the Gel Doc XR+Molecular Imager (BIO-RAD, USA). Purification and sequencing of PCR products were carried out at Sun biotech Company, Beijing, China. DNA sequences generated in this study were deposited in the GenBank for further studies.

### **Phylogenetic analysis**

New sequence data and the related sequences obtained from Genbank were aligned in MAFFT v. 6.864b (<http://mafft.cbrc.jp/alignment/server/index.html>; Katoh et al. 2019) edited and improved using Bioedit v.7 (Hall 1999) and MEGA 5.0 (Tamura et al. 2013). Maximum likelihood (ML) and Bayesian inference analysis (BI) analyses were performed. ML analyses were performed using raxmlGUI version 1.3 (Silvestro & Michalak 2012). The optimal ML tree search was searched with 1000 separate runs, using the default algorithm of the program from a random starting tree for each run. The final tree was selected among suboptimal trees from each run by comparing the likelihood scores under the GTRGAMMA substitution model. The best scoring tree was selected. BI analyses were performed using MrBayes v. 3.0b4 (Ronquist & Huelsenbeck 2003), and nucleotide substitution model were determined with MrModeltest v. 2.2 (Nylander 2004). Posterior probabilities (PP) (Rannala & Yang 1996, Zhaxybayeva & Gogarten 2002) were defined by Bayesian Markov Chain Monte Carlo (BMCMC) sampling method in MrBayes v. 3.0b4 (Huelsenbeck & Ronquist 2001). Resulting trees were visualized with TreeView v. 1.6.6 (Rambaut 2012).

### **Taxonomy**

**Ascomycota** R.H. Whittaker

We follow the latest treatments and updated accounts of Ascomycota in Wijayawardene et al. (2020).

**Class Dothideomycetes** sensu O.E. Erikss & Winka

Dothideomycetes is considered to be the largest and most phylogenetically diverse class in the phylum Ascomycota (Schoch et al. 2009, Hyde et al. 2013). Liu et al. (2017) provided the divergence time estimations at different levels for the class Dothideomycetes and reported that divergence times can provide additional evidence to support the establishment of higher-level taxa, such as families, orders and classes. The subclasses of Dothideomycetes and their families reported in this study are listed in alphabetical order.

**Table 1** Genes/loci used in the study with respective PCR primers and protocols

Gene/loci	Primer		PCR protocol				Reference	
	Forward	Reverse	Initial Denaturation	Denaturation	Annealing	Extension		Final extension
<b>Internal transcribed spacer (ITS)</b>	ITS5	ITS4	94°C, 4 min 1 cycle	94°C, 45 sec 35 cycles	56°C, 45 sec	72°C, 1 min	72°C, 10 min 1 cycle	White et al. (1990)
<b>Large subunit (LSU)</b>	LROR	LR5	94°C, 4 min 1 cycle	94°C, 45 sec 35 cycles	56°C, 45 sec	72°C, 1 min	72°C, 10 min 1 cycle	Rehner & Samuels (1994) Vilgalys & Hester (1990)
<b>Small subunit (SSU)</b>	NS1	NS4	94°C, 4 min 1 cycle	94°C, 45 sec 35 cycles	56°C, 45 sec	72°C, 1 min	72°C, 10 min 1 cycle	White et al. (1990)
<b>Elongation factor-1 alpha (TEF1)</b>	EF1-728F	EF1- 986R	94°C, 3 min 1 cycle	94°C, 30 sec 35 cycles	55°C, 50 sec	72°C, 1 min	72°C, 10 min 1 cycle	Carbone & Kohn (1999)
<b>RNA polymerase II second largest subunit (RBP2)</b>	fRPB2-5F	fRPB2-7cr	95°C, 5 min 1 cycle	95°C, 45 sec 40 cycles	55°C, 2 min	72°C, 1.5 min	72°C, 10 min 1 cycle	Liu et al. (1999)
<b>Beta tubulin (β-tubulin)</b>	Bt2a	Bt2b	94°C, 3 min 1 cycle	94°C, 30 sec 35 cycles	55°C, 50 sec	72°C, 1 min	72°C, 10 min 1 cycle	Glass & Donaldson (1995)
<b>Glyceraldehyde-3-phosphate dehydrogenase (GADPH)</b>	gpd1	gpd2	94°C, 5 min 1 cycle	94°C, 30 sec 35 cycles	59°C, 30 sec	72°C, 1 min	72°C, 7 min 1 cycle	Berbee et al. (1999)

**Subclass Pleosporomycetidae** C.L. Schoch et al.

**Bambusicolaceae** D.Q. Dai & K.D. Hyde

Bambusicolaceae was introduced by Hyde et al. (2013) with four genera, viz. *Bambusicola* D.Q. Dai & K.D. Hyde, *Leucaenicola* Jayasiri, E.B.G. Jones & K.D. Hyde, *Neobambusicola* Crous & M.J. Wingf. and *Palmiascoma* Phookamsak & K.D. Hyde (Liu et al. 2015, Wijayawardene et al. 2018, Jayasiri et al. 2019). Later, Wijayawardene et al. (2020) accepted *Neobambusicola* in Sulcatisporaceae. Bambusicolaceae shares similar morphological characteristics with some families in Pleosporales (i.e. Didymosphaeriaceae, Massarinaceae and Tetraplosphaeriaceae), in having cylindrical to clavate asci and fusiform to

ellipsoidal, hyaline to brown, 1-septate ascospores (Dai et al. 2015). Bambusicolaceae differs from related families with asexual morph having holoblastic, annelidic or phialidic conidiogenous cells (Dai et al. 2015).

***Bambusicola*** D.Q. Dai & K.D. Hyde

*Bambusicola* D.Q. Dai & K.D. Hyde was introduced and typified with *B. massarinia* D.Q. Dai & K.D. Hyde (Dai et al. 2012), and was previously placed in Trematosphaeriaceae based on ribosomal LSU gene sequence analysis. The genus is known for its asexual and sexual morphs. Hyde et al. (2013) provided a combined phylogenetic analysis of LSU, SSU, RPB2 and TEF1 data for the families in Dothideomycetes. Species of *Bambusicola* aggregated into a separate clade from other families in Massarineae, for which Hyde et al. (2013) introduced the new family Bambusicolaceae. We herein introduce a novel *Bambusicola* species from Thailand.

***Bambusicola ficuum*** N.I. de Silva & K.D. Hyde, sp. nov.

Fig. 2

Index Fungorum number: IF 557332; Facesoffungi number: FoF 07740

Etymology – The specific epithet reflects the host *Ficus* sp.

Holotype – MFLU 17-0677

*Saprobic* on dead twigs of *Ficus* sp. Sexual morph: *Ascomata* 140–200 µm high, 165–210 µm diam. ( $\bar{x}$  = 155 × 180 µm, n = 10), immersed to semi-immersed on host surface, solitary, globose to sub-globose, dark brown. *Neck* small, short, elongate, and central with minute papilla. *Peridium* 20–30 µm wide, unequally thick, comprises two layers, outer 1–3 cell layers of hyaline to brown *textura angularis* cells and inner 1–4 cell layers of hyaline *textura prismatica* cells. *Hamathecium* comprising 1–2 µm wide, cylindrical to filiform, septate, pseudoparaphyses. *Asci* 90–140 × 17–24 µm ( $\bar{x}$  = 120 × 20 µm, n = 20), 8-spored, bitunicate, fissitunicate, cylindric-clavate to clavate, short pedicellate, apically rounded, with an ocular chamber. *Ascospores* 42–50 × 6–9 µm ( $\bar{x}$  = 47 × 7 µm, n = 30), overlapping bi-seriate or multi-seriate, hyaline, fusiform, with rounded to acute ends, 1-septate, constricted at the septum, upper cell larger than lower cell, smooth-walled, hyaline, guttulate, surrounded by a mucilaginous sheath. Asexual morph: Undetermined.

Culture characteristics – Colonies on PDA reaching 25 mm diameter after 1 week at 20–25°C, colonies medium sparse, circular, surface slightly rough with edge entire, cottony to fairly fluffy with sparse aspects, colony from above: yellowish white; reverse: brown at the center and yellow at the margin.

Material examined – THAILAND, Chiang Mai Province, Mae Tang district, Ban Pa Deng, Mushroom Research Center, dead twigs (attached to the tree) of *Ficus* sp. (Moraceae), 25 January 2017, N. I. de Silva, NI108 (MFLU 17-0677, holotype), ex-type living culture, MFLUCC 17-0872.

GenBank Numbers – LSU: MT215580; SSU: MT215581; TEF1: MT199326

Notes – *Bambusicola ficuum* shows a close phylogenetic affinity to *B. dimorpha* and *B. pustulata* (Fig. 1). There are six base pair differences in TEF nucleotide sequences between *Bambusicola ficuum* and *B. pustulata* (0.87%). The TEF sequence data for *Bambusicola dimorpha* is not available for the current phylogenetic analyses. Morphologically, *Bambusicola ficuum* differs from *B. dimorpha* and *B. pustulata* in having longer ascospores (42–50 µm) with sheath, in contrast to the longer ascospores without sheath in *Bambusicola dimorpha* (17–25 µm) and *B. pustulata* (11–17 µm). *Bambusicola dimorpha* was collected in Chiang Mai Province, Thailand on dead bamboo culms (Thambugala et al 2017), while *B. pustulata* was reported in Phang-Nga Province, Thailand on dead bamboo culms (Dai et al. 2015). The new strain, *Bambusicola ficuum* was collected in Chiang Mai Province, Thailand on dead twigs of *Ficus* sp.

**Lentitheciaceae** Y. Zhang et al.

Lentitheciaceae was introduced by Zhang et al. (2009) with *Lentithecium fluviatile* (Aptroot & Van Ryck.) K.D. Hyde, J. Fourn. & Ying Zhang as the type species. Wanasinghe et al. (2014) listed six genera under this family and 14 genera are accepted in Wijayawardene et al. (2020).

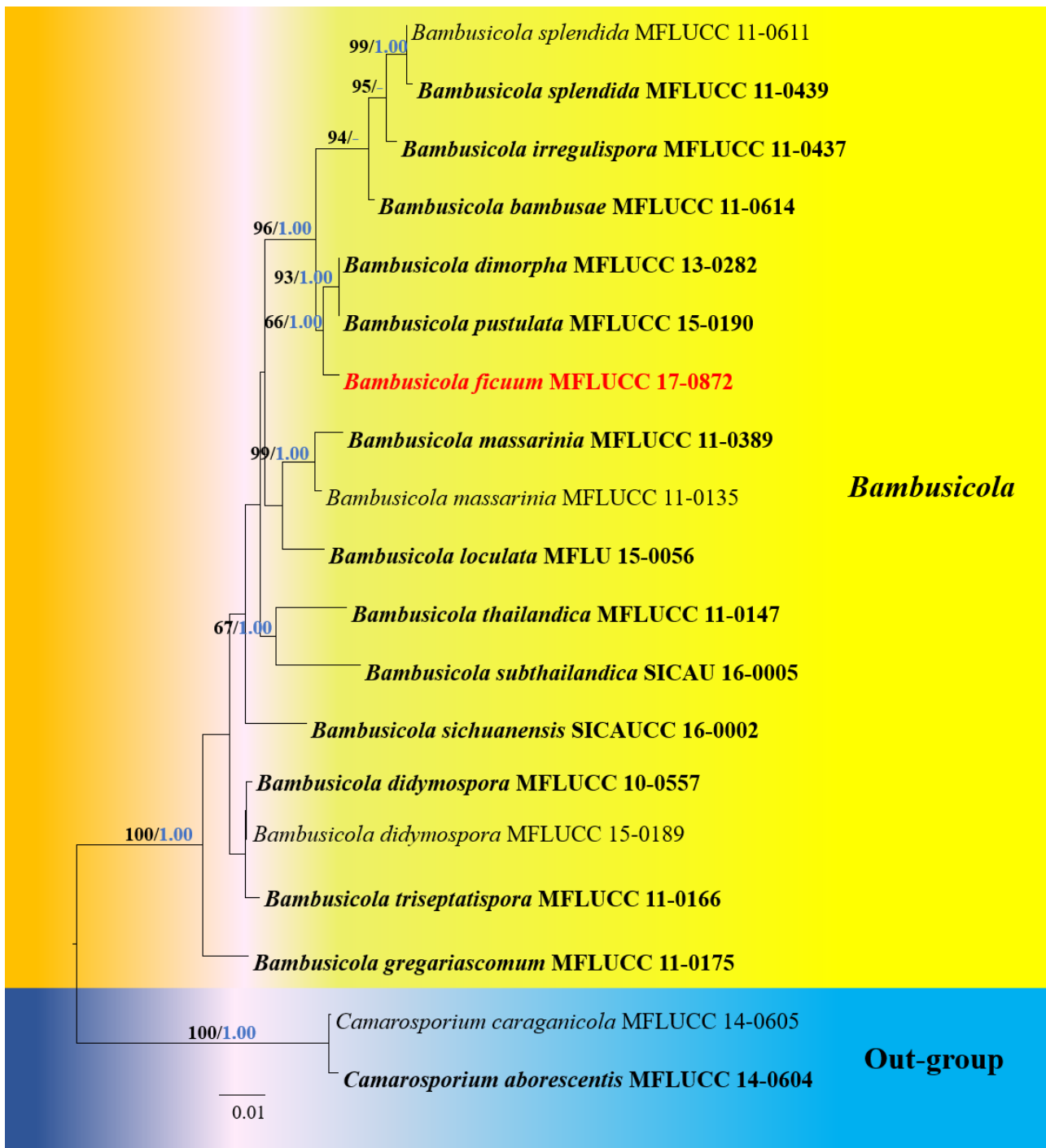


**Figure 1** – Maximum likelihood analysis with 1000 bootstrap replicates yielded a best tree with the likelihood value of -6126.199615. The combined LSU, SSU and TEF sequence datasets comprised 19 strains of *Bamusicola* with *Camarosporium aborescentis* (MFLUCC 14-0604) and *Camarosporium caraganicola* (MFLUCC 14-0605) as the outgroup taxa. Tree topology of the ML analysis was similar to the BI. The matrix had 310 distinct alignment patterns, with 21.56% of undetermined characters or gaps. Estimated base frequencies were as follows; A = 0.239116, C = 0.247058, G = 0.277564, T = 0.236262; substitution rates AC = 0.583379, AG = 2.265165, AT = 0.909124, CG = 0.754568, CT = 11.365613, GT = 1.000000; gamma distribution shape parameter  $\alpha = 0.020000$ . Maximum likelihood bootstrap (ML, black) values equal to or greater than 65% and Bayesian posterior probabilities (PP, blue) equal to or greater than 0.90% are given above the nodes. The scale bar indicates 0.01 changes. The ex-type strains are in black bold and new isolates in red bold.



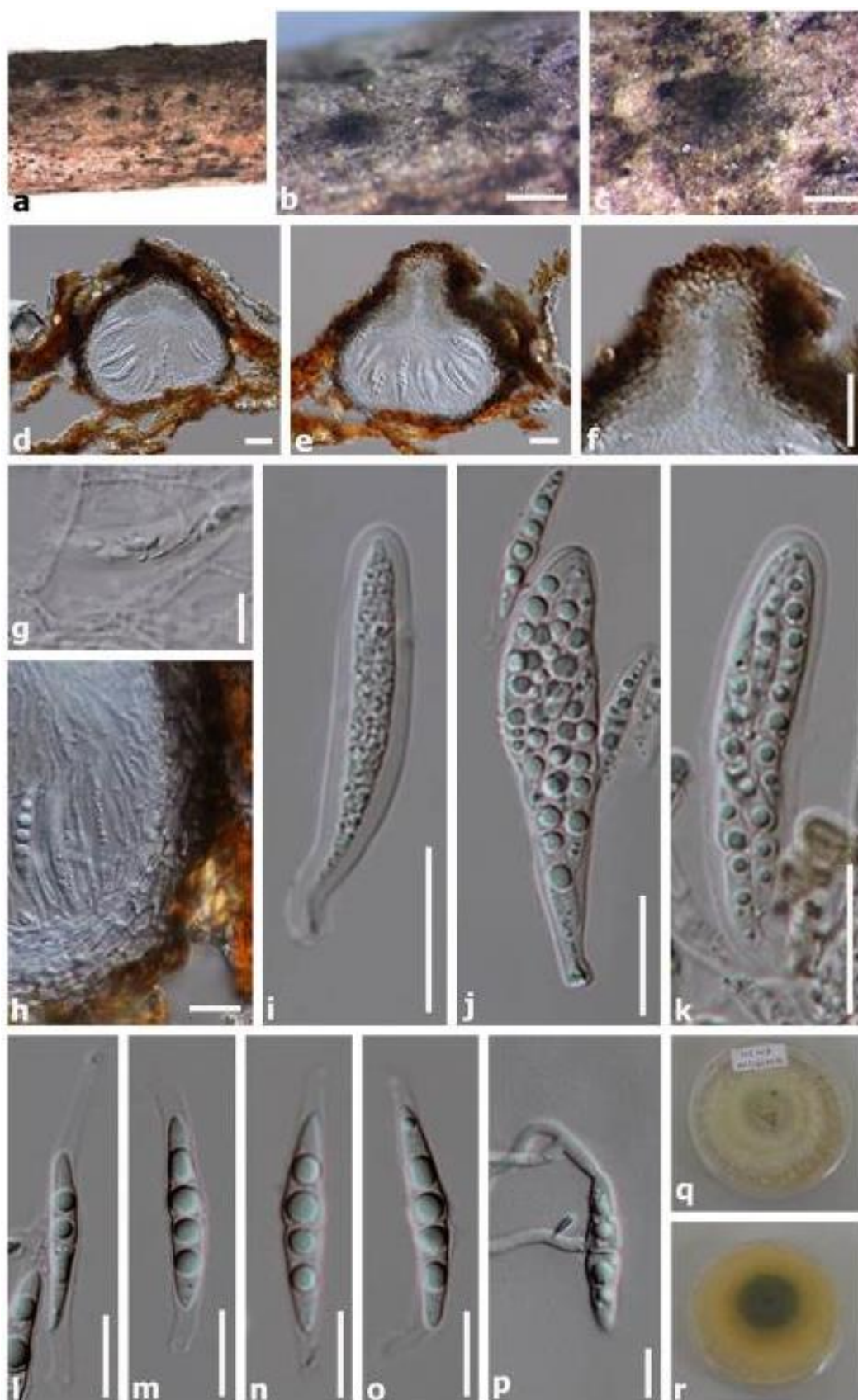


**Figure 2** – *Bambusicola ficuum* (MFLU 17-0677, holotype). a Apices of ascomata. b, c Appearance of ascomata on the host material. d, e, f Section through an ascoma. g Pseudoparaphyses. h Peridium. i–k. Asci l–o Ascospores. p Germinating ascospore. q Culture on PDA upper view. r Culture on PDA lower view. Scale bars: b, c = 100  $\mu$ m, d–f = 50  $\mu$ m, g, h = 20  $\mu$ m, i–k = 30  $\mu$ m, l–p = 20  $\mu$ m.

### ***Keissleriella* Höhn.**

Höhn (1919) introduced *Keissleriella* to accommodate *K. aesculi* (Höhn.) Höhn. (= *Pyrenochaeta aesculi* Höhn.). This genus is characterized by ascomata with ostiolar necks filled with black setae, and one to multi-septate, hyaline to pale brown ascospores (Barr 1990, Liu et al. 2015, Wanasinghe et al. 2018b, Phookamsak et al. 2019). The asexual morph comprises unbranched or branched, smooth, flexuous, hyaline conidiophores, phialidic conidiogenous cells and hyaline to brown, aseptate or septate conidia (Hyde et al. 2020). Munk (1957) placed *Keissleriella* in Lophiostomataceae, and then von Arx & Muller (1975) included it in Pleosporaceae. Subsequently, Barr (1990) placed it in Melanommataceae, while Lumbsch & Huhndorf (2007) transferred *Keissleriella* in to Massarinaceae. Zhang et al. (2009) included the genus in Lentitheciaceae, and this is followed by many subsequent authors (Zhang et al. 2012, Hyde et al. 2013, Wijayawardene et al. 2014, Tanaka et al. 2015, Wanasinghe et al. 2017b, 2018b, Phookamsak et al. 2019, Hyde et al. 2020).

### ***Keissleriella italica* Brahmanage, Camporesi & K.D. Hyde, sp. nov.**

Fig. 4

Index Fungorum number: IF557623; Facesoffungi number: FoF 08006

Etymology – Epithet refers to the country, Italy where the specimen was collected.

Holotype – MFLU 20-0394

*Saprobic* on dead aerial stems of *Brassica* sp. (Brassicaceae). Sexual morph: *Ascomata* 120–240 × 110–120 µm ( $\bar{x}$  = 210 × 105 µm), immersed to semi-immersed, appearing as black raised spots on the host, solitary, globose to subglobose, uniloculate, black, ostiolate with papilla filled with black setae. *Peridium* 18–25 µm wide, composed of 4–6 layers of pale brown to brown cells of *textura angularis*. *Hamathecium* comprising numerous, 0.8–1.3 µm wide, cellular, branched, septate, anastomosed pseudoparaphyses. *Asci* 50–70 × 12–18 µm ( $\bar{x}$  = 60 × 16 µm, n = 20), bitunicate, 8-spored, clavate, rounded at the apex with a short furcate pedicel. *Ascospores* 8–10 × 2–3 µm ( $\bar{x}$  = 8.5 × 2.5 µm, n = 20), overlapping uniseriate to biseriate, fusiform, hyaline, 1-septate, constricted at the septum, smooth-walled, guttulate and lacks a sheath. Asexual morph: Undetermined.

Material examined – ITALY, Province of Forlì-Cesena [FC], Forlì, via Correcchio, on dead aerial stems of *Brassica* sp. (Brassicaceae), 24 February 2018, E. Camporesi, IT 3746 (MFLU 20-0394, holotype; JZBH3490001, isotype).

GenBank Accessions – LSU: MT370427; SSU: MT370371

Notes – *Keissleriella italica* is typical of *Keissleriella* with its ostiolar neck, and fusiform, septate ascospores (Munk 1953, Tanaka et al. 2015). *Keissleriella italica* clustered sister to *K. dactylidicola* Mapook, Camporesi & K.D. Hyde and *K. phragmiticola* Wanas., E.B.G. Jones & K.D. Hyde with relatively poor bootstrap support (Fig. 3). *Keissleriella italica* has smaller ascomata (120–240 × 110–120 µm vs 160–210 × 200–230 µm vs 400–500 × 400–450 µm), asci (50–70 × 12–18 µm vs 60–80 × 8–10 µm vs 120–160 × 16–20 µm) and ascospores (8–10 × 2–3 µm vs 15–19 × 4–5 µm vs 35–50 × 7–11 µm) than that of *K. dactylidicola* and *K. phragmiticola*, respectively (Ariyawansa et al. 2015a, Wanasinghe et al. 2018a). Further, *K. dactylidicola* has surrounded by a hyaline, gelatinous sheath around the ascospores while *Keissleriella italica* lacks a sheath and their ascospore arrangement and the asci are also different from each other. Base pair differences of the LSU region of *Keissleriella italica* to *K. dactylidicola* and *K. phragmiticola* are 0.99% (6 bp out of 602 bp without gaps) and 1.3% (8 bp out of 602 bp without gaps) respectively. Even though there is less support in our phylogenetic analyses, we rely mostly on its independent lineage, nucleotide and morphological differences to treat it as a new species.

### ***Pseudomurilentithecium* Mapook & K.D. Hyde**

*Pseudomurilentithecium* was introduced by Hyde et al. (2020) based on the combined LSU and ITS phylogeny. The genus clusters within Lentitheciaceae (Fig. 3). *Pseudomurilentithecium* shows close phylogenetic affinities to *Poaceascoma* and *Setoseptoria* (Hyde et al. 2020). However, *Pseudomurilentithecium* can be distinguished from *Setoseptoria* in having brown, fusiform and

muriform ascospores whereas *Poaceascoma* has hyaline, filiform ascospores without vertical septa (Phookamsak et al. 2015). In this study, we introduce another species to the genus from *Clematis vitalba*.

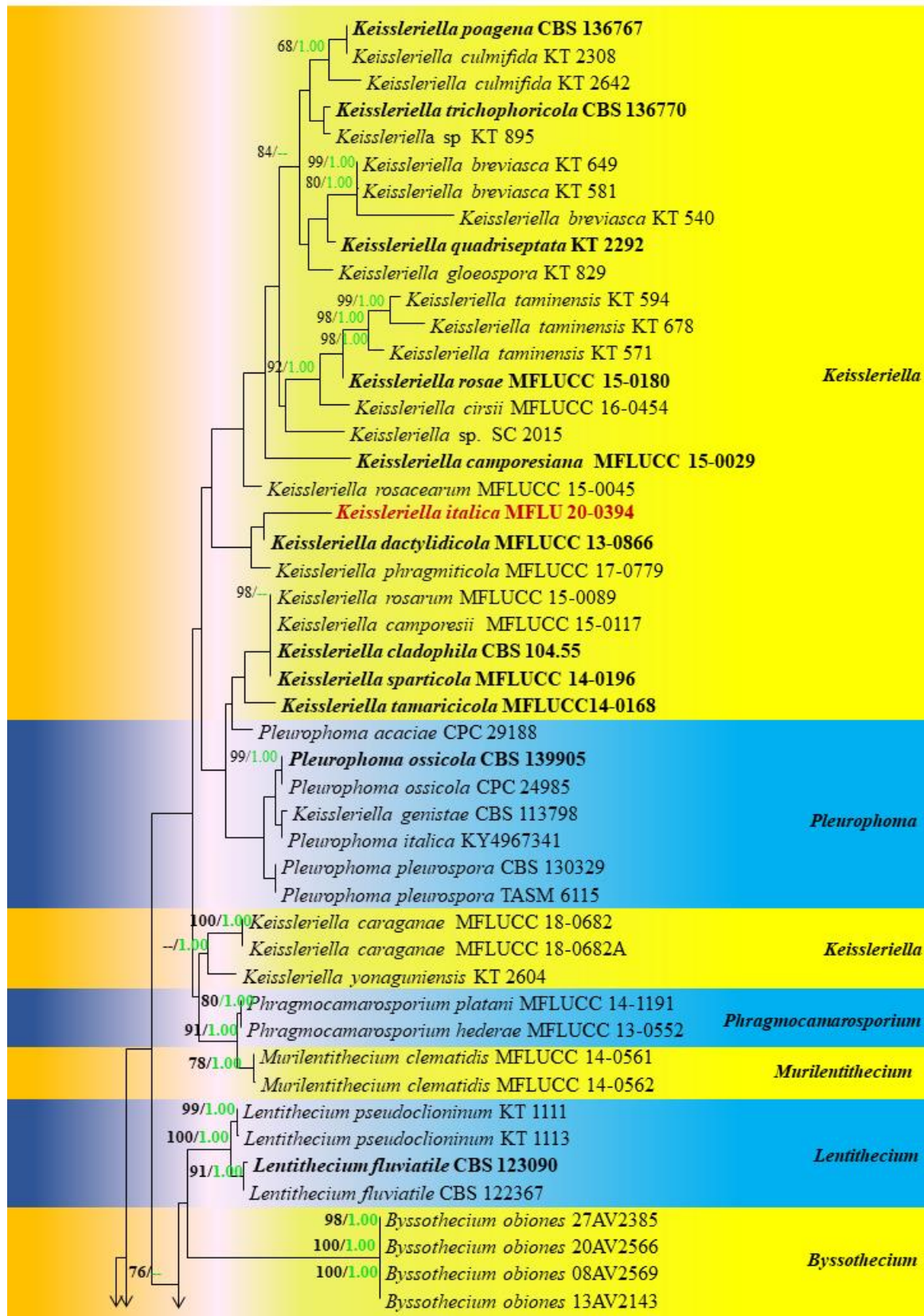


**Figure 3** – Maximum likelihood analysis with 1000 bootstrap replicates yielded a best tree with the likelihood value of -12505.847030. The combined LSU, SSU and ITS sequence datasets comprised

69 strains with *Massarina cisti* (CBS 266.62) and *M. pandanicola* (MFLUCC 17-0596) as the outgroup taxa. The matrix had 542 distinct alignment patterns, with 25.87% of undetermined characters or gaps. Estimated base frequencies were as follows; A = 0.244251, C = 0.220423, G = 0.272920, T = 0.262407; substitution rates AC = 1.276940, AG = 2.987661, AT = 1.881985, CG = 0.507025, CT = 6.404577, GT = 1.000000; gamma distribution shape parameter  $\alpha = 0.534298$ . Maximum likelihood bootstrap (ML, black) values equal to or greater than 65% and Bayesian posterior probabilities (PP, green) equal to or greater than 0.95 PP are given above the nodes. The scale bar indicates 0.03 changes. The ex-type strains are in black bold and new isolates are in red bold.

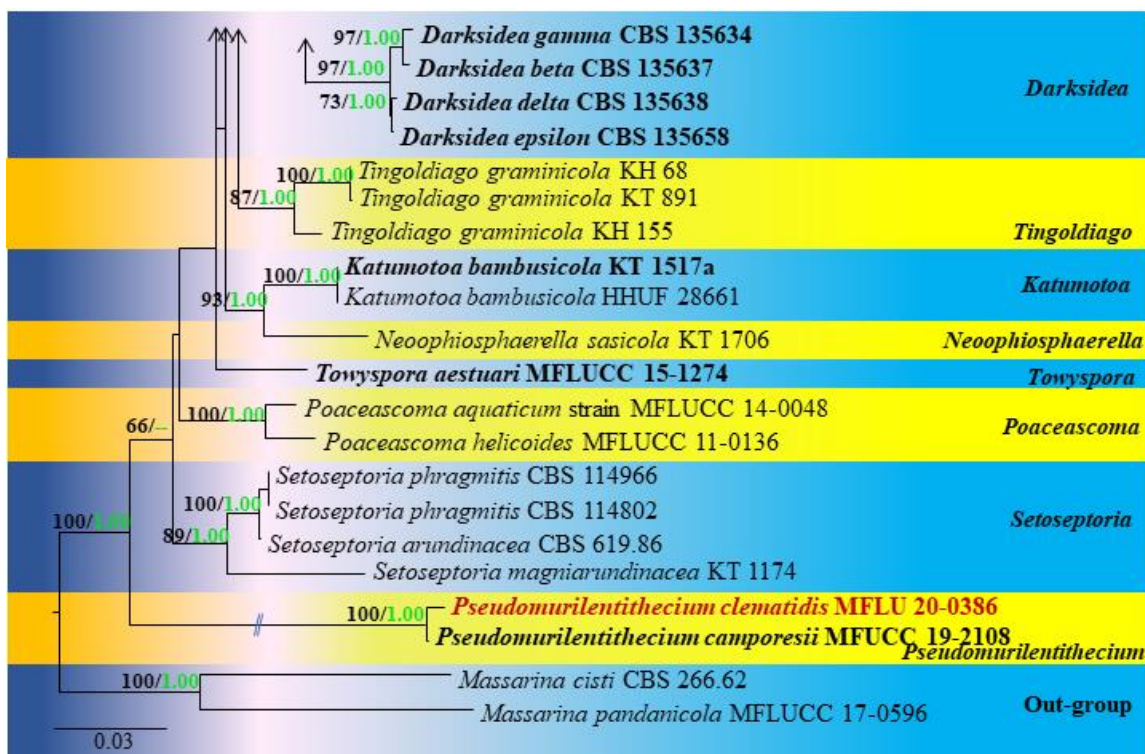


Figure 3 – Continued.

*Pseudomurilentithecium clematidis* Brahmanage, Camporesi & K.D. Hyde, sp. nov.

Fig. 5

Index Fungorum number: IF557595; Facesoffungi number: FOF 08007

Etymology – The species epithet refers to the host genus “*Clematis*”.

Holotype – MFLU 20-0386

*Saprobic* on dead aerial branches of *Clematis vitalba*. Sexual morph: *Ascomata* 650–1500  $\mu\text{m}$  high  $\times$  600–900  $\mu\text{m}$  diam., immersed, solitary, scattered, coriaceous, subglobose to globose, dark brown to black. *Ostiolar* neck protruding. *Peridium* 12–18  $\mu\text{m}$  wide, composed of two layers, outer layer comprises 2–3 layers, dark brown cells of *textura angularis* and inner layer comprises hyaline cells of *textura angularis*. *Hamathecium* comprising 1.2–2  $\mu\text{m}$  wide, cylindrical, septate, branched pseudoparaphyses. *Asci* 80–120  $\times$  8–15  $\mu\text{m}$  ( $\bar{x}$  = 102  $\times$  14  $\mu\text{m}$ , n = 10), bitunicate, 8-spored, cylindric-clavate, straight or slightly curved, apically rounded, short pedicellate. *Ascospores* 25–35  $\times$  10–15  $\mu\text{m}$  ( $\bar{x}$  = 28  $\times$  12  $\mu\text{m}$ , n = 30), overlapping, uni–bi-seriate, initially hyaline to pale yellow, 1-septate when immature, becoming golden-brown to brown at maturity, ellipsoid to broadly fusiform, muriform, 3–8-transversely septate, with 1–2 vertical septa, constricted at the central septum, upper half wider than the lower half, straight or curved, surrounded by hyaline, thick gelatinous sheath. Asexual morph: Undetermined.

Material examined – ITALY, Province of Forlì-Cesena [FC], Fiumicello-Premilcuore, dead branches of *Clematis vitalba* (Ranunculaceae), 5 December 2013, E. Camporesi, IT 1559 (MFLU 20-0386, holotype; JZBH3490002, isotype).

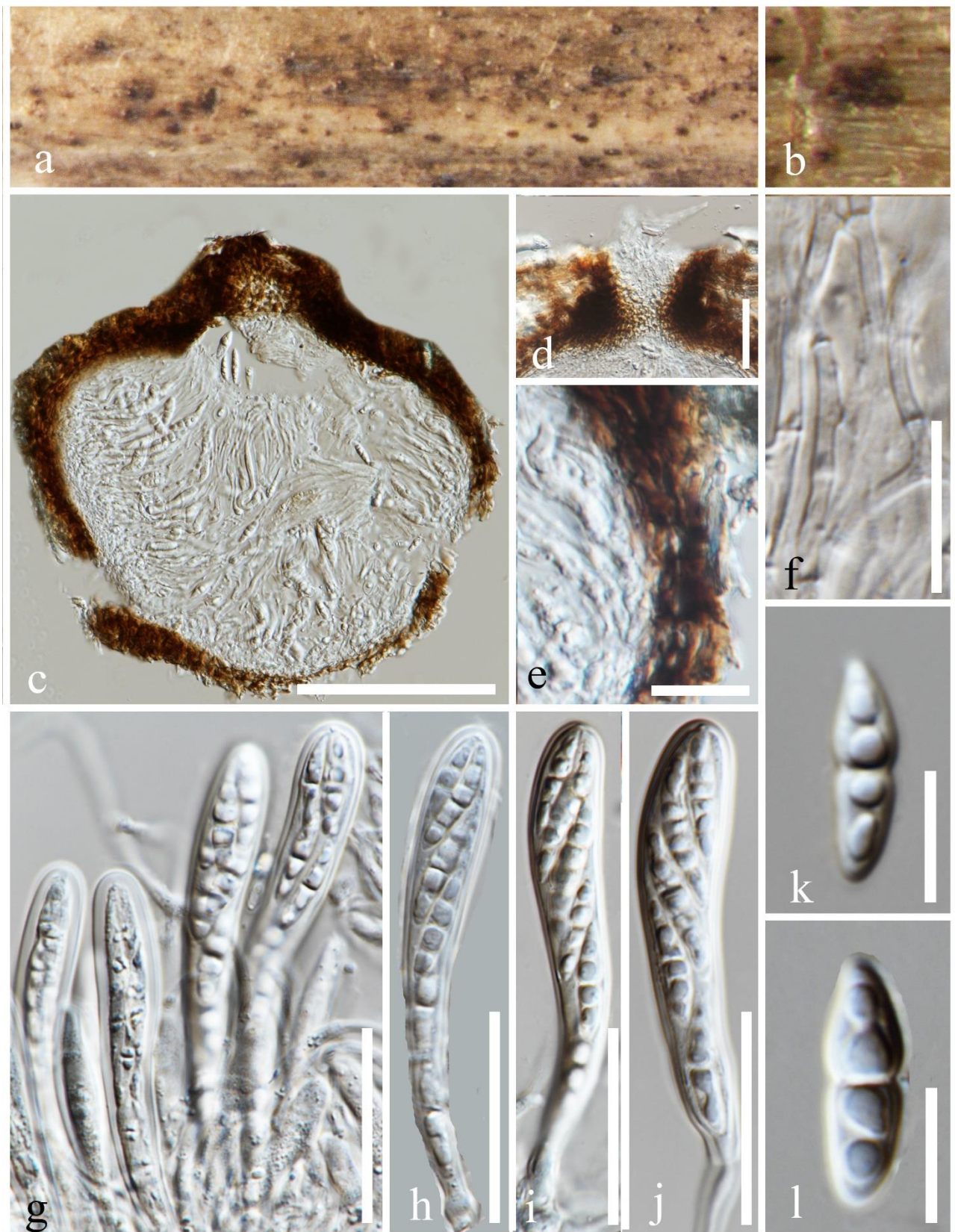


**Figure 4** – *Keissleriella italica* (MFLU 20-0394, holotype). a Appearance of ascomata on host. b Close up of an ascoma. c Section through an ascoma. d Ostiolar region. e Peridium. f Pseudoparaphyses. g–j Asci. k, l Ascospores. Scale bars: c = 100  $\mu$ m, g–j = 20  $\mu$ m, d, e, f = 10  $\mu$ m, k, l = 5  $\mu$ m.

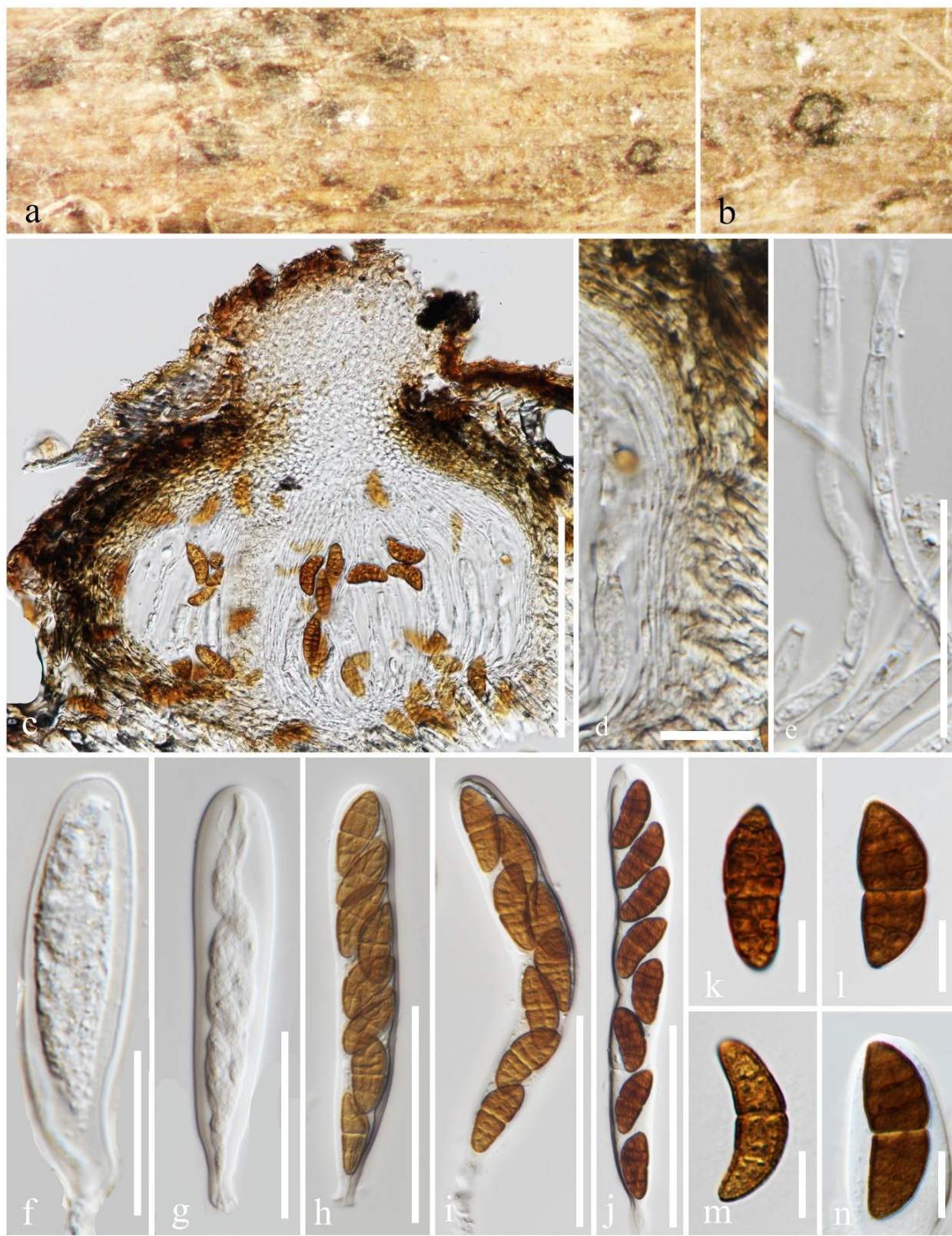


**Figure 5** – *Pseudomurilentithecium clematidis* (MFLU 20-0386, holotype). a Appearance of ascomata on host. b Close up of an ascoma. c Section through an ascoma. d Peridium. e Pseudoparaphyses. f–i Asci. j–m Ascospores n. Ascospore showing thick gelatinous sheath. Scale bars: c = 500  $\mu$ m, f–j = 50  $\mu$ m, e = 20  $\mu$ m, d, k–n = 10  $\mu$ m

Notes – *Pseudomurilentithecium clematidis* shares similar features with *P. camporesii* in having ascomata with protruding ostiolar necks, cylindrical, septate, branched pseudoparaphyses,

cylindric-clavate asci and ascospores that are initially hyaline to pale yellow which becomes golden-brown to brown at maturity and with a hyaline gelatinous sheath (Hyde et al. 2020). *Pseudomurilentithecium clematidis* has curved ascospores with a wider upper half than the lower half, while *P. camporesii* has mostly straight slightly curved ascospores with equal upper and lower portions. Size of ascomata ( $650\text{--}1500 \times 600\text{--}900 \mu\text{m}$  vs  $130\text{--}145 \times 140\text{--}160 \mu\text{m}$ ) and asci ( $80\text{--}120 \times 8\text{--}15 \mu\text{m}$  vs  $90\text{--}115 \times 16\text{--}22 \mu\text{m}$ ) of *P. clematidis* and *P. camporesii* are also different. Based on a phylogenetic analysis of combined LSU and ITS sequence dataset, *P. clematidis* is related to *P. camporesii* (Fig. 3). However, base pair differences of the ITS region of *P. clematidis* and *P. camporesii* is 1.9% (11 bp out of 590 bp without gaps). Thus, *P. clematidis* is introduced as a novel species based on both morphology and DNA sequence data.

### **Leptosphaeriaceae** M.E. Barr

Members of Leptosphaeriaceae are saprobes, hemibiotrophs or pathogens on stems and leaves of herbaceous or woody plants in terrestrial and aquatic habitats (Hyde et al. 2013, Ariyawansa et al. 2015b, Dayarathne et al. 2015, Jones et al. 2015, Liu et al. 2015, Wanasinghe et al. 2016, Tennakoon et al. 2017). Barr (1987) introduced Leptosphaeriaceae, and designated *Leptosphaeria* Ces. & De Not. as the type of the family. Species in Leptosphaeriaceae are characterized by immersed, erumpent or superficial, perithecial ascomata with single papillate ostioles, fissitunicate, cylindrical asci and hyaline to brown, transversely septate ascospores (Hyde et al. 2013, Ariyawansa et al. 2015b, Phookamsak et al. 2019, Hongsanan et al. 2020). The asexual morphs of taxa in Leptosphaeriaceae are coelomycetes (*Heterospora chenopodii* (Westend.) Gruyter) or hyphomycetes (De Gruyter et al. 2013, Hyde et al. 2013, Wanasinghe et al. 2016, Tennakoon et al. 2017). Twelve genera are accepted in Leptosphaeriaceae (Wijayawardene et al. 2020, Hongsanan et al. 2020).

### **Plenodomus** Preuss

*Plenodomus* was introduced by Preuss (1851) with *P. rabenhorstii* Preuss as the type species. However, *P. rabenhorstii* was replaced by *P. lingam* (Tode) Höhn. (sexual morph: *Leptosphaeria maculans* Ces. & De Not.) by Boerema & Kesteren (1964) due to the type material of *P. rabenhorstii* being lost during the World War II (Torres et al. 2005, Ariyawansa et al. 2015b, Phookamsak et al. 2019). The connection between *L. maculans* (sexual morph) and *P. lingam* (asexual morph) has been confirmed by single spore isolation (Boerema & Kesteren 1964). We herein introduce two new host record of *Plenodomus* species in Italy.

### **Plenodomus biglobosus** (Shoemaker & H. Brun) Gruyter, Aveskamp & Verkley

Fig. 7

Index Fungorum number: IF564727; Facesoffungi number: FoF08008

*Saprobic on Alliaria petiolata*. Sexual morph: Not observed. Asexual morph: Coelomycetous. *Conidiomata*  $110\text{--}180 \times 165\text{--}225 \mu\text{m}$  ( $\bar{x} = 150 \times 180 \mu\text{m}$ ,  $n = 5$ ), pycnidial, solitary, scattered, erumpent, mostly subglobose, ostiolate. *Ostiole* papillate with a narrow pore. *Pycnidial wall*  $20\text{--}30 \mu\text{m}$  wide, composed of several layers with thick-walled, brown to lightly pigmented cells of *textura angularis*. *Conidiogenous cells*  $1\text{--}2.5 \times 1\text{--}1.2 \mu\text{m}$  ( $\bar{x} = 2 \times 1 \mu\text{m}$ ,  $n = 20$ ), phialidic, hyaline, smooth, ampulliform. *Conidia*  $4\text{--}8 \times 1.5\text{--}2.5 \mu\text{m}$  ( $\bar{x} = 6.2 \times 2 \mu\text{m}$ ,  $n = 30$ ), hyaline, aseptate, ellipsoidal to subcylindrical, with two large guttules.

Material examined – ITALY, Province of Forlì-Cesena [FC], San Martino in Villafranca, on dead aerial stem of *Alliaria petiolata* (Brassicaceae), 12 February 2018, E. Camporesi, IT 3725 (MFLU 20-0393, JZBH3480002).

GenBank Accessions – LSU: MT370425; SSU: MT370369; ITS: MT370401

Notes – Our new isolate (MFLU 20-0393) comprises phialidic, hyaline, smooth, ampulliform conidiogenous cells and hyaline, aseptate, ellipsoidal to subcylindrical conidia. Our new isolate forms a well-supported lineage (96% ML, 1.00 PP; Fig. 6) in a clade comprising *P. biglobosus* (Shoemaker & H. Brun) Gruyter, Aveskamp & Verkley, *P. pimpinellae* (Lowen & Sivan.) Gruyter,

Aveskamp & Verkley, *P. guttulatus* Ariyaw. & K.D. Hyde and *P. hendersoniae* (Fuckel) Gruyter, Aveskamp & Verkley.

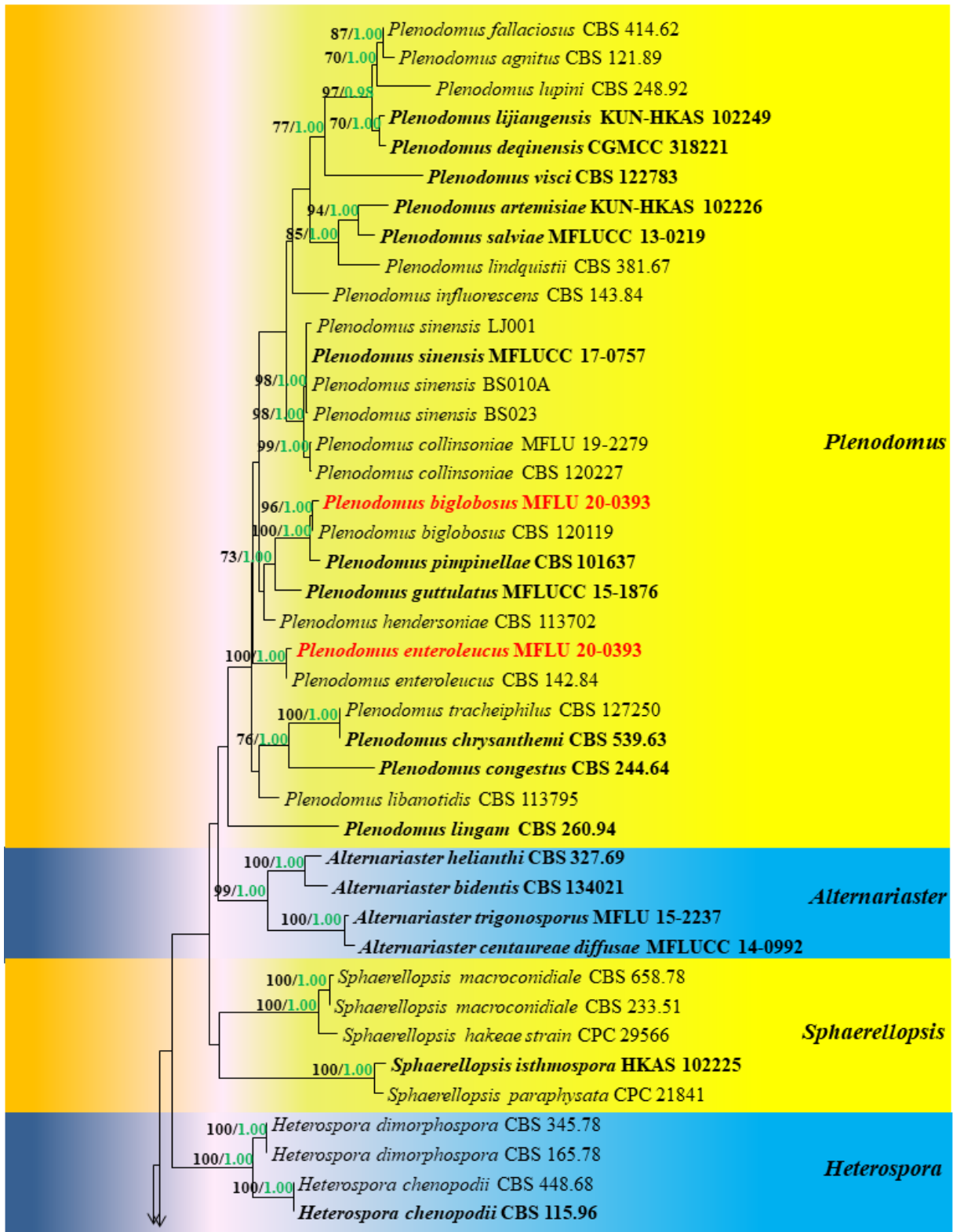


**Figure 6** – Maximum likelihood analysis with 1000 bootstrap replicates yielded a best tree with the likelihood value of -12505.847030. The combined LSU, SSU, ITS and TEF1 sequence dataset comprised 101 strains of *Leptosphaeriaceae* with *Phaeosphaeria oryzae* (CBS 110110), *Phaeosphaeriopsis glaucopunctata* (MFLUCC 13-0265) and *Paraphoma radicina* (CBS 111.79) as the outgroup taxa. Tree topology of the ML analysis was similar to the BI analysis. The matrix had



542 distinct alignment patterns, with 25.87% of undetermined characters or gaps. Estimated base frequencies were as follows; A = 0.244251, C = 0.220423, G = 0.272920, T = 0.262407; substitution rates AC = 1.276940, AG = 2.987661, AT = 1.881985, CG = 0.507025, CT = 6.404577, GT = 1.000000; gamma distribution shape parameter  $\alpha$  = 0.534298. Maximum likelihood bootstrap (ML, black) values equal to or greater than 65% and Bayesian posterior probabilities (PP, green) equal to or greater than 0.95 PP are given above the nodes. The scale bar indicates 0.03 changes. The ex-type strains are in black bold and new isolates are in red bold.

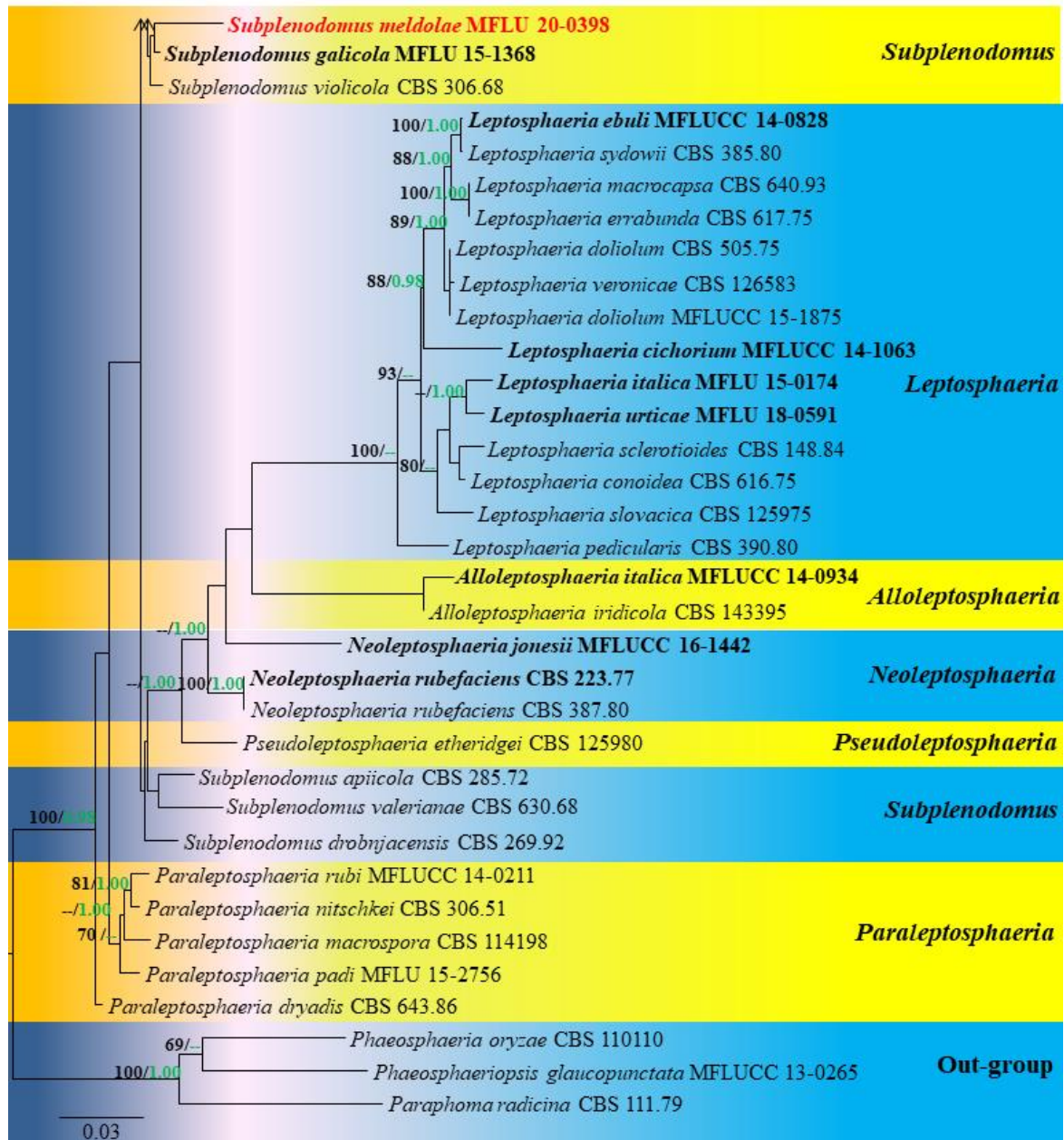


**Figure 6** – Continued.

New isolate (MFLU 20-0393) shows a closer phylogenetic and morphological affinity to *P. biglobosus* (CBS 120119), which has been described from cultivated *Brassica* species as the cause of upper stem lesions. There are no significant differences in the base pair differences of LSU (0.11%, 1/875) and ITS (0.60%, 3/506] loci of our new isolate (MFLU 20-0393) and *P. biglobosus* (CBS 120119). Therefore, we identified our isolate (MFLU 20-0393) as *P. biglobosus*. This is the first record of *P. biglobosus* from *Alliaria petiolata* (Brassicaceae) in Italy.

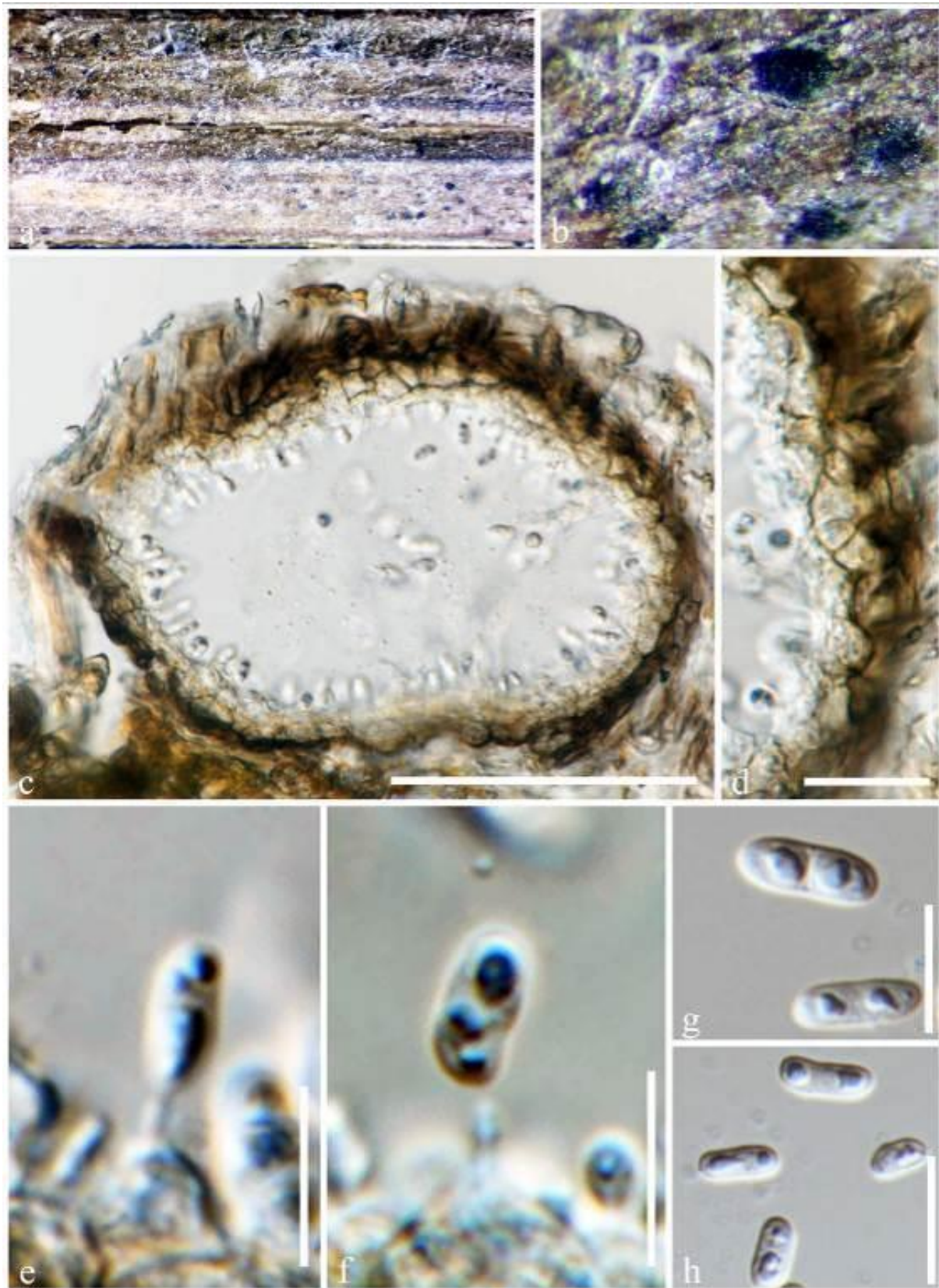


**Figure 7** – *Plenodomus biglobosus* (MFLU 20-0393). a, b Conidiomata on host surface. c Vertical section through a conidioma. d Pycnidial wall. e, f Developing conidia. g, h Conidia. Scale bars: c = 100  $\mu$ m, d = 20  $\mu$ m, g, h = 10, e, f = 5  $\mu$ m.

*Plenodomus enteroleucus* (Sacc.) Gruyter, Aveskamp & Verkley  
 Index Fungorum number: IF564753; Facesoffungi number: FoF08009

Fig. 8

*Saprobic* on *Picris hieracioides*. Sexual morph: Undetermined. Asexual morph: Coelomycetous. *Conidiomata* 150–270 × 255–360 µm ( $\bar{x}$  = 200 × 280 µm, n = 5), pycnidial, solitary, scattered, erumpent, mostly subglobose, ostiolate. *Ostiole* slightly papillate with a narrow pore or opening via a rupture. *Pycnidial wall* 20–35 µm wide, composed of several layers with thick-walled, brown to lightly pigmented cells of *textura angularis*, surface heavily pigmented. *Conidiogenous cells* 1–2.5 µm long, holoblastic, phialidic, globose to oblong, individually hyaline and pale brown when in a mass, and formed from the inner layer of pycnidial wall. *Conidia* 5–8 × 1.5–2.8 µm ( $\bar{x}$  = 6.5 × 2 µm, n = 20), hyaline, aseptate, ellipsoidal to oblong, with guttules.

Material examined – ITALY, Province of Forlì-Cesena [FC], Saviana-Santa Sofia, on dead aerial stems of *Picris hieracioides* (Asteraceae), 8 November 2017, E. Camporesi, IT 3575a (MFLU 20-0389, JZBH3480001).

GenBank Accessions – LSU: MT370423, ITS: MT370399

Notes – Our new isolate (MFLU 20-0389) shows a closer phylogenetic affinity to *P. enteroleucus* (Fig. 6) and it morphologically resembles the holotype PAD, Gillet, 1878. However, MFLU 20-0389 has comparatively longer conidia (5–8 vs 3–4 µm) than the type. There are no base pair differences in the ITS region of MFLU 20-0389 and CBS 142.84 strains. Therefore, by considering both phylogenetic and morphological data, we confirmed our new strain as *P. enteroleucus*. This is the first record of *P. enteroleucus* from *Picris hieracioides* (Asteraceae) in Italy.

### ***Subplenodomus*** Gruyter, Aveskamp & Verkley

De Gruyter et al. (2013) introduced *Subplenodomus* with *S. violicola* (P. Syd.) Gruyter, Aveskamp & Verkley, as the type species, to accommodate selected phoma-like species that belong to Leptosphaeriaceae. Based on morphological and multi-gene phylogenetic analyses, *Subplenodomus* was accepted as an asexual morph of Leptosphaeriaceae (De Gruyter et al. 2013, Hyde et al. 2013, Ariyawansa et al. 2015b). *Subplenodomus* is characterized by thick-walled, ostiolate pycnidia, consisting of pseudoparenchymatous or sometimes scleroplectenchymatous cell types, phialidic, ampulliform to doliiform conidiogenous cells and hyaline, aseptate, and ellipsoid conidia (De Gruyter et al. 2013). *Subplenodomus* species formed two distant subclades in our phylogenetic analyses (Fig. 6). *Subplenodomus sensu stricto* comprises *S. galicola*, *S. violicola* and our new species, *S. meldolae*, while *S. apiicola* (Kleb.) Gruyter, Aveskamp & Verkley, *S. drobnjacensis* (Bubák) Gruyter, Aveskamp & Verkley and *S. valerianae* (Henn.) Gruyter, Aveskamp & Verkley are grouped in *Subplenodomus sensu lato*. The genus comprises five species and here we introduce a new species from Italy.

### ***Subplenodomus meldolanus*** Brahmanage & K.D. Hyde, sp. nov.

Fig. 9

Index Fungorum number: IF557592; Facesoffungi number: FoF08010

Etymology – Epithet refers to the geographical region “Meldola” where the species was found.

Holotype – MFLU 20-0398

*Saprobic* on dead aerial stems of *Medicago* sp. (Fabaceae). Sexual morph: *Ascomata* 185–300 × 260–420 µm ( $\bar{x}$  = 240 × 350 µm, n = 5), immersed, slightly erumpent through the host tissues, globose to subglobose, dark brown, with a central ostiole. *Peridium* 12–18 µm wide, composed of 4–6 layers of brown to dark brown, thick-walled cells of *textura angularis*. *Hamathecium* composed on pseudoparaphyses, 0.8–1.5 µm diam., intermingled among asci, subcylindrical, smooth, hyphae-like. *Asci* 80–100 × 12–13 µm ( $\bar{x}$  = 92 × 12.6 µm, n = 20), 8-spored, bitunicate, cylindrical to subcylindrical, sessile to short pedicellate, with an indistinct ocular chamber. *Ascospores* 20–35 × 5–10 µm ( $\bar{x}$  = 30 × 8 µm, n = 30), bi-seriate, partially overlapping, fusoid-ellipsoid, pale brown, finely roughened, 3-septate, slightly constricted at the septa, at times first cell above median septum becomes slightly swollen. Asexual morph: Undetermined.

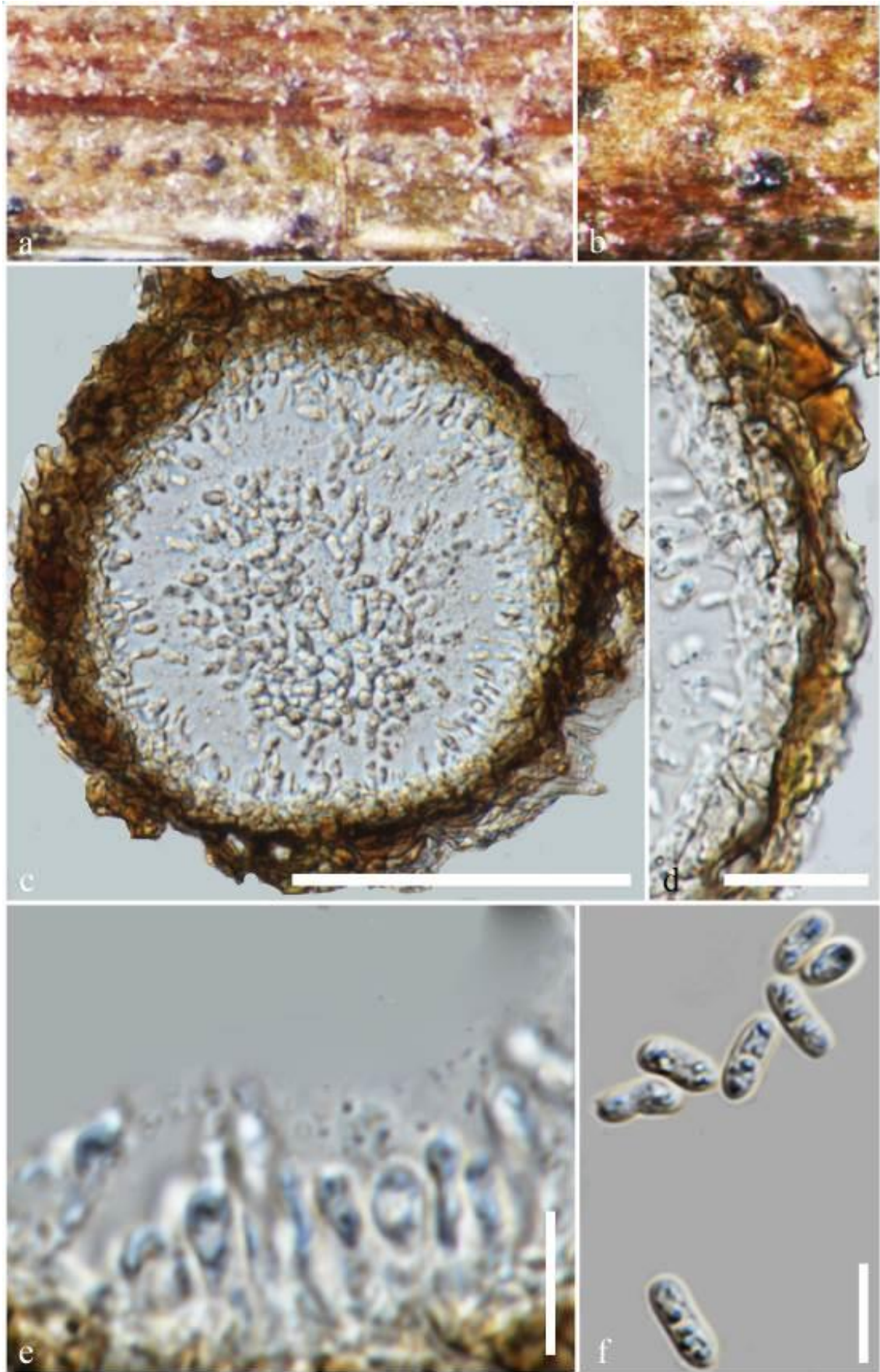


**Figure 8** – *Plenodomus enteroleucus* (MFLU 20-0389). a, b Conidiomata on host surface. c Vertical section through a conidioma. d Pycnidial wall. e Developing conidia. f Conidia. Scale bars: c = 50  $\mu$ m, d = 20  $\mu$ m, e, f = 5  $\mu$ m.



**Figure 9** – *Subplenodomus meldolanus* (MFLU 20-0398, holotype). a Appearance of ascomata on host. b Close up of ascomata. c Section through an ascoma. d Peridium. e Pseudoparaphyses. f–h Asci. i Ascospores. Scale bars: c = 100  $\mu$ m, f–h = 50  $\mu$ m, e = 20  $\mu$ m, d, i = 10  $\mu$ m.

Material examined – ITALY, Province of Forlì-Cesena [FC], near Meldola, on a dead aerial stem of *Medicago* sp. (Fabaceae), 18 December 2017, E. Camporesi, IT 3625 (MFLU 20-0398, holotype; JZBH3480003 isotype).

GenBank Accessions – LSU: MT370424; ITS: MT370400

Notes – Phylogenetically, *Subplenodomus meldolanus* is closely related to *S. galicola* Phukhams., Tibpromma, Camporesi & K.D. Hyde described from a dead stem of *Galium* sp. collected in Italy. *Subplenodomus galicola* has larger ascospores (30–40 × 6–9 µm) that are constricted only at the median septa and asci (66–120 × 12–17 µm) (Tibpromma et al. 2017). Base pair differences of the ITS region of *S. meldolanus* as compared to *S. galicola* and *S. violicola* are 3.4% (30 bp out of 555 bp, without gaps) and 8.9% (44 bp out of 490 bp, without gaps), respectively.

### Lophiostomataceae Luerss.

Lophiostomataceae was erected by Saccardo (1883) with *Lophiostoma macrostomum* (Tode) Ces. & De Not. as the type species (Hashimoto et al. 2018) and is characterized by slit-like ostiolar openings on a laterally compressed papilla, mostly clavate asci and 1- to multi-septate and hyaline to dark brown ascospores with terminal appendages or mucilaginous sheaths (Hyde et al. 2013, Ariyawansa et al. 2015a, Liu et al. 2015, Thambugala et al. 2015, Hyde et al. 2017, Tibpromma et al. 2017). Members of some genera also have trabeculate pseudoparaphyses (Liew et al. 2000). There are 27 accepted genera viz. *Crassiclypeus* A. Hashim., K. Hiray. & Kaz. Tanaka, *Decaisnella* Fabre, *Dimorphiopsis* Crous, *Flabellascoma* A. Hashim., K. Hiray. & Kaz. Tanaka, *Guttulispora* Thambug., Qing Tian & K.D. Hyde, *Kiskunsagia* D.G. Knapp, Imrefi & Kovács, *Lentistoma* A. Hashim., K. Hiray. & Kaz. Tanaka, *Leptoparies* A. Hashim., K. Hiray. & Kaz. Tanaka, *Lophiohelichrysum* Dayar., Camporesi & K.D. Hyde, *Lophiopoacea* Ariyaw., Thambug. & K.D. Hyde, *Lophiostoma* Ces. & De Not., *Neotrematosphaeria* Thambug., Kaz. Tanaka & K.D. Hyde, *Neovaginatisspora* A. Hashim., K. Hiray. & Kaz. Tanaka, *Parapaucispora* A. Hashim., K. Hiray. & Kaz. Tanaka, *Paucispora* Thambug., Kaz. Tanaka & K.D. Hyde, *Platystomum* Trevis., *Pseudocapulatispora* Mapook & K.D. Hyde, *Pseudolophiostoma* Thambug., Kaz. Tanaka & K.D. Hyde, *Pseudopaucispora* A. Hashim., K. Hiray. & Kaz. Tanaka, *Pseudoplatystomum* Thambug. & K.D. Hyde, *Sigarispora* Thambug. & K.D. Hyde, *Tumularia* Descals & Marvanová and *Vaginatisspora* K.D. Hyde (Hongsanan et al. 2020).

### *Pseudopaucispora* A. Hashim., K. Hiray. & Kaz. Tanaka

*Pseudopaucispora* was introduced to accommodate *P. brunneospora* A. Hashim., K. Hiray. & Kaz. Tanaka, with pseudopycnidia and small, brown ascospores (Hashimoto et al. 2018). This genus is somewhat similar to *Paucispora* (Thambugala et al. 2015). *Pseudopaucispora* differs from *Paucispora* in having a single zone ascomatal peridium and an ascus with a short pedicel, whereas *Paucispora* has two zones in the peridium and an ascus with a relatively long pedicel (Thambugala et al. 2015, Hashimoto et al. 2018).

### *Pseudopaucispora hyalinospora* Samarak. & K.D. Hyde, sp. nov.

Fig. 11

Index Fungorum number: IF557374; Facesoffungi number: FoF08003

Etymology – Refers to its hyaline ascospores

Holotype – MFLU 18-0803

*Saprobic* on dead branches in terrestrial habitat. Sexual morph *Ascomata* 475–510 µm high, 350–400 µm diam. ( $\bar{x}$  = 490 × 375 µm, n = 5), scattered, immersed, dark brown to black, globose to subglobose, ostiolate. *Papilla* 310–350 µm length, erumpent through host surface, coriaceous to carbonaceous. *Ostiole* crest-like, central, periphysate, broadly papillate, with an irregular pore-like opening, plugged by hyaline, filamentous hyphae. *Peridium* 30–60 µm wide ( $\bar{x}$  = 39.5 µm, n = 20), single stratum, with 4–6 layers of dark brown to black cells of *textura prismatica*, fusing and indistinguishable from the host tissues. *Hamathecium* comprising 1.3–2 µm wide ( $\bar{x}$  = 1.6 µm, n = 25), numerous, filamentous, septate, branched, trabeculate pseudoparaphyses, embedded in a

gelatinous matrix. *Asci* 100–130 × 13–18 μm ( $\bar{x}$  = 110 × 15.8 μm, n = 25), 8-spored, bitunicate, fissitunicate, cylindrical-clavate, with a short pedicel, apically rounded, with an ocular chamber. *Ascospores* 33.5–38.5 × 7–8 μm ( $\bar{x}$  = 38 × 7.3 μm, n = 30), L/W 5.2, uni- to bi-seriate, hyaline, light brown when mature, fusiform, 3-septate including 2 eusepta, constricted at the median septum, guttulate, smooth-walled, with a distinct narrow sheath at the end, 6–9 μm long ( $\bar{x}$  = 7.8 μm, n = 15). Asexual morph Undetermined.

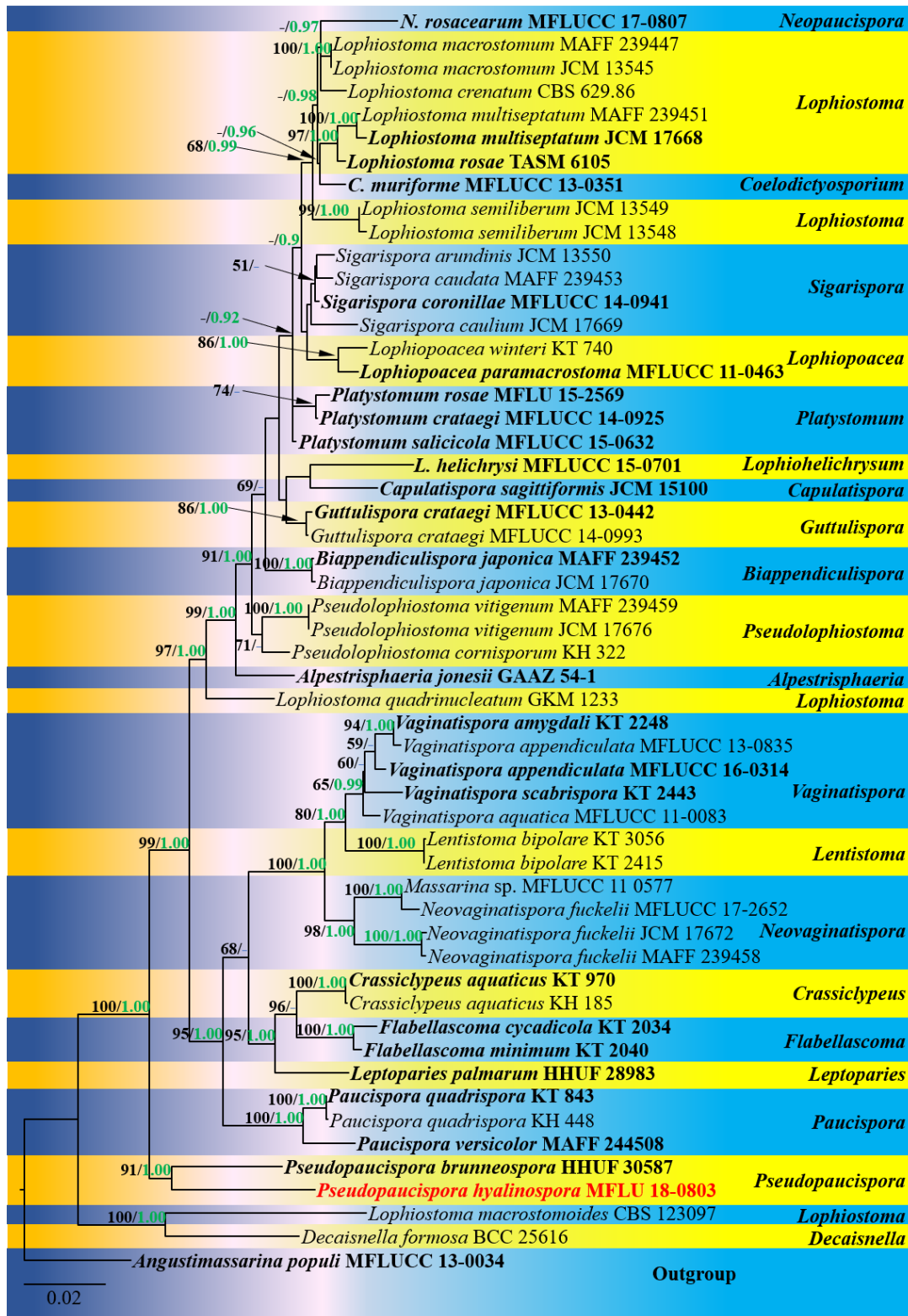


**Figure 10** – Maximum likelihood analysis with 1000 bootstrap replicates yielded a best tree with the likelihood value of -12454.204760. The combined LSU, SSU and TEF1 sequence dataset

comprised 54 strains of *Lophiostomataceae* with *Anguistimassarina populi* (MFLUCC 13-0034) as the outgroup taxon. Tree topology of the ML analysis was similar to the BI analysis. The matrix had 709 distinct alignment patterns, with 9.91% of undetermined characters or gaps. Estimated base frequencies were as follows; A = 0.246305, C = 0.242924, G = 0.273454, T = 0.237317; substitution rates AC = 1.155343, AG = 3.247931, AT = 1.046007, CG = 1.482199, CT = 9.600596, GT = 1.000000; gamma distribution shape parameter  $\alpha$  = 0.652364. Maximum likelihood bootstrap (ML, black) values equal to or greater than 50% and Bayesian posterior probabilities (PP, green) equal to or greater than 0.90 PP are given above the nodes. The scale bar indicates 0.02 changes. The ex-type strains are in bold and new isolate is in red bold.



**Figure 11** – *Pseudopaucispora hyalinospora* (MFLU 18–0803, holotype). a–c Ascomata on the substrate. d Section of the peridium. e–g Cross sections of ascomata. h Pseudoparaphyses. i–l Asci (l in congo red). m–q Ascospores (p in congo red, q in Indian ink). r Germinating ascospore. s Upper view of the colony. t Reverse view of the colony. Scale bars: a–c = 500  $\mu$ m, e–g = 200  $\mu$ m, d, i–l = 50  $\mu$ m, m–r = 20  $\mu$ m, h = 10  $\mu$ m.



Culture characteristics – Ascospores becoming light brown and germinating on PDA within 18 h and producing germ tubes from the ends. Colonies on PDA reaching 16 mm diam. after 4 weeks at 25°C, circular, filiform margin, effuse to raised, surface grey, reverse yellowish brown, dense, with greyish green edge.

Material examined – THAILAND, Chiang Rai Province, Mueang District, on dead branch, 28 July 2017, M.C. Samarakoon, SAMC026 (MFLU 18–0803, holotype; HKAS 102296 isotype), ex-type living culture, MFLUCC 18–0360.

GenBank Accessions – LSU: MT435501, SSU: MT435504, TEF1: MT729647

Notes – *Pseudopaucispora hyalinospora* (MFLU 18–0803) possesses scattered, immersed ascomata with an elongated and laterally compressed ostiole, a single-layered peridium composed of rectangular, brown cells, cylindrical to clavate asci and fusiform, 1-septate, smooth-walled ascospores with a narrow bipolar sheath at the end. *Pseudopaucispora hyalinospora* differs from *P. brunneospora* in having larger ascomata (475–510 µm high, 350–400 µm diam. vs 210–300 µm high, 215–355 µm diam.), a thicker peridium (30–58 vs 15–18 µm) and larger asci (110 × 15.8 vs 75.0 × 8.7 µm) and ascospores (38 × 7.3 vs 15.3 × 4.0; l/w 5.2 vs 3.8) (Hashimoto et al. 2018). *Pseudopaucispora brunneospora* is characterized by brown ascospores in contrast to the hyaline spores in *P. hyalinospora* (Hashimoto et al. 2018). Phylogenetic analysis of combined LSU, SSU and TEF1 sequence data revealed that *P. hyalinospora* strain MFLUCC 18–0360 clusters with *P. brunneospora* with high statistical support (91 % ML, 1.00 PP; Fig. 10). Hence, we introduce *P. hyalinospora* isolated from dead branches as a new species.

### Massarinaceae Munk

Munk (1956) introduced Massarinaceae typified by *Massarina* Sacc. with *M. eburnea* (Tul. & C. Tul.) Sacc. as the type species. *Byssothecium* Fuckel, *Helminthosporiella* Hern.-Restr., Sarria & Crous, *Helminthosporium* Link, *Massarina* Sacc., *Pseudodidymosphaeria* Thambug. & K.D. Hyde, *Pseudosplanchnonema* Chethana & K.D. Hyde, *Semifissispora* H.J. Swart, *Stagonospora* (Sacc.) Sacc and *Suttonomyces* Wijayaw., Camporesi & K.D. Hyde are accepted in Massarinaceae (Wijayawardene et al. 2020). In this study, we introduce a new species of *Stagonospora*.

### *Stagonospora* (Sacc.) Sacc.

*Stagonospora* is typified by *S. paludosa* (Sacc. & Speg.) Sacc., a species isolated from *Carex pseudocyperus*. Quaedvlieg et al. (2013) re-evaluated septoria-like genera and introduced *Stagonospora sensu stricto* in Massarinaceae due to pycnidial, immersed, globose, ostiolate conidiomata, conidiophores reduced to holoblastic conidiogenous cells with percurrent proliferations, and doliiform, cylindrical to ellipsoid, hyaline, guttulate conidia. Tanaka et al. (2015) revised Massarinaceae and accepted 12 species in *Stagonospora* based on both morphology and phylogeny data.

### *Stagonospora poaceicola* Tennakoon, Phookamsak R & K.D. Hyde, sp. nov.

Fig. 13

Index Fungorum number: IF557371; Facesoffungi number: FoF07748;

Etymology – Name reflects the host family (Poaceae) of the new species.

Holotype – MFLU 17-0769

*Saprobic* on dead stems of grasses. Sexual morph: *Ascomata* 170–220 × 160–190 µm diam. ( $\bar{x}$  = 197 × 177 µm, n = 8), solitary or aggregated, semi-immersed to erumpent, elongate, uniloculate, subglobose or obpyriform, coriaceous, black, ostiolate. *Peridium* 20–25 µm wide composed of 3–4 layers of thin-walled, lightly pigmented to dark brown, somewhat flattened cells of *textura angularis*. *Hamathecium* composed of dense, 1.8–2.5 µm wide, filamentous, distinctly septate, broad, cellular pseudoparaphyses, slightly constricted at the septum, anastomosing at the apex, embedded in a hyaline gelatinous matrix. *Asci* (65–)70–110(–115) × (12–)14–21(–23) µm ( $\bar{x}$  = 89 × 17 µm, n = 35), 8-spored, bitunicate, fissitunicate, clavate, short pedicellate (7–17.5 µm long), apically rounded with a shallow ocular chamber. *Ascospores* 21–28(–30) × 4.5–6.5 µm ( $\bar{x}$  = 24.4 × 5.5 µm, n = 35), overlapping, uniseriate to biseriate or triseriate, hyaline, narrowly fusiform,

2–3-septate, slightly constricted at the middle septum, straight to curved, with or without guttules, smooth-walled, without a sheath. Asexual morph: Undetermined.

Material examined – CHINA, Yunnan Province, Xishuangbanna, Nabanhe, on dead stems of grass sp. (Poaceae), 25 November 2015, D.S. Tennakoon, KIB 029 (MFLU 17-0769, holotype; KUN-HKAS 96342, isotype).

GenBank Accessions – ITS: MT199603, LSU: MT199604, SSU: MT199602, TEF1: MT199325.

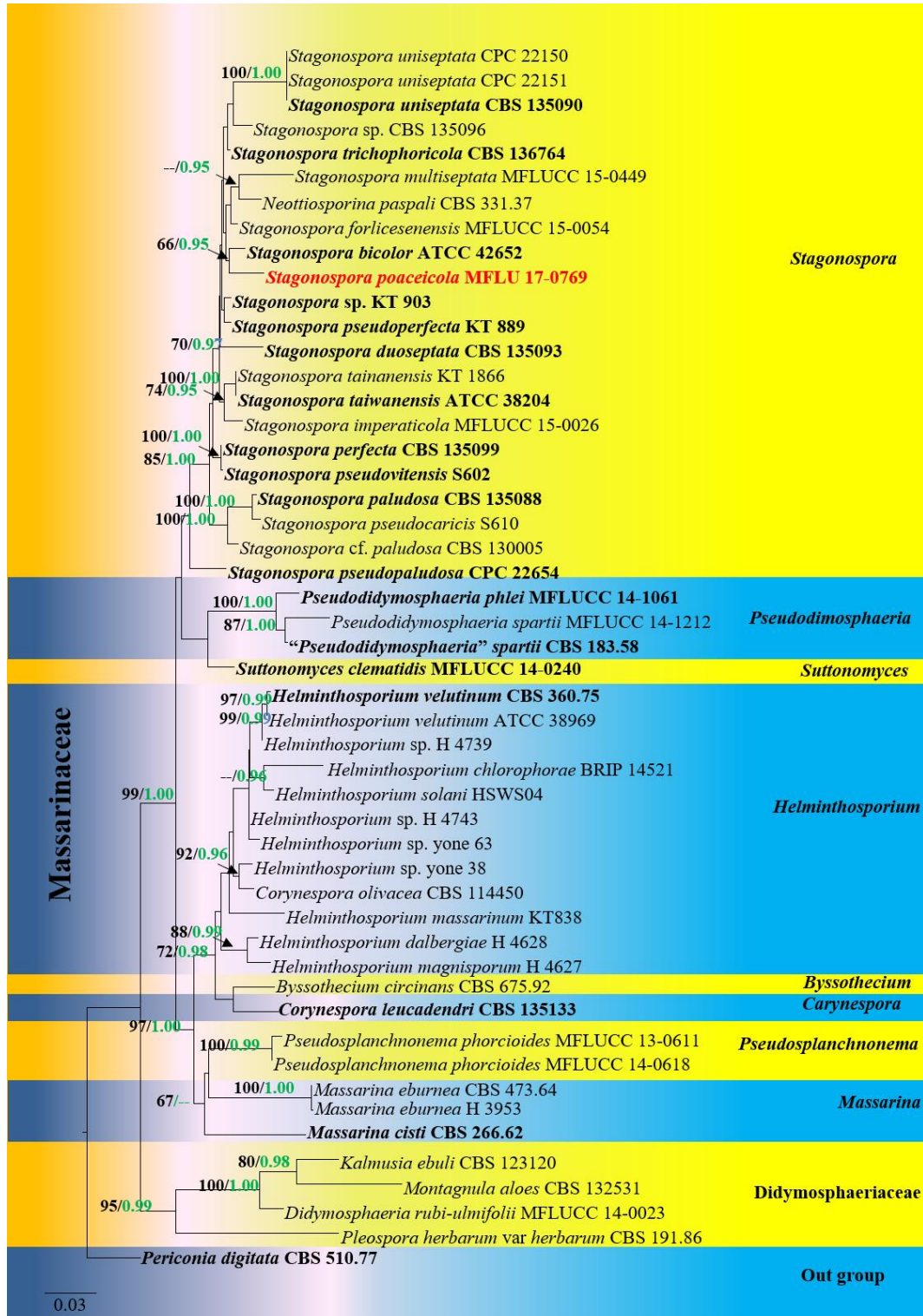


**Figure 12** – Maximum likelihood analysis with 1000 bootstrap replicates yielded a best tree with the likelihood value of -14639.631854. The combined LSU, SSU, ITS and TEF1 sequence dataset

comprised 50 strains with *Periconia digitata* (CBS 510.77) as the outgroup taxon. Tree topology of the ML analysis was similar to the BI. The matrix had 898 distinct alignment patterns, with 39.41 % of undetermined characters or gaps. Estimated base frequencies were as follows; A = 0.239744, C = 0.237635, G = 0.270639, T = 0.251148; substitution rates AC = 1.597454, AG = 2.732638, AT = 1.893531, CG = 1.067351, CT = 8.759818, GT = 1.000000; gamma distribution shape parameter  $\alpha = 0.486600$ . Maximum likelihood bootstrap (ML, black) values equal to or greater than 60% and Bayesian posterior probabilities (PP, green) equal to or greater than 0.90% are given above the nodes. The scale bar indicates 0.03 changes. The ex-type strains are in black bold and new isolates are in red bold.

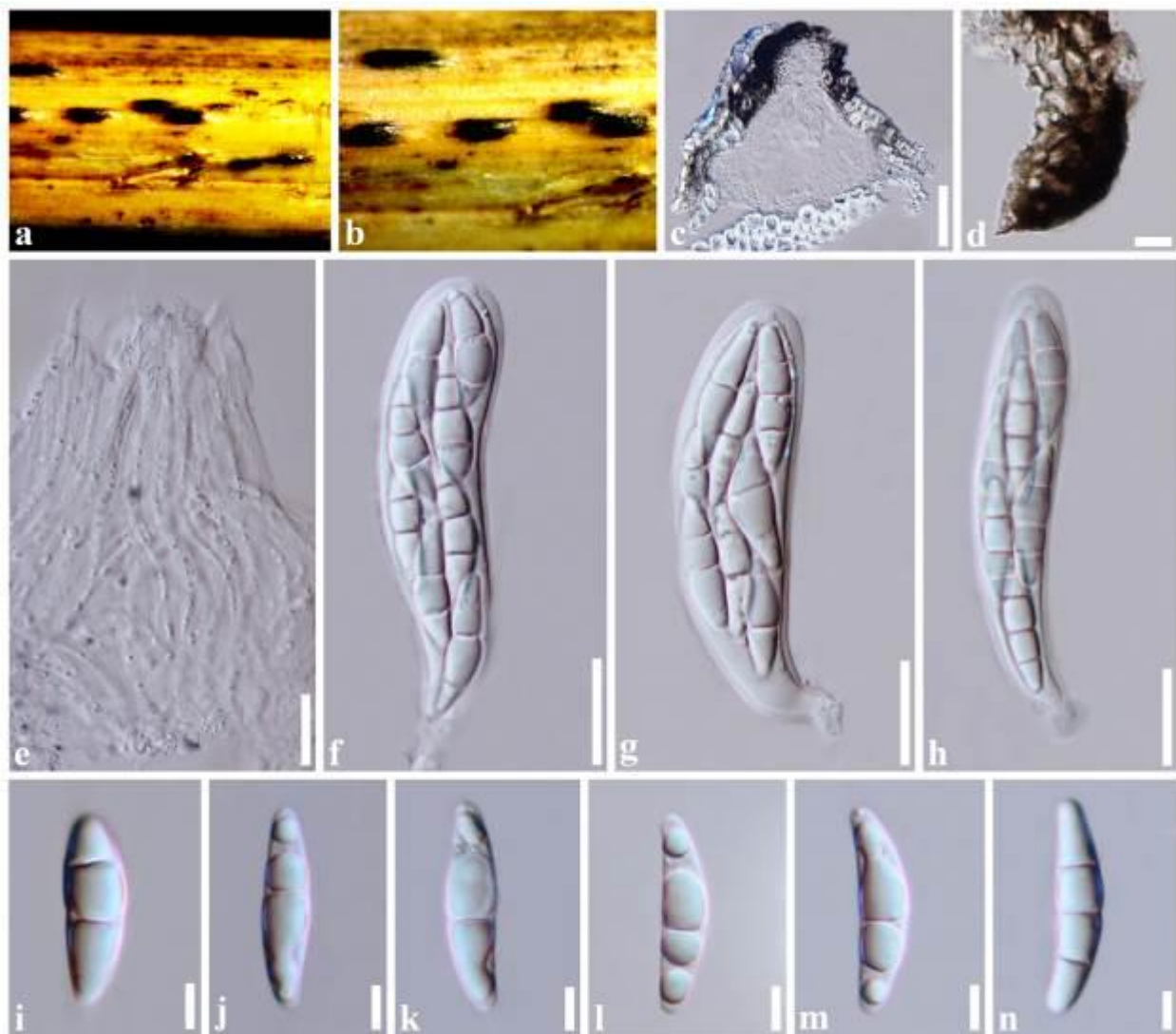


**Figure 13** – *Stagonospora poaeicola* (MFLU 17-0769, holotype). a Appearance of ascomata on host. b Close-up of ascomata. c Section of an ascoma. d Section of peridium. e Pseudoparaphyses. f–h Asci. i–n Ascospores. Scale bars: c = 50  $\mu\text{m}$ , d = 10  $\mu\text{m}$ , e–h = 20  $\mu\text{m}$ , i–n = 5  $\mu\text{m}$ .

Notes – *Stagonospora poaeicola* shares similar morphological characteristics to *S. perfecta* Quaedvl., Verkley & Crous and *S. pseudoperfecta* Kaz. Tanaka & K. Hiray. in having short pedicellate asci and hyaline, fusiform, straight to curved ascospores. However, *S. perfecta* and *S. pseudoperfecta* differs from *S. poaeicola* by having ascospores with clear sub-median septum surrounded by a mucilaginous sheath (Tanaka et al. 2015). Furthermore, *S. poaeicola* has semi-immersed to erumpent ascomata, whereas *S. perfecta* and *S. pseudoperfecta* have immersed

ascomata. According to the combined multi-gene phylogeny (LSU, SSU, ITS and TEF1), *S. poaceicola* grouped with other *Stagonospora* species and shows a closer affinity to *S. bicolor* (Fig. 12). However, *S. bicolor* (D. Hawksw., W.J. Kaiser & Ndimande) Kaz. Tanaka & K. Hiray. can be distinguished from *S. poaceicola* by having melanized ascospores. These ascospores appeared to be released in a hyaline or very pale brown stage with 1–3 septa, but later the upper central cell in the 3-septate spores slightly inflated and can become dark brown to almost black at maturity (Eriksson & Hawksworth 2003).

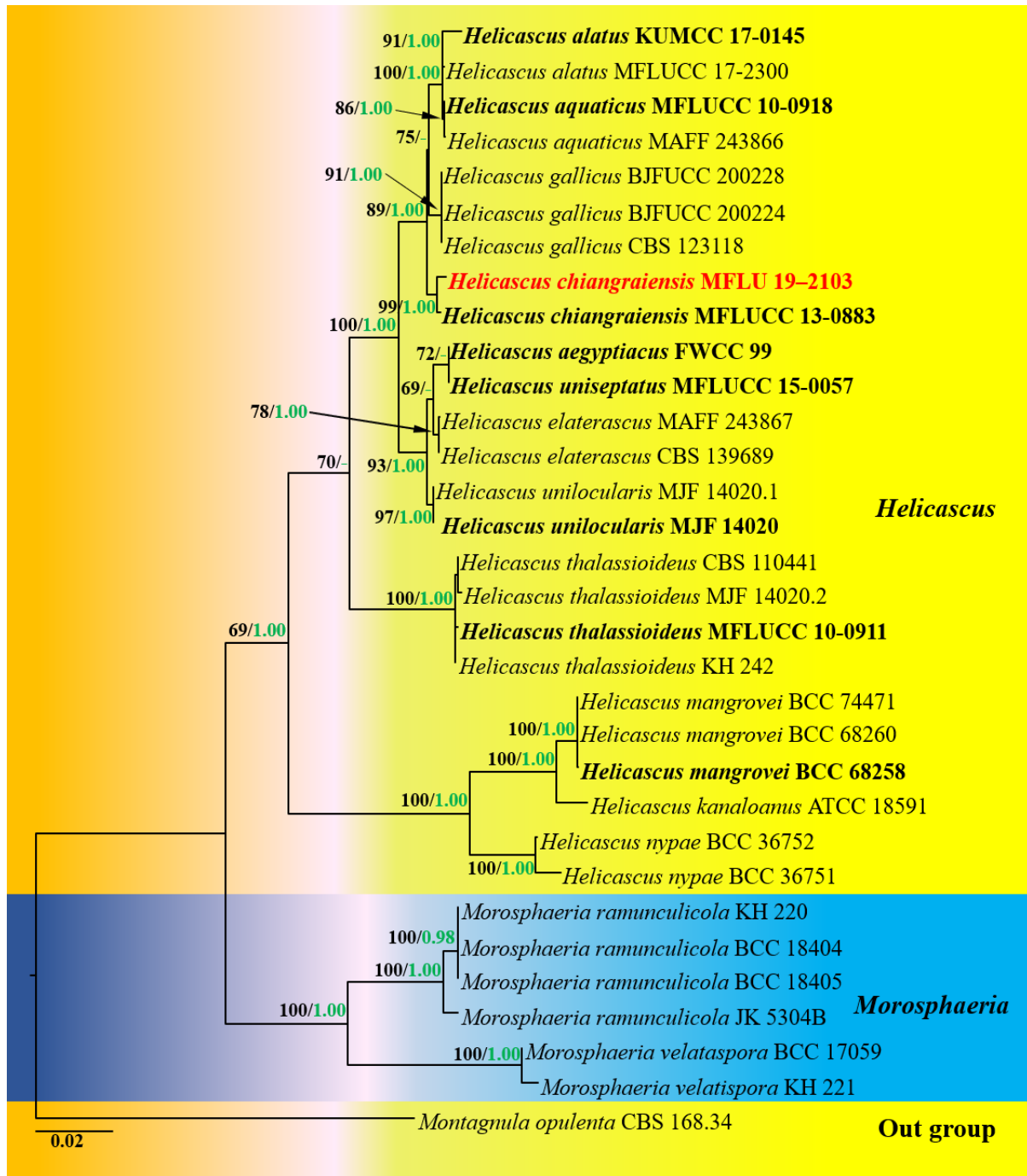


**Figure 14** – Maximum likelihood analysis with 1000 bootstrap replicates yielded a best tree with the likelihood value of -14639.631854. The combined LSU, SSU, ITS and TEF1 sequence dataset comprised 32 strains with *Montagnula opulenta* (CBS 168.34) as the outgroup taxon. Tree topology of the ML analysis was similar to the BI analysis. The matrix had 898 distinct alignment patterns, with 39.41 % of undetermined characters or gaps. Estimated base frequencies were as follows; A = 0.250353, C = 0.237635, G = 0.270639, T = 0.251148; substitution rates AC =

1.597454, AG = 2.732638, AT = 1.893531, CG = 1.067351, CT = 8.759818, GT = 1.000000; gamma distribution shape parameter  $\alpha = 0.486600$ . Maximum likelihood bootstrap (ML, black) values equal to or greater than 65% and Bayesian posterior probabilities (PP, green) equal to or greater than 0.95 PP are given above the nodes. The scale bar indicates 0.02 changes. The ex-type strains are in black bold and new isolate is in red bold.

### **Morosphaeriaceae** Suetrong et al.

Morosphaeriaceae was introduced by Suetrong et al. (2009) in Pleosporales to accommodate *Massarina ramunculicola* K.D. Hyde and *M. velatispora* K.D. Hyde & Borse, which did not group in Massarinaceae in their phylogenetic analyses. Morosphaeriaceae includes four genera, namely: *Aquilomyces* D.G. Knapp, Kovács, J.Z. Groenew. & Crous, *Clypeolocus* Kaz. Tanaka & K. Hiray., *Helicascus* Kohlm. and *Morosphaeria* Suetrong et al. (Jones et al. 2015, 2019, Wijayawardene et al. 2017).

### **Helicascus** Kohlm.

*Helicascus* was established by Kohlmeyer (1969) and is typified by *H. kanaloanus* Kohlm. (Kohlmeyer 1969). This genus includes 11 species (Wijayawardene et al. 2017, 2018, Zeng et al. 2018). *Helicascus* is characterized by immersed ascostromata comprising several locules that share a common periphysate ostiole lying under a more or less conspicuous pseudostromatic tissue or solitary to clustered unilocular ascostromata, which may be immersed to almost superficial and septate ascospores with or without a mucilaginous sheath (Kohlmeyer 1969). *Helicascus* species have been reported from Australia, Brunei, Chile, China, Egypt, France, Philippines, South Africa, Thailand and the USA associated with freshwater habitats (Kohlmeyer 1969, Hyde 1991, Hyde et al. 1998, Cai et al. 2002, 2003, Zhang et al. 2013, 2014, Luo et al. 2016, Preedanon et al. 2017).

### **Helicascus chiangraiensis** Z.L. Luo, J.K Liu, H.Y. Su & K.D. Hyde

Fig. 15

Index Fungorum number: IF552003; Facesoffungi number: FoF02019

*Saprobic* on dead wood, submerged in freshwater. Sexual morph: *Ascomata* 200–290  $\mu\text{m}$  diam, 250–400  $\mu\text{m}$  high ( $\bar{x} = 250 \times 325 \mu\text{m}$ ,  $n = 5$ ), solitary, scattered, black, immersed, unilocular, globose to subglobose, ostiolate. *Peridium* 34–52  $\mu\text{m}$ , subhyaline to dark brown, composed of several layers of pseudoparenchymatous cells, outer layer dark brown, with thick-walled cells, arranged in a *textura angularis*, inner layer hyaline with flattened, thin-walled cells. *Hamathecium* composed of 1.8–2.4  $\mu\text{m}$  ( $\bar{x} = 2.1 \mu\text{m}$ ,  $n = 20$ ) wide, septate, hypha-like pseudoparaphyses, slightly constricted at the septa, embedded in a gelatinous matrix. *Asci* 78–110  $\times$  13–20  $\mu\text{m}$  ( $\bar{x} = 93.5 \times 16.9 \mu\text{m}$ ,  $n = 20$ ), 8-spored, bitunicate, fissionate, clavate, apically rounded, dehiscent, endoascus narrow, coiled within ectoascus, ectoascus forming a long tail-like extension. *Ascospores* 19.5–32  $\times$  5.5–8.7  $\mu\text{m}$  ( $\bar{x} = 26.6 \times 7.5 \mu\text{m}$ ,  $n = 20$ ), uni to bi-seriate and partially overlapping, ellipsoid-fusiform, verruculose, upper end narrowly rounded, lower end tapering, slightly curved in side view, with 2–4 large refractive guttules, 1-euseptate, septum submedian, hyaline when young, becoming brown when mature, thick-walled, verruculose, slightly constricted at the septum, surrounded by a 2.9–5.2  $\mu\text{m}$  ( $\bar{x} = 4.1 \mu\text{m}$ ,  $n = 10$ ) wide sheath. Asexual morph: Undetermined.

Culture characteristics – Ascospores becoming blackish brown and germinating on PDA within 15 h. Colonies on PDA reaching 13–15 mm diam. after one week at 25°C, circular, undulate margin, smooth and effuse surface, yellowish white, reverse yellowish brown.

Material examined – CHINA, Guizhou Province, Guiyang City, Tongxin, Yan Lou, on dead wood submerged in an inland tank, 17 June 2018, M.C. Samarakoon, SAMC160 (MFLU 19–2103; HKAS 102391), living culture MFLUCC 20–0092.

GenBank Accessions – ITS: MT425059; LSU: MT435500, SSU: MT435503, TEF1: MT462701

Notes – *Helicascus chiangraiensis* was introduced by Luo et al. (2016) on decaying wood submerged in a pond from northern Thailand. The species is characterized by unilocular ascomata, coiling asci and verruculose ascospores with a mucilaginous sheath. The specimen in this study

(MFLU 19–2103) is similar to *H. chiangraiensis*. In addition, the molecular analysis showed that our strain clusters with *H. chiangraiensis* with high statistical support (99 % ML, 1.00 PP; Fig. 14). The base pairs comparisons of LSU and TEF1 sequences also show 100 % similarity among MFLU 15–0084 and MFLU 19–2103. Our isolate (MFLU 19–2103) is the first record of *H. chiangraiensis* from China.



**Figure 15** – *Helicascus chiangraiensis* (MFLU 19–2103). a–c Ascomata on the substrate. d Cross section of ascoma. e Section of the peridium. f Pseudoparaphyses. g–i Asci. j–o Ascospores (o in Indian ink). p Verruculose ascospores. Culture grow on PDA q. upper side, r. reverse side. Scale bars: a = 1 cm, b = 1000 μm, c = 500 μm, d = 100 μm, e, h, i = 20 μm, g, j–p = 10 μm, f = 5 μm.

#### Phaeosphaeriaceae M.E. Barr

Barr (1979) introduced Phaeosphaeriaceae which comprises 83 genera (Phookamsak et al. 2014, 2017, 2019, Wijayawardene et al. 2014, 2017a, 2018a, b, Hyde et al. 2016, Yang et al. 2019,

Bakhshi et al. 2019, Maharachchikumbura et al. 2019, Marin-Felix et al. 2019, Hongsanan et al. 2020). Species in this family are often necrotrophic pathogens or saprobes on plants (Shoemaker & Babcock 1992, Carson 2005, Stukenbrock et al. 2006, Cannon & Kirk 2007, Tibpromma et al. 2017).

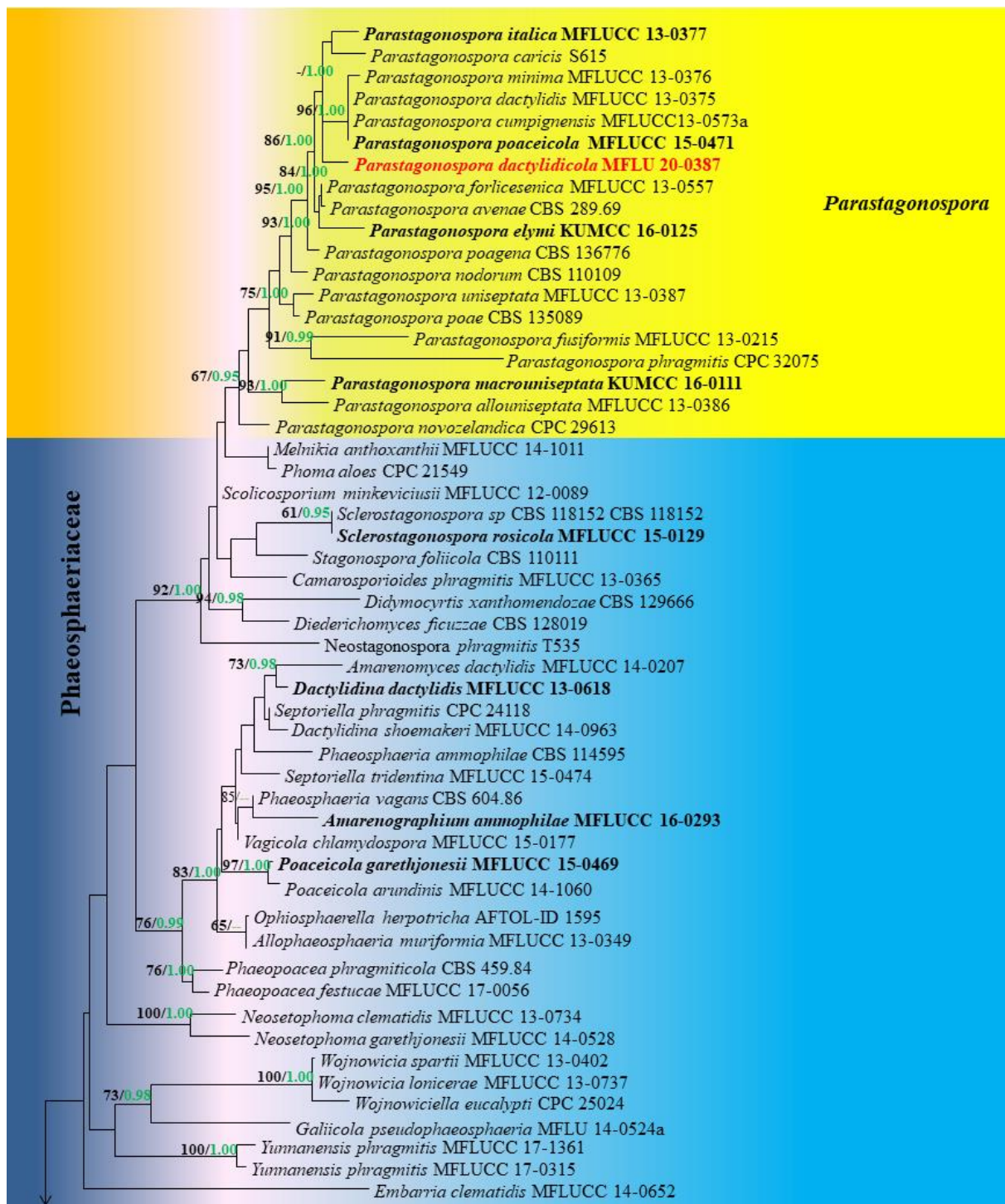


**Figure 16** – Maximum likelihood analysis with 1000 bootstrap replicates yielded a best tree with the likelihood value of -25654.433343. The combined LSU, SSU and ITS sequence dataset comprised 117 strains of *Phaeosphaeriaceae* with *Staurosphaeria rhamnicola* (MFLUCC 17-0813) and (MFLUCC 17-0814) as the outgroup taxa. Tree topology of the ML analysis was similar to the BI analysis. The matrix had 1059 distinct alignment patterns, with 29.42% of undetermined characters or gaps. Estimated base frequencies were as follows; A = 0.244002, C = 0.232592, G = 0.265733, T = 0.257673; substitution rates AC = 1.239463, AG = 3.249856, AT = 2.647426, CG =

0.669460, CT = 7.008165, GT = 1.000000; gamma distribution shape parameter  $\alpha = 0.610808$ . Maximum likelihood bootstrap (ML, black) values equal to or greater than 65% and Bayesian posterior probabilities (PP, green) equal to or greater than 0.95 PP are given above the nodes. The scale bar indicates 0.02 changes. The ex-type strains are in black bold and new isolates are in red bold.

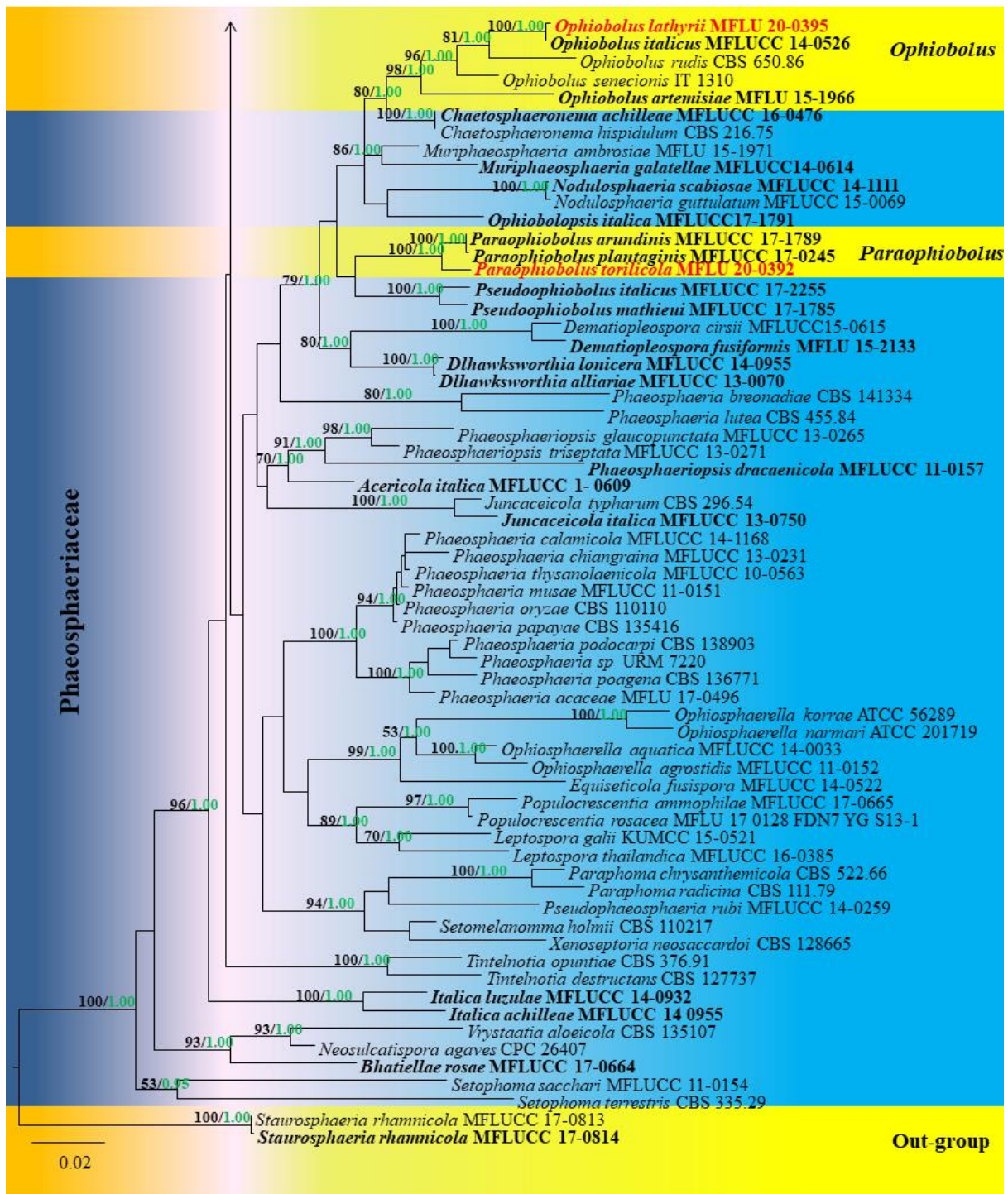


Figure 16 – Continued.

*Parastagonospora* Quaedvl., Verkley & Crous, Stud. Mycol. 75: 362 (2013)

*Parastagonospora* is characterized by immersed ascomata with slightly papillate ostioles, bitunicate, short pedicellate asci, fusoid, subhyaline to pale brown, septate ascospores and coelomycetous asexual morphs with hyaline, cylindrical, granular to multi-guttulate, transversely



euseptate conidia (Quaedvlieg et al. 2013, Li et al. 2015). Quaedvlieg et al. (2013) introduced this genus to accommodate several serious cereal-pathogens that were previously placed in either *Septoria/Stagonospora* or *Leptosphaeria/Phaeosphaeria*.

***Parastagonospora dactylidicola*** Brahmanage, Camporesi & K.D. Hyde, sp. nov.

Fig. 17

Index Fungorum number: IF557589; Facesoffungi number: FoF 08011

Entomology: Epithet refers to the host genus *Dactylis* of the new species.

Holotype – MFLU 20-0387

*Saprobic* on dead aerial stems of *Dactylis glomerata*. Sexual morph: Undetermined. Asexual morph: *Conidiomata* 100–110 × 85–115 μm ( $\bar{x}$  = 105 × 100 μm, n = 5), pycnidial, brown to black, erumpent or immersed to semi-immersed, globose to subglobose, ampulliform, or obpyriform, with central papillate ostiole. *Pycnidial wall* 35–10 μm wide, composed of outer layers of brown to dark brown cells and inner layers of hyaline cells of *textura angularis*. *Conidiophores* reduced to conidiogenous cells. *Conidiogenous cells* phialidic, hyaline, smooth-walled, aggregated, lining the inner cavity, ampulliform to subcylindrical, broadly cylindrical or broadly conical, with percurrent proliferation near apex. *Conidia* 7.5–10 × 2.5–3.5 μm ( $\bar{x}$  = 8 × 3 μm, n = 30), hyaline or subhyaline, smooth-walled, thin- or thick-walled, ellipsoid to oblong, or subcylindrical, multi-guttulate, with obtuse or subobtuse apex, straight to gently curved, transversely 1-septate, sometimes constricted at the septa.

Material examined – ITALY, Province of Forlì-Cesena [FC], San Lorenzo in Noceto, on dead aerial stems of *Dactylis glomerata* (Poaceae), 6 April 2015, E. Camporesi, IT 2433 (MFLU 20-0387, holotype; JZBH3460001, isotype).

GenBank Accessions – LSU: MT370430, ITS: MT370412

Notes – *Parastagonospora dactylidicola* is similar to stagonospora-like asexual morph. Phylogeny based on LSU and ITS sequence analyses shows that *P. dactylidicola* forms a separate lineage basal to a clade comprising *Parastagonospora campignensis*, *P. dactylidis*, *P. minima*, *P. poaceicola* (MFLUCC 15-0471) (Fig. 16). However, *P. dactylidicola* can be distinguished from *P. dactylidis* and *P. minima* based on conidial morphology. *Parastagonospora dactylidicola* has cylindrical to subcylindrical or fusiform conidia with narrow ends, while *P. dactylidis* has fusiform conidia with a slightly narrower base, and distinctly granular cytoplasm, whereas *P. minima* has subcylindrical conidia which are wider in the basal half, and narrow at the apex (Ghaderi & Razavi 2018). In addition, the conidia of *P. dactylidicola* are smaller (7.5–10 × 2.5–3.5 μm) than that of *P. dactylidis* and *P. minima*. However, *P. campignensis* is known only from its asexual morph. Base pair differences of ITS gene region of the novel species to *P. campignensis*, *P. dactylidis* and *P. minima* are 4.7% (24 bp out of 506 bp, without gaps), 4.5% (23 bp out of 505 bp, without gaps) and 4.4% (22 bp out of 492 bp, without gaps) respectively.

### ***Ophiobolus*** Reiss

*Ophiobolus* was established based on the type species *O. phiobolus disseminans* by Reiss (1854). Species in *Ophiobolus* are characterized by ascomata with a long cylindrical erumpent beak lined with hyaline periphyses, cylindrical to cylindrical-clavate asci usually in linear fascicles, and tetraseriate, multiseptate, phragmosporous to scolecosporous, elliptical to fusiform ascospores, sometimes bearing globose appendages at each end, sometimes with band-like or cushion-shaped appendages near the first-formed septum (Shoemaker & Babcock 1989, Phookamsak et al. 2014, 2017). Phookamsak et al. (2017) reported a polyphyletic nature of *Ophiobolus*-like fungi in Phaeosphaeriaceae. The type, *Ophiobolus disseminans*, showed close phylogenetic affinities with species of *Entodesmium* and *Premilcurensis* species. Those species were synonymized under *Ophiobolus* (Phookamsak et al. 2017).

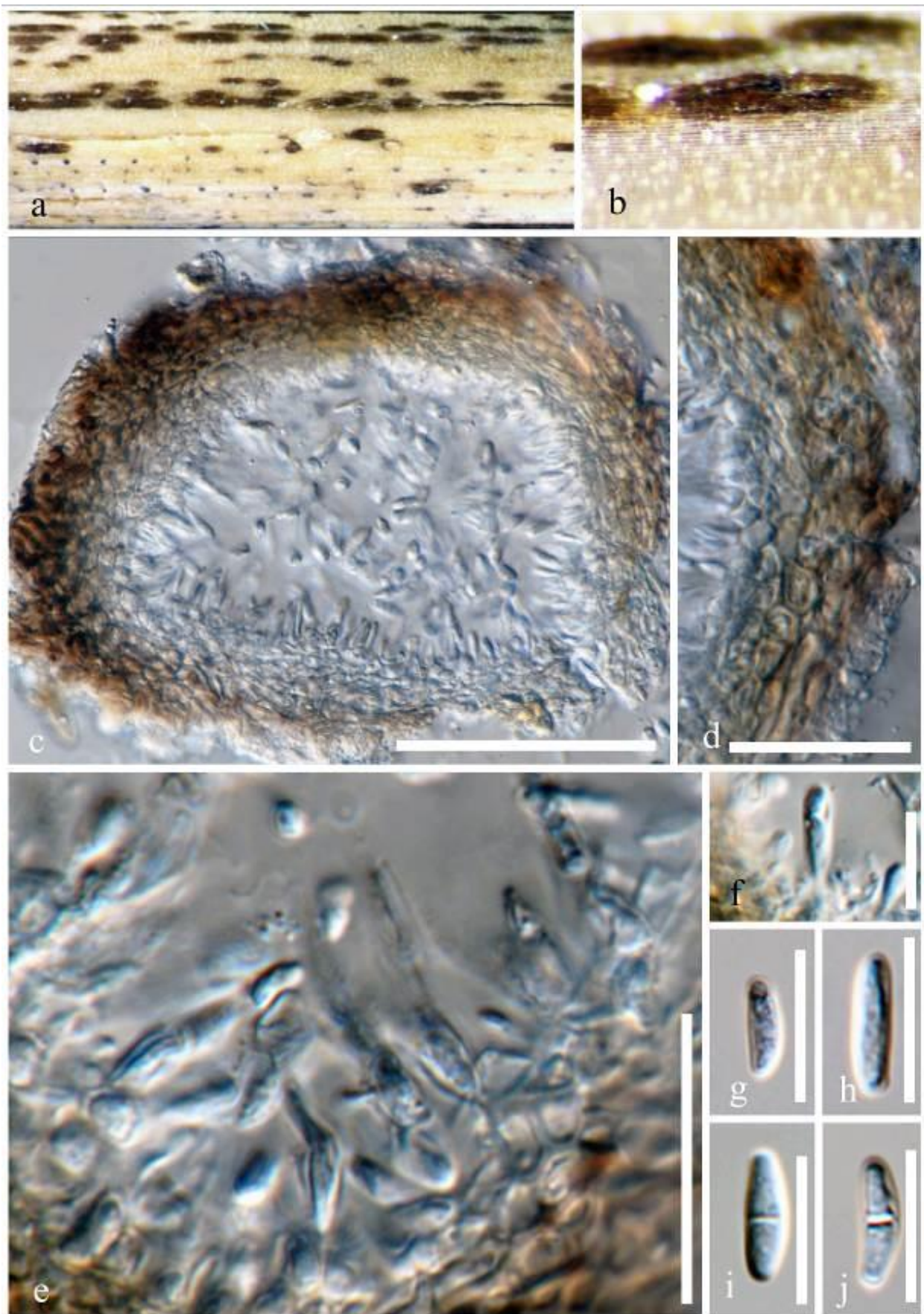


**Figure 17** – *Parastagonospora dactylidicola* (MFLU 20-0387, holotype). a, b Conidiomata on host surface. c Vertical section through a conidioma. d Pycnidial wall. e, f Developing conidia. g–j Conidia. Scale bars: c = 50 µm, d, e = 20 µm, f–j = 10 µm.

***Ophiobolus lathyri*** Brahmanage, Camporesi & K.D. Hyde, sp. nov.

Fig. 18

Index Fungorum number: IF557591; Facesoffungi number: FoF 08012

Etymology – Epithet refers to the host genus *Lathyrus* of the new species.

Holotype – MFLU 20-0395

*Saprobic* on dead aerial stem of *Lathyrus* sp. Sexual morph: *Ascomata* 730–990 µm high, 430–560 µm diam. ( $\bar{x}$  = 465 × 500 µm, n = 5), immersed to slightly erumpent, scattered beneath the host periderm or on decorticated wood, visible as small black dots on the host surface, ampulliform, solitary, ostiolate. *Ostiole* central, inconspicuous at the surface. *Peridium* 120–132 µm wide, comprising an inner layer of hyaline 2–3 elongated cell layers and an outer layer of 3–4 layers, of dark brown, thick-walled cells of *textura angularis*. *Hamathecium* comprising numerous, 2–3.5 µm wide, filamentous, unbranched, cellular, guttulate pseudoparaphyses. *Asci* 180–325 × 14–18 µm ( $\bar{x}$  = 260 × 16.2 µm, n = 20), 8-spored, bitunicate, fissitunicate, cylindric-clavate, with a pedicel. *Ascospores* 150–175 × 4–6 µm ( $\bar{x}$  = 168 × 5.2 µm, n = 30), overlapping triseriate, hyaline, usually 12-euseptate, not constricted at septa, rounded at the ends, guttulate, smooth-walled, lacking a mucilaginous sheath. Asexual morph: Undetermined.

Material examined – ITALY, Province of Ravenna [RA], Fognano di Brisighella, on a dead aerial stem of *Lathyrus* sp. (Fabaceae), 16 March 2018, E. Camporesi, IT 3782b (MFLU 20-0395, holotype).

GenBank Accessions – LSU: MT370429; SSU: MT370372, ITS: MT893362

Notes – The present molecular analyses indicate that the new strain MFLU 20-0395 clusters in *Ophiobolus* (Fig. 16) and we recognized it as a new species, *Ophiobolus lathyri*. *Ophiobolus lathyri* showed a close phylogenetic affinity to *O. italicus* (Fig. 18). *Ophiobolus lathyri* can be distinguished from *O. italicus* by the ascospore shape and septation. *Ophiobolus lathyri* has filiform, 12-euseptate ascospores, while *O. italicus* has fusiform, 4-septate ascospores (Tibpromma et al. 2017). *Ophiobolus lathyri* can be easily distinguished from *O. rudis* in having relatively longer ascospores (150–175 × 4–6 µm vs 110–120 × 3–4 µm) and 18–20 septate ascospores. Base pair differences of the LSU region of *O. lathyri* to *O. italicus* and *O. rudis* are 0.24% (2 bp out of 818 bp, without gaps) and 0.9% (7 bp out of 796 bp) respectively. ITS base pair differences of *O. lathyri* to *O. italicus* and *O. rudis* are 2.3% (12 bp out of 512 bp, without gaps) and 4.3% (22 bp out of 314 bp, without gaps) which are in recommended range to consider them as different species according to Jeewon & Hyde (2016).

***Paraophiobolus*** Phookamsak, Wanas. & K.D. Hyde

*Paraophiobolus* was introduced by Phookamsak et al. (2017) to accommodate *P. arundinis* Phookamsak, Phookamsak, Wanas., Camporesi & K.D. Hyde and *P. plantaginis* (Qing Tian, Camporesi & K.D. Hyde) Phookamsak Wanas. & K.D. Hyde. We follow the latest treatment and updated account of *Paraophiobolus* in Phookamsak et al. (2017). Here, a novel species *P. torilicola* is introduced based on both morphology and phylogeny data.

***Paraophiobolus torilicola*** Brahmanage, Camporesi & K.D. Hyde, sp. nov.

Fig. 19

Index Fungorum number: IF557590; Facesoffungi number: FoF 08013

Etymology – Epithet refers to the host genus *Torilis* of the new species.

Holotype – MFLU 20-0392

*Saprobic* on dead aerial stems of *Torilis arvensis*. Sexual morph: *Ascomata* 180–310 × 150–200 µm ( $\bar{x}$  = 220 × 180 µm, n = 5), immersed to slightly erumpent through epidermis of host, light brown at base, brown to dark brown towards the apex, scattered, solitary to gregarious, globose to subglobose, uniloculate, glabrous, ostiolate, papillate. *Papilla* 60–75 × 50–70 µm, mammiform to oblong, with rounded to truncate apex, composed of several layers of dark brown to black cells, arranged in a *textura angularis* to *textura prismatica*, glabrous, ostiole central, without periphyses. *Peridium* 16–18 µm wide, thick-walled, outer layer composed of 5–7 layers of brown to dark brown, thick-walled cells, arranged in a *textura angularis*, inner layer composed of 3–4 layers of hyaline, thin-walled cells of *textura angularis*, thicker towards the apex. *Hamathecium* comprising

numerous, 1–2.5  $\mu\text{m}$  wide, broad, branched, septate, cellular pseudoparaphyses, embedded in a gelatinous matrix. *Asci* 45–100  $\times$  4.5–5  $\mu\text{m}$  ( $\bar{x}$  = 65  $\times$  4.8  $\mu\text{m}$ , n = 40), 8-spored, bitunicate, cylindrical to cylindrical-clavate, with short furcate pedicel, apically rounded, ocular chamber clearly visible when immature. *Ascospores* 40–60  $\times$  1–2  $\mu\text{m}$  ( $\bar{x}$  = 78  $\times$  3  $\mu\text{m}$ , n = 30), fasciculate, scolecosporeous, filiform, with rounded ends, tapered towards the lower cells, hyaline to pale yellowish when young, becoming yellowish green at maturity, slightly curved near the apex, with around 11–13 eu-septa, swollen near the base of the 4<sup>th</sup> cell, slightly constricted at the 4<sup>th</sup> septum, not constricted at the other septa, not separating into part spores, smooth-walled, with terminal appendages at the ends. Asexual morph: Undetermined.

Material examined – ITALY, Province of Forlì-Cesena [FC], Voltre – Civitella di Romagna, dead aerial stem of *Torilis arvensis* (Huds.) Link (Apiaceae), 22 January 2018, E. Camporesi, IT 3689 (MFLU 20-0392, holotype; JZBH3460002, isotype).

GenBank Accessions – LSU MT370428, ITS: MT370411

Notes – Multi-gene phylogenetic analyses of combined LSU, SSU and ITS sequence dataset indicate that *Paraophiobolus torilicola* groups with the members of *Paraophiobolus* with high statistical support (100% ML, 1.00 PP) (Fig. 16). *Paraophiobolus torilicola* is phylogenetically closely related to *P. arundinis* and *P. plantaginis*. However, *P. arundinis* is different from *P. torilicola* in having relatively larger ascospores (70–85  $\times$  2.5–3  $\mu\text{m}$  vs 40–60  $\times$  1–2  $\mu\text{m}$ ). *Paraophiobolus plantaginis* is easily distinguished from *P. torilicola* by the number of ascospore septa (5–8 vs 11–13). A synopsis of the host and the morphological characteristics of *Paraophiobolus* species is given in Table 2. Base pair differences of the ITS region of *P. torilicola* with *P. arundinis* and *P. plantaginis* are 1.8% (16 bp out of 899 bp) and 1.7% (15 bp out of 899 bp), respectively.

**Table 2** Synopsis of *Paraophiobolus* species discuss in this study

Species	Hosts	Ascomata ( $\mu\text{m}$ )	Asci ( $\mu\text{m}$ )	Ascospores ( $\mu\text{m}$ )
<i>P. arundinis</i>	<i>Arundo pliniana</i>	170–410 $\times$ 110–400	75–110 $\times$ 7–12	70–85 $\times$ 2.5–3, 12(–16)-septate
<i>P. plantaginis</i>	<i>Plantago</i> sp.	145–205 $\times$ 135–220	69–124 $\times$ 7.4–9.5	50–72 $\times$ 4–6, 5–8-septate
<i>P. torilicola</i>	<i>Torilis arvensis</i>	100–110 $\times$ 102–106	45–100 $\times$ 4.5–5	40–60 $\times$ 1–2, 11–13-septate

## Pleosporaceae

Pleosporaceae was introduced by Nitschke (1869) based on the immersed ascomata and presence of pseudoparaphyses, which was assigned to Sphaeriales. Pleosporaceae species are pathogens or saprobes on wood and dead herbaceous stems or leaves (Sivanesan 1984). The asexual morphs of Pleosporaceae can be hyphomycetes (Hyde et al. 2013, Ariyawansa et al. 2015c). Pleosporaceae comprises 24 genera (Wijayawardene et al. 2020).

## *Alternaria* Nees

Nees (1816) introduced *Alternaria* based on *A. tenuis* as the only species. Later the type specimen of *Torula alternata* Fr. 1832 was identified by Simmons as synonymous with Nees (1816) description of *A. tenuis*; therefore, he declared *A. alternata* as the type for the genus (Simmons 1967). *Alternaria* species can be saprobes or pathogens on vegetation and often found on soil, air, dust and water-damaged buildings (Ellis 1971, Ellis & Sinclair 1976, Runa et al. 2009, Woudenberg et al. 2013, Lawrence et al. 2016). Some species have been described from polypropylene, rubber, fluorine plastics and jet fuel (Sheridan & Soteris 1974, Lugauskas et al. 2003, Al Ghafri et al. 2019). However, the majority of species are pathogens, infecting number of host species, including major greenhouse and field crops such as carrot, cucurbits, date, palm, tomato, tobacco and wheat (Al-Nadabi et al. 2018, Jayawardena et al. 2019a). Other species of *Alternaria* have been reported as food spoilers and postharvest pathogens that contaminate cereals, fruit and nuts (Pitt & Hocking 1997, Andersen & Hollensted 2008, Lawrence et al. 2016, Al Ghafri

et al. 2019).

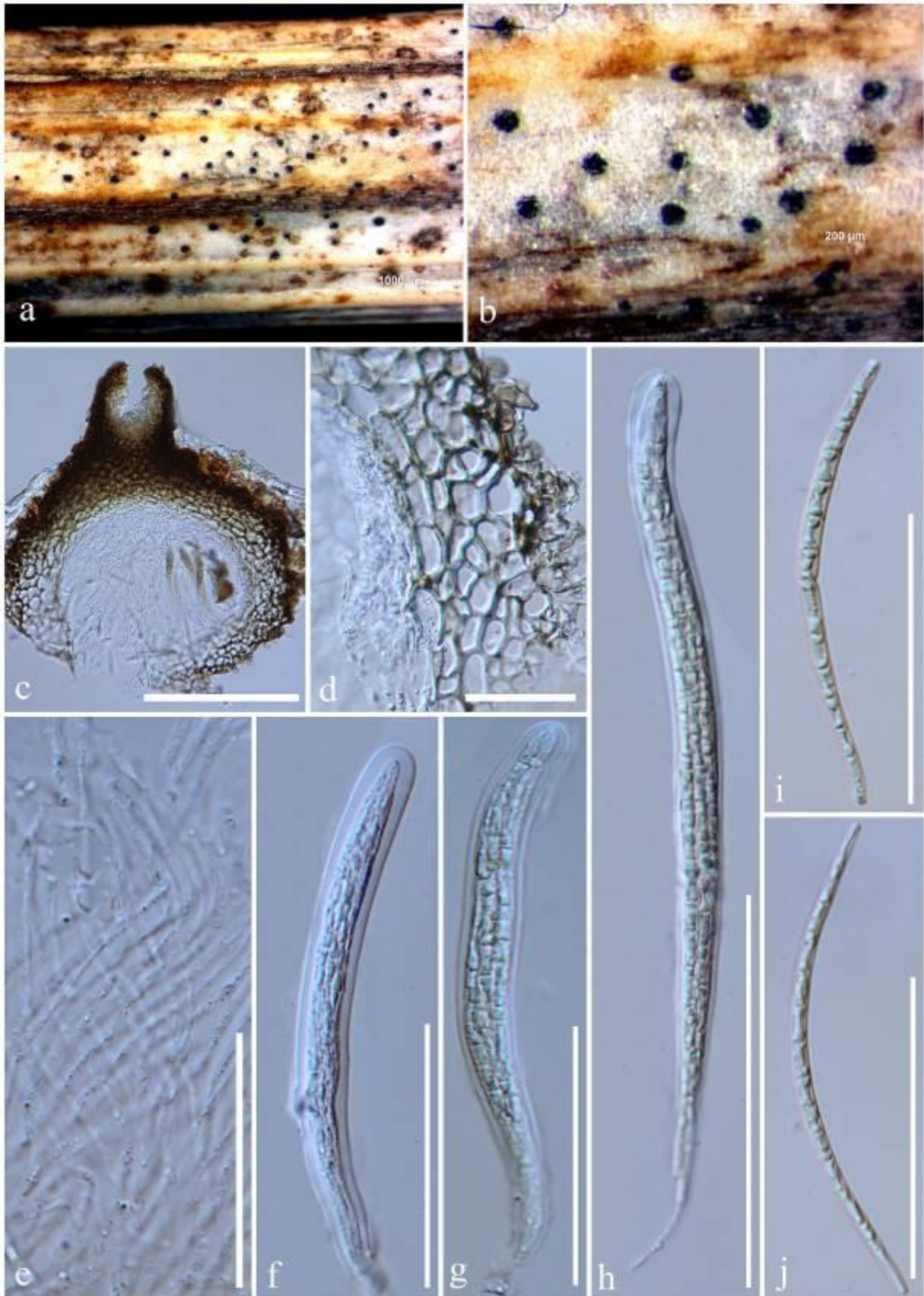


**Figure 18** – *Ophiobolus lathyri* (MFLU 20-0395, holotype). a Appearance of ascomata on host. b Close-up of ascomata. c Section of an ascoma. d Section of peridium. e Pseudoparaphyses. f–h Asci. i, j Ascospores. Scale bars: c = 500  $\mu\text{m}$ , d = 100  $\mu\text{m}$ , f–h = 200  $\mu\text{m}$ , i–j = 100  $\mu\text{m}$ .



**Figure 19** – *Paraophiobolus torilicola* (MFLU 20-0392, holotype). a Appearance of ascomata on host. b Close-up of ascomata c Section of an ascoma. d Section of peridium. e Pseudoparaphyses. f–j Asci. k, l Ascospores. Scale bars: c = 100  $\mu$ m, e–j = 50  $\mu$ m, d, k–l = 20  $\mu$ m.

*Alternaria rumicis* Brahmanage, Camporesi & K.D. Hyde, sp. nov.

Fig. 21

Index Fungorum number: IF557587; Facesoffungi number: FoF 08017

Etymology – Species epithet refers to the host genus *Rumex*, of the new species

Holotype – MFLU 20-0396

*Saprobic* on dead aerial stems. Sexual morph: *Ascomata* 180–250 × 220–260 μm ( $\bar{x}$  = 210 × 250 μm, n = 5), black, solitary to gregarious, semi-immersed to erumpent, base fused with host substrate, globose to subglobose, with broadly to narrowly, oblong and flattened papilla. *Papilla* smooth, ostiolar canal filled with hyaline cells. *Peridium* 30–42 μm wide, slightly thin, thick at the sides and thinner at the base, composed of heavily pigmented, thick-walled cells of *textura angularis*, coriaceous. *Hamathecium* of 1–2 μm wide, cellular, septate, broad, dense pseudoparaphyses. *Asci* 110–150 × 25–35 μm ( $\bar{x}$  = 140 × 30 μm, n = 20), 8-spored, bitunicate, cylindrical to clavate, with short pedicel and minute ocular chamber. *Ascospores* 25–38 × 14–16 μm ( $\bar{x}$  = 35 × 15 μm, n = 30), partially overlapping, uni- to bi-seriate, mostly ellipsoidal, muriform, 3–5 transverse septa with 1 longitudinal septum in the central segments, end cells without septa, brown or pale brown, with a thick sheath. Asexual morph: Undetermined.

Culture characteristics – Conidia germinating on PDA within 14 h and reaching 4 cm diam. in 15 days at 25°C. Colonies growing on PDA, hairy or cottony, white to grey, mycelium superficial, effuse, radially striate, white to grey.

Material examined – ITALY, Province of Forlì-Cesena [FC], Magliano-Forlì, dead aerial stems of *Sinapis alba* (Brassicaceae), 28 April 2018, E. Camporesi, IT 3866 (MFLU 20-0396, holotype; JZBH3180036, isotype), ex-type living culture, JZB3180036; *ibids.*, Collina-Forlì, dead aerial stem of *Dactylis glomerata* (Poaceae), 28 April 2018, E. Camporesi, IT 3683 (MFLU 20-0400; JZBH3180037); Santa Sofia, dead aerial stem of *Rumex* sp. (Polygonaceae), 8 March 2014, E. Camporesi, IT 1758 (MFLU 20-0401; JZBH3180038); Tontola di Predappio, dead aerial stem of *Scabiosa* sp. (Caprifoliaceae), 19 March 2018, E. Camporesi, IT 3803 (MFLU 20-0402; JZBH3180039); Ravenna, Fognano di Brisighella, dead aerial stem of *Lathyrus* sp. (Fabaceae), 16 March 2018, E. Camporesi, IT 3779 (MFLU 20-0403; JZBH3180040).

GenBank Accessions – (MFLU 20-0396) ITS: MT370417; GAPDH: MT994321 (MFLU 20-0400) ITS: MT370416; GAPDH: MT994318; (MFLU 20-0401) ITS: MT370413; GAPDH: MT729647; (MFLU 20-0402) ITS: MT370415; GAPDH: MT994320; (MFLU 20-0403) ITS: MT370414; GAPDH: MT994319 Notes – *Alternaria rumicis* is phylogenetically closely related to *A. ventricosa* R.G. Roberts in *Alternaria* section *infectoria* (96% ML, 1.00 PP; Fig. 20). *Alternaria ventricosa* is known only from the sexual morph (Roberts 2007). Base pair differences of *A. rumicis* and *A. ventricosa* for ITS and GAPDH regions are 0.6% (3 bp out of 531 bp) and 1.56% (8 bp out of 519 bp).

### *Comoclathris* Clem.

*Comoclathris* typified by *Comoclathris lanata* Clem., is characterized by ascomata with circular lid-like openings and applanate, reddish-brown to dark reddish-brown, muriform ascospores (Zhang et al. 2012, Ariyawansa et al. 2014, 2015a). Based on phylogenetic analyses *Comoclathris* was accepted in Pleosporaceae (Ariyawansa et al. 2015a, b, Wijayawardene et al. 2017). There are 44 epithets listed in Index Fungorum (2020) under this genus and most of them lack DNA sequence data. In this study we updated the genus with three new species which were collected from Italy.

*Comoclathris europaeae* Brahmanage, Camporesi & K.D. Hyde, sp. nov.

Fig. 23

Index Fungorum number: IF557585, Facesoffungi number: FoF08014

Etymology – Species epithet refers to the host epithet “*Olea europaea*”.

Holotype: MFLU 20-0391

*Saprobic* on dead stems of dead land leaves of *Olea europaea*. Sexual morph: *Ascomata* 240–250 μm × 145–165 μm ( $\bar{x}$  = 245 × 150 μm, n = 5), solitary, scattered, semi-immersed to slightly erumpent, dark brown to black, globose to subglobose, without a distinct ostiole.

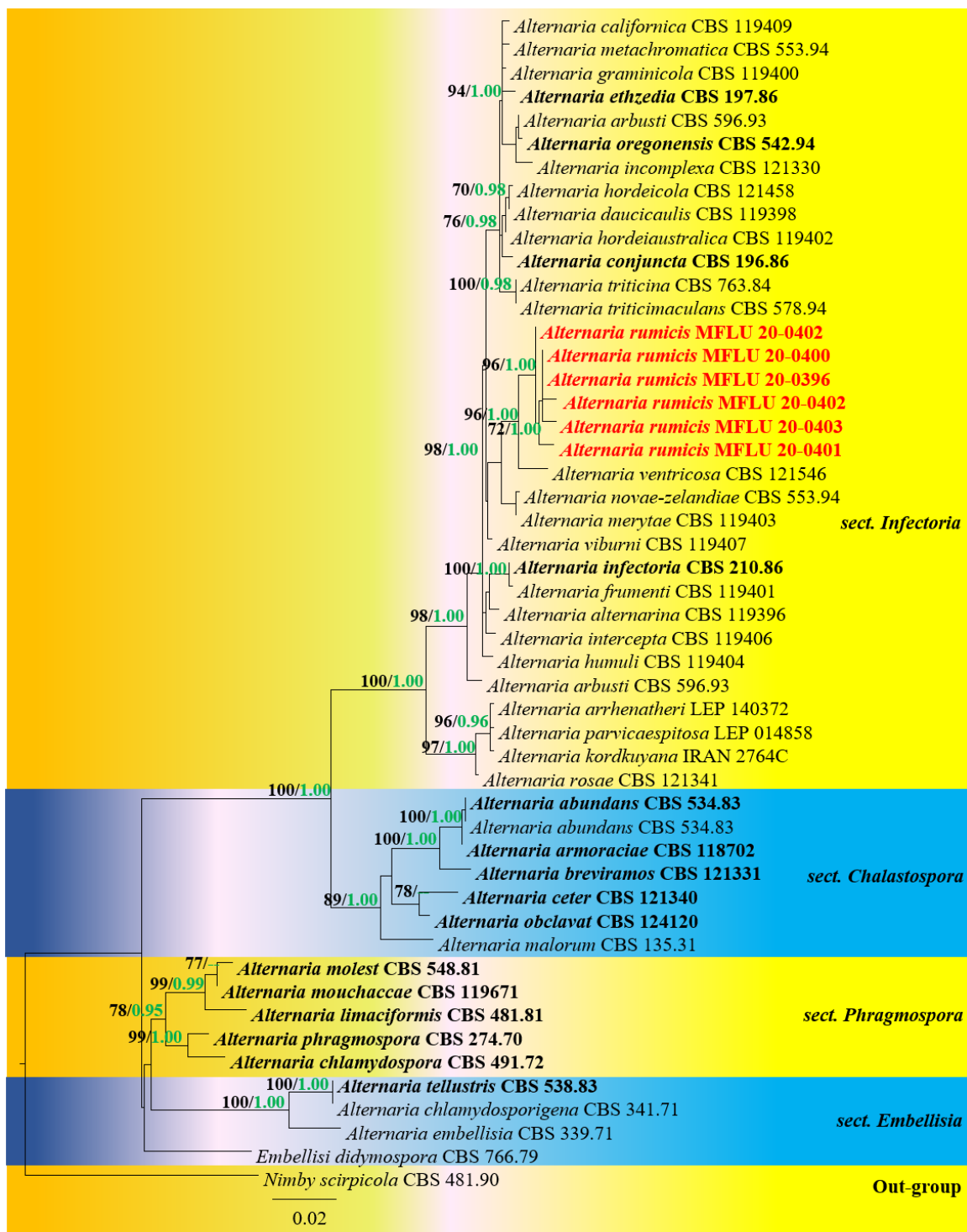


**Figure 20** – Maximum likelihood analysis with 1000 bootstrap replicates yielded a best tree with the likelihood value of -18854.981529. The combined ITS and GAPDH sequence dataset comprised 50 strains of *Alternaria* with *Nimby scirpicola* (CBS 481.90) as the outgroup taxon. Tree topology of the ML analysis was similar to the BI analysis. The matrix had 764 distinct alignment patterns, with 4.72% of undetermined characters or gaps. Estimated base frequencies were as follows; A = 0.241585, C = 0.261062, G = 0.262479, T = 0.234874; substitution rates AC = 1.843223, AG = 4.648646, AT = 1.463605, CG = 0.917951, CT = 7.866437, GT = 1.000000; gamma distribution shape parameter  $\alpha$  = 0.182190. Maximum likelihood bootstrap (ML, black) values equal to or greater than 65% and Bayesian posterior probabilities (PP, green) equal to or greater than 0.95 PP are given above the nodes. The scale bar indicates 0.02 changes. The ex-type strains are in black bold and new isolates are in red bold.





**Figure 21** – *Alternaria rumicis* (MFLU 20-0396, holotype). a, b Ascomata on host surface. c Vertical section through an ascoma. d Peridium. f-h Asci. i-k Ascospores. l Culture on PDA (upper view). Scale bars: c = 100  $\mu$ m, e-i = 50  $\mu$ m, d, j, k = 20  $\mu$ m.

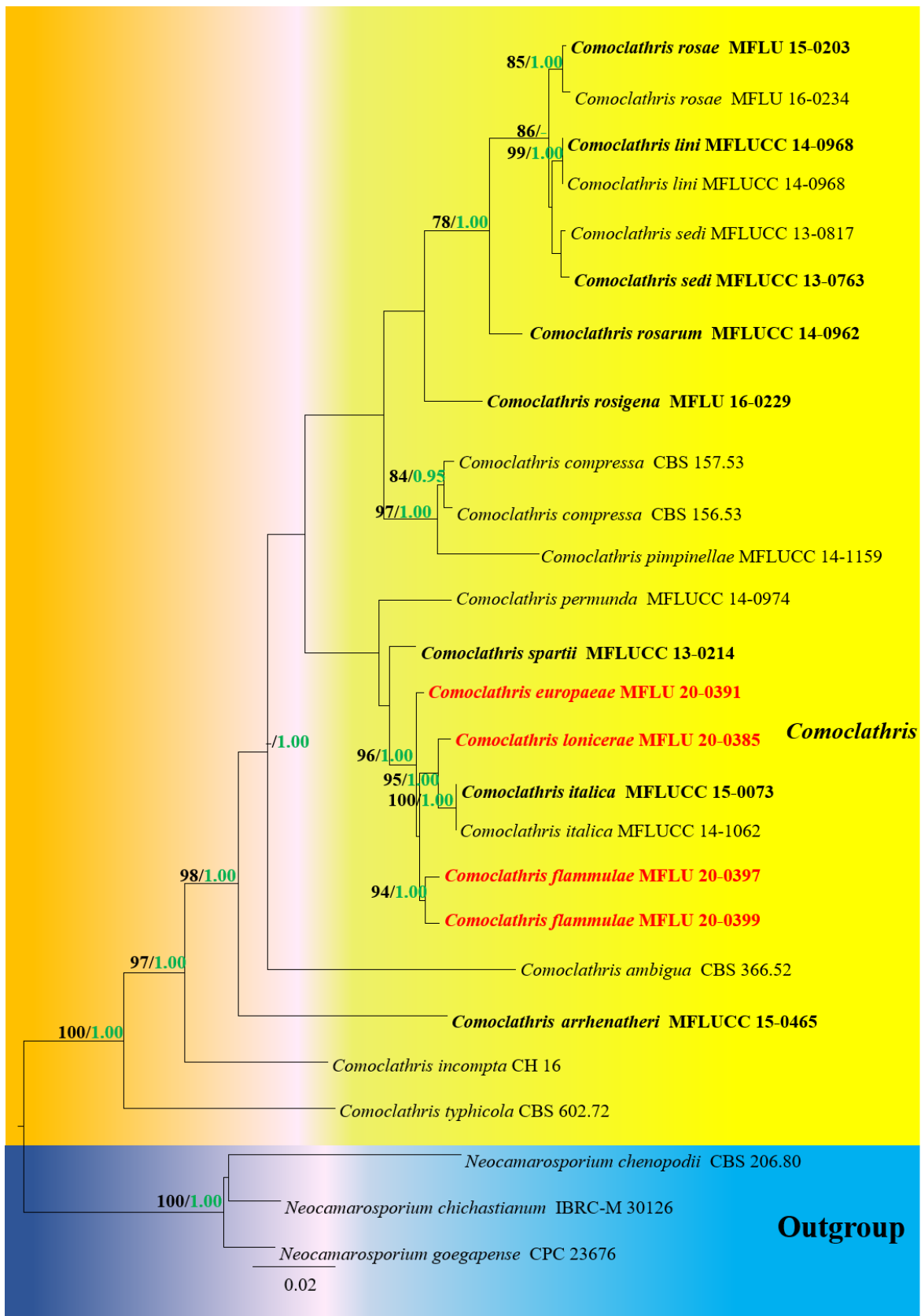


**Figure 22** – Maximum likelihood analyses with 1000 bootstrap replicates yielded a best tree with the likelihood value of -10271.393559. The combined LSU, SSU, ITS and RPB2 sequence dataset comprised 25 strains with *Neocamarosporium chichastianum* (IBRC M 30126), *N. chenopodii* (CBS206.80) and *N. goegapense* (CPC 23676) as the outgroup taxa. Tree topology of the ML analysis was similar to the BI analysis. The matrix had 393 distinct alignment patterns, with 26.53% of undetermined characters or gaps. Estimated base frequencies were as follows; A =

0.250308, C = 0.247190, G = 0.270102, T = 0.232400; substitution rates AC = 2.125141, AG = 4.267562, AT = 1.161328, CG = 0.955650, CT = 7.483498, GT = 1.000000; gamma distribution shape parameter  $\alpha = 0.162915$ . Maximum likelihood bootstrap (ML, black) values equal to or greater than 65% and Bayesian posterior probabilities (PP, green) equal to or greater than 0.95 PP are given above the nodes. The scale bar indicates 0.03 changes. The ex-type strains are in black bold and new isolates are in red bold.

*Peridium* 10–30  $\mu\text{m}$  wide, dark brown to lightly pigmented cells of *textura angularis*. *Hamathecium* composed of 1–1.5  $\mu\text{m}$  diam., hyaline, septate, anastomosed pseudoparaphyses. *Asci* 60–70  $\times$  15–18  $\mu\text{m}$  ( $\bar{x} = 65 \times 16.5 \mu\text{m}$ ,  $n = 10$ ), 8-spored, bitunicate, fissitunicate, cylindro-clavate, pedicellate, apex rounded, with an indistinct ocular chamber. *Ascospores* 20–22  $\times$  11–13  $\mu\text{m}$  ( $\bar{x} = 21 \times 12.8 \mu\text{m}$ ,  $n = 20$ ), uni- to biseriate, partially overlapping, muriform, brown, transversely septate or muriform, with 7 transverse septa, one longitudinal septum at central segments, ellipsoidal to clavate, with acute end at the apex and rounded end at the base, upper half slightly wider and shorter than the lower half cell, constricted at the primary septum, surrounded by a mucilaginous sheath. Asexual morph: Undetermined.

Material examined – ITALY, Province of Forlì-Cesena [FC], Vitignano-Meldola, on dead land leaves of *Olea europaea* (Oleaceae), 20 January 2018, E. Camporesi, IT 3684 (MFLU 20-0391, holotype; JZBH3450002, isotype).

GenBank Accessions – LSU: MT370421; SSU: MT370367; ITS: MT370396; RPB2: MT729650

Notes – *Comoclathris europaeae* is similar to *C. flammulae* and it shows close phylogenetic affinities to *C. lonicerae* (MFLU 20-0385), *C. flammulae* (MFLU 20-0397, MFLU 20-0399) and *C. italica* (MFLUCC 15-0073, MFLUCC 14-1062) with high statistical support (96% ML, 1.00 PP; Fig 22). Their base pair differences within the ITS regions are *C. flammulae* (9/562 (1.60%), no gaps), *C. italica* (5/480 (1.04%), no gaps) and *C. lonicerae* (5/500 (1.00%), no gaps). Base pair differences within the RPB2 region are (7/521 (1.34 %), no gaps), *C. italica* (25/847 (2.95 %)) and *C. lonicerae* (17/869 (1.95%), no gaps). Furthermore, *C. europaeae* has smaller asci (60–70  $\times$  15–18  $\mu\text{m}$ ) than those of *C. lonicerae* (180–192  $\times$  60–74  $\mu\text{m}$ ). *Comoclathris europaeae* has smaller asci (60–70  $\times$  15–18  $\mu\text{m}$ ) and ascospores (20–22  $\times$  11–13  $\mu\text{m}$ ) than those of *C. italica* (asci: 100–120  $\times$  30–35  $\mu\text{m}$  and ascospores: 30–35  $\times$  10–15  $\mu\text{m}$ ).

***Comoclathris flammulae*** Brahmanage, Camporesi & K.D. Hyde, sp. nov.

Fig. 24

Index Fungorum number: IF557584; Facesoffungi number: FoF 08015

Etymology – Species epithet refers to the host species epithet “*flammula*”

Holotype: MFLU 20–0397

*Saprobic* on dead aerial branches of *Clematis flammula* and *Colutea arborescens*. Sexual morph: *Ascomata* 105–130  $\mu\text{m} \times$  80–90  $\mu\text{m}$  ( $\bar{x} = 120 \times 86 \mu\text{m}$ ,  $n = 5$ ), solitary or aggregated, immersed, globose to subglobose, dark brown to black, without a distinct ostiole. *Peridium* 14–30  $\mu\text{m}$  wide, comprising 2–4 layers of dark brown to brown, thick-walled cells of *textura angularis*. *Hamathecium* comprising numerous, 1–1.5  $\mu\text{m}$  wide, septate, pseudoparaphyses. *Asci* 50–55  $\times$  13–17  $\mu\text{m}$  ( $\bar{x} = 52 \times 15 \mu\text{m}$ ,  $n = 10$ ), 8-spored, bitunicate, fissitunicate, cylindric-clavate, short pedicellate, rounded at the apex, with an indistinct ocular chamber. *Ascospores* 16–22  $\times$  10–16  $\mu\text{m}$  ( $\bar{x} = 20 \times 15 \mu\text{m}$ ,  $n = 20$ ), overlapping uni- to bi-seriate, yellowish brown when immature, becoming dark brown at maturity, clavate, with acute ends, muriform, with 6 transverse septa, 1–2 longitudinal septa, upper part is wider than the lower part, smooth, with a thick, hyaline, mucilaginous sheath. Asexual morph: Undetermined.

Material examined – ITALY, Province of Forlì-Cesena [FC], Bonalda-Civitella di Romagna, on dead aerial branches of *Clematis flammula* (Ranunculaceae), 1 June 2018, E. Camporesi, IT 3922 (MFLU 20-0397, holotype; JZBH3450003, isotype); *ibid.*, San Martino-Predappio, dead aerial branch of *Colutea arborescens* (Fabaceae), 23 October 2015, E. Camporesi, 13 (MFLU 20-0399; JZBH3450004).

GenBank Accessions – MFLU 20-0397) LSU: MT370397; SSU: MT370368; ITS: MT370397; RPB2: MT729651, (MFLU 20-0399) LSU: MT370420; SSU: MT370366; ITS: MT370395.

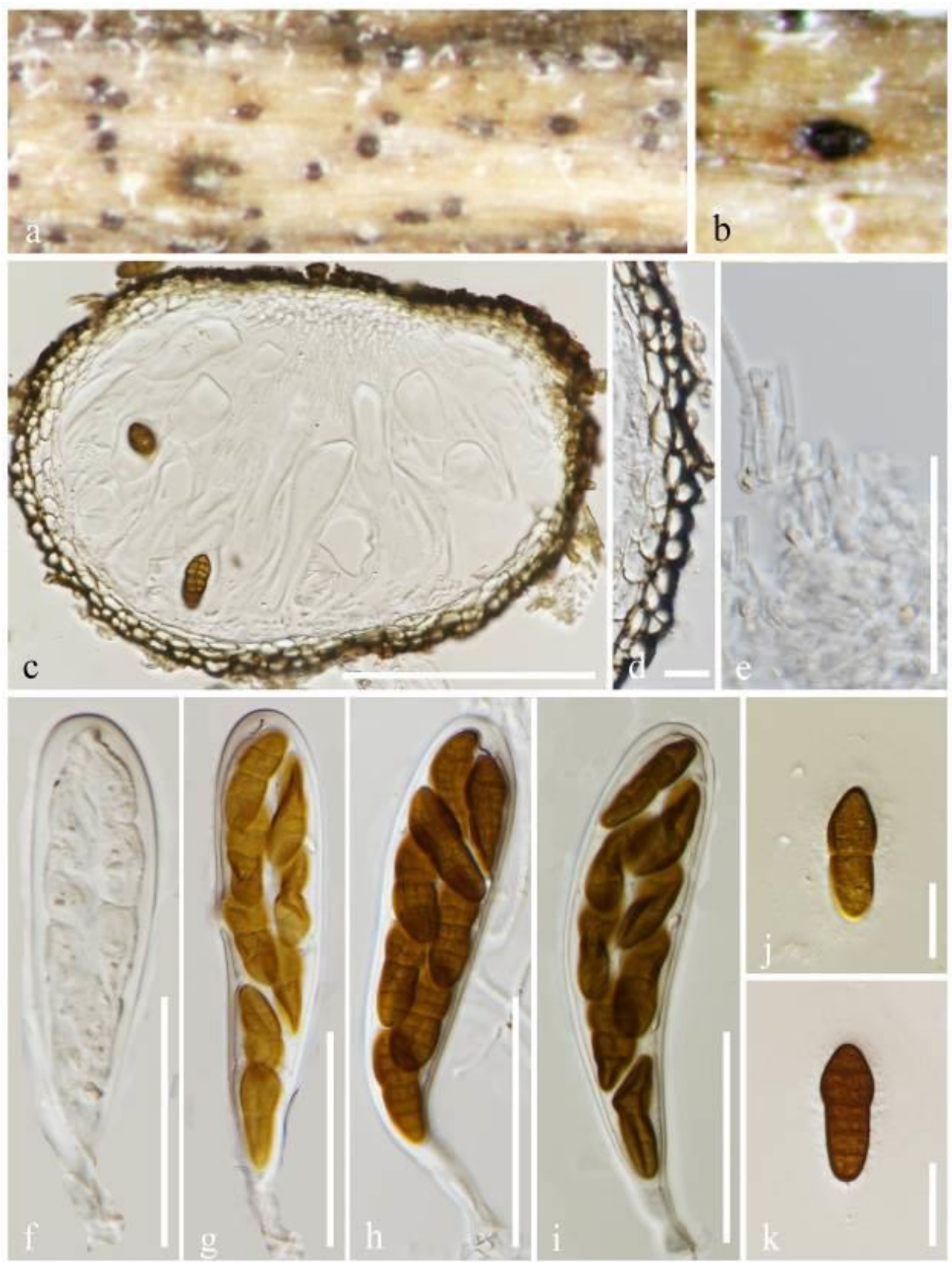


**Figure 23** – *Comoclathris europaeae* (MFLU 20-0391, holotype). a Appearance of ascomata on host. b Close up of an ascoma. c Section through an ascoma. d Peridium. e Pseudoparaphyses. f–i Ascii. j, k Ascospores. Scale bars: c = 100  $\mu$ m, f–i = 20  $\mu$ m, d, e, j–k = 10  $\mu$ m.



**Figure 24** – *Comoclathris flammulae* (MFLU 20-0397, holotype). a Appearance of ascomata on host. b Close up of ascomata. c Section through an ascoma. d Peridium. e Pseudoparaphyses. f–j Asci k, l Ascospores. Scale bars: c = 100 µm, e–j = 20 µm, d, k, l = 10 µm.

Notes – Isolates of *Comoclathris flammulae* (MFLU 20-0397 and MFLU 20-0399) grouped with statistical support (94% ML, 1.00 PP; Fig. 22) and are closely related to *C. europaeae*, *C. italica* and *C. lonicerae*. *Comoclathris flammulae* differs from *C. europaeae* by having smaller

ascomata (105–130  $\mu\text{m}$   $\times$  80–90  $\mu\text{m}$  vs 240–250  $\mu\text{m}$   $\times$  145–165  $\mu\text{m}$ ) and smaller asci (48–55  $\times$  13–17  $\mu\text{m}$  vs 60–70  $\times$  15–18  $\mu\text{m}$ ). *Comoclathris flammulae* has smaller asci (50–55  $\times$  13–17  $\mu\text{m}$  vs 100–120  $\times$  30–35  $\mu\text{m}$ ) and shorter ascospores (16–22 vs 30–35  $\mu\text{m}$ ) than those of *C. italica*. *Comoclathris flammulae* can be distinguished from *C. lonicerae* mainly by their ascospore septation (6 transverse septa vs 3–5 transverse septa). Base pair differences of ITS region of *Comoclathris flammulae* to *C. italica*. and *C. lonicerae* are (7/550 (1.3%), no gaps) and (13/564 (2.3%), no gaps) respectively while RPB2 base pair differences are (20/861 (2.3%), no gaps) and (12/861 (2.4%), no gaps). *Comoclathris compressa* (Harkn.) Shoemaker & C.E. Babcock, *C. pentamera* (P. Karst.) S. Ahmad and *C. sedi* Wanas., Ariyaw., Camporesi & K.D. Hyde have previously been reported from *Clematis* host species. This is the first report of *Comoclathris* species from *Colutea* species.

***Comoclathris lonicerae*** Brahmanage, Camporesi & K.D. Hyde, sp. nov.

Fig. 25

Index Fungorum number: IF557586; Facesoffungi number: FoF 08016

Etymology – Species epithet refers to the host genus *Lonicera*.

Holotype – MFLU 20-0385

*Saprobic* on dead stems of living branches of *Lonicera* sp., appearing as black spots on the host surface. Sexual morph: *Ascomata* 370–485  $\mu\text{m}$   $\times$  255–360  $\mu\text{m}$  ( $\bar{x}$  = 460  $\times$  300  $\mu\text{m}$ , n = 10), solitary or aggregated, scattered, semi-immersed to erumpent, globose to subglobose, dark brown to black, without a distinct ostiole. *Peridium* 12–27  $\mu\text{m}$  wide, comprising 2–4 layers of brown to dark brown cells of *textura angularis*. *Hamathecium* comprising numerous, 1.4–2.4  $\mu\text{m}$  wide, septate, pseudoparaphyses. *Asci* 180–192  $\times$  60–74  $\mu\text{m}$  ( $\bar{x}$  = 185  $\times$  68  $\mu\text{m}$ , n = 20), 8-spored, bitunicate, fissitunicate, broadly cylindrical to cylindrical-clavate, short pedicellate, rounded at the apex, with an indistinct, shallow ocular chamber. *Ascospores* 55–70  $\times$  20–30  $\mu\text{m}$  ( $\bar{x}$  = 65  $\times$  28  $\mu\text{m}$ , n = 30), overlapping uni- or bi-seriate, yellowish brown, transversely septate or muriform, with 3–5 transverse septa, 1–2 longitudinal septa, with rounded ends, constricted at the middle septum, smooth with a thick mucilaginous sheath. Asexual morph Undetermined.

Material examined – ITALY, Province of Arezzo (AR), Montalone-Bibbiena, on living branches of *Lonicera* sp. (Caprifoliaceae), 5 May 2013, E. Camporesi, IT 1248 (MFLU 20-0385, holotype; JZBH3450001, isotype).

GenBank Accessions – LSU: MT370419; SSU: MT370365; ITS: MT370394; RPB2: MT729649

Notes – *Comoclathris lonicerae* is phylogenetically closely related to *C. italica* (MFLUCC 15-0073, MFLUCC 14-1062), but forms a well-separated lineage (95% ML, 1.00 PP) in the present phylogenetic analyses (Fig. 22). *Comoclathris lonicerae* can easily be distinguished from *C. italica* by their larger asci (180–192  $\times$  60–74  $\mu\text{m}$  vs 100–120  $\times$  30–35  $\mu\text{m}$ ) and larger ascospores (55–70  $\times$  20–30  $\mu\text{m}$  vs 30–35  $\times$  10–15  $\mu\text{m}$ ) (Thambugala et al. 2017). The ITS and RPB2 base pair difference among these isolates are 0.58% (3 bp without gaps out of 521bp) and 1.4% (12 bp without gaps out of 856 bp), respectively. Based on phylogenetic and morphological differences, we introduced this taxon as a new *Comoclathris* species. *Comoclathris emodi* reported from *Lonicera* sp. in India differs from *C. lonicerae* by having 4 transverse septa (Shoemaker & Babcock 1992). However, there is no sequence data available to compare the phylogenetic relationship of our new species to *C. emodi*.

### ***Stemphylium*** Wallr.

*Stemphylium* is a well-established genus typified with *S. botryosum* Wallr. (Woudenberg et al. 2017). It includes dematiaceous hyphomycetes and can be distinguished from other hyphomycetes in Pleosporaceae by having phaeodictyospores produced by the percurrent proliferation in its conidiophores, and apically swollen conidiogenous cells (Köhl et al. 2009). *Stemphylium* species are mostly pathogens on a wide range of vegetable plants, including tomato, lettuce, beans, pea and fruits (Câmara et al. 2002, Woudenberg et al. 2017, Brahmanage et al. 2018, 2019).

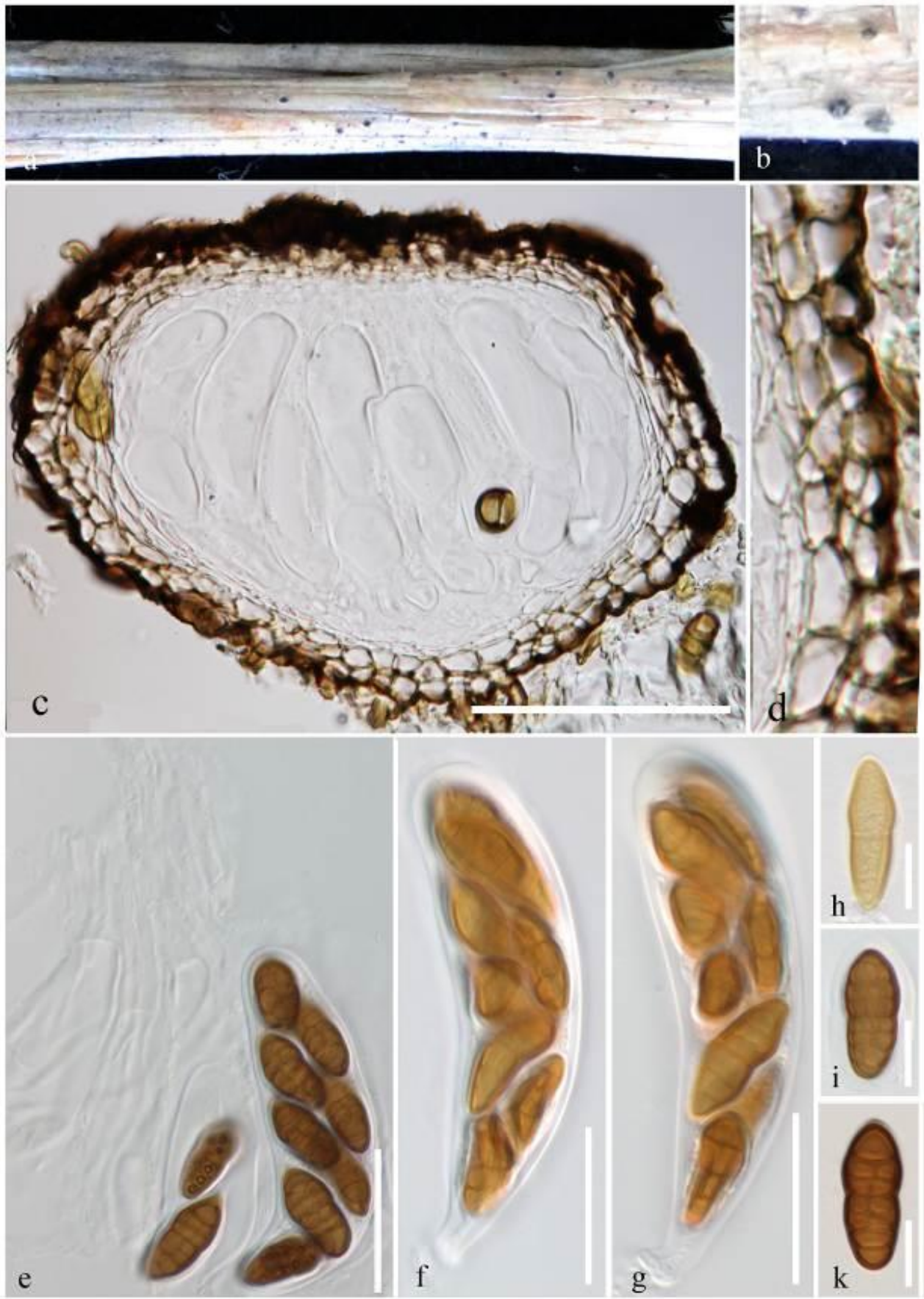


**Figure 25** – *Comoclathris loniceræ* (MFLU 20-0385, holotype). a Appearance of ascomata on host. b Close up of ascomata. c Section through an ascoma. d Peridium. e Pseudoparaphyses and asci. f, g Asci. h–k Ascospores. Scale bars: c = 100  $\mu$ m, e–g = 50  $\mu$ m, h–k = 20  $\mu$ m.

*Stemphylium artemisiae* Brahmanage, Camporesi & K.D. Hyde, sp. nov.

Fig. 27

Index Fungorum number: IF557588; Facesoffungi number: FoF08018

Etymology: Name referring to the host genus *Artemisia* of the new species

Holotype – MFLU 20-0404

*Saprobic* on dead aerial stems of *Artemisia* sp. Sexual morph: *Ascomata* 80–100 × 130–140 µm ( $\bar{x}$  = 90 × 138 µm, n = 5), black, solitary, immersed to erumpent, base not easy to remove from the substrate, subglobose to ampulliform, coriaceous, with flattened ostiolate. *Ostiole* minute papillate, smooth, ostiolar canal filled with hyaline cells. *Peridium* 10–30 µm wide, usually composed with two layers, thick at the sides and thinner at the base, outer layer of heavily pigmented thick-walled cells of *textura angularis*, inner layer composed of hyaline to pale brown, thin-walled cells of *textura angularis*. *Hamathecium* of 1–2 µm wide, cellular, septate, broad, dense pseudoparaphyses. *Asci* 40–60 × 12–16 µm ( $\bar{x}$  = 55 × 14 µm, n = 20), 8-spored, bitunicate, fissitunicate, broadly cylindrical to cylindrical-clavate, with a short pedicel and a minute ocular chamber. *Ascospores* 16–20 × 10–12 µm ( $\bar{x}$  = 18 × 11.5 µm, n = 30), uni- to bi-seriate, partially overlapping, pale brown to brown, mostly ellipsoidal, muriform with 4–7 transverse septa and 1–3 longitudinal septa, sectored, with a sheath. Asexual morph: Undetermined.

Culture characteristics – Colonies on PDA reaching 8 cm diam. after 2 weeks at 24°C, later with dense mycelium, circular, smooth margin, yellowish grey, reverse brownish yellow.

Material examined – ITALY, Province of Forlì-Cesena [FC], Monte Poggiolo – Castrocaro Terme e Terra del Sole, on a dead aerial stem of *Artemisia* sp. (Asteraceae), 22 February 2018, E. Camporesi, IT 3742 (MFLU 20-0404, holotype; JZBH3240016, isotype), ex-type living culture JZB3240016.

GenBank Accessions – ITS: MT370409; CAL: MT729657; GAPDH: MT729664

Notes – In our phylogenetic analysis based on combined ITS, CAL and GAPDH DNA sequences, *Stemphylium artemisiae* clustered with members of *Stemphylium* (Fig. 29). *Stemphylium artemisiae* shows close phylogenetic affinities with *S. amaranthi*, *S. halophilum* and *S. lycii*, but forms a distinct lineage with moderate statistical support (76% ML, 0.91 PP) (Fig. 26). Base pair differences of *S. artemisiae* with *S. amaranthi*, *S. halophilum* and *S. lycii* are shown in Table 3. *Stemphylium artemisiae* differs from *S. amaranthi*, *S. lycii* and *S. halophilum* based on their ascospore measurements (16–20 × 10–12 µm vs 34–41 × 14–18 µm vs 35–38 × 13–15 µm), respectively (Woudenberg et al. 2017, Poursafar et al. 2018).

**Table 3** Base pair differences of *Stemphylium artemisiae* to its related species

Species	ITS	GAPDH	CAL
<i>S. amaranthi</i>	0.55% (3 bp out of 545 bp)	2.8% (20 bp out of 700 bp)	1.3% (7 bp out of 584 bp)
<i>S. halophilum</i>	1.5% (8 bp out of 545 bp)	2.8% (20 bp out of 700 bp)	5.1% (20 bp out of 584 bp)
<i>S. lycii</i>	1.1% (6 bp out of 545 bp)	2.6% (18 bp out of 700bp)	3.6% (21 bp out of 584 bp)

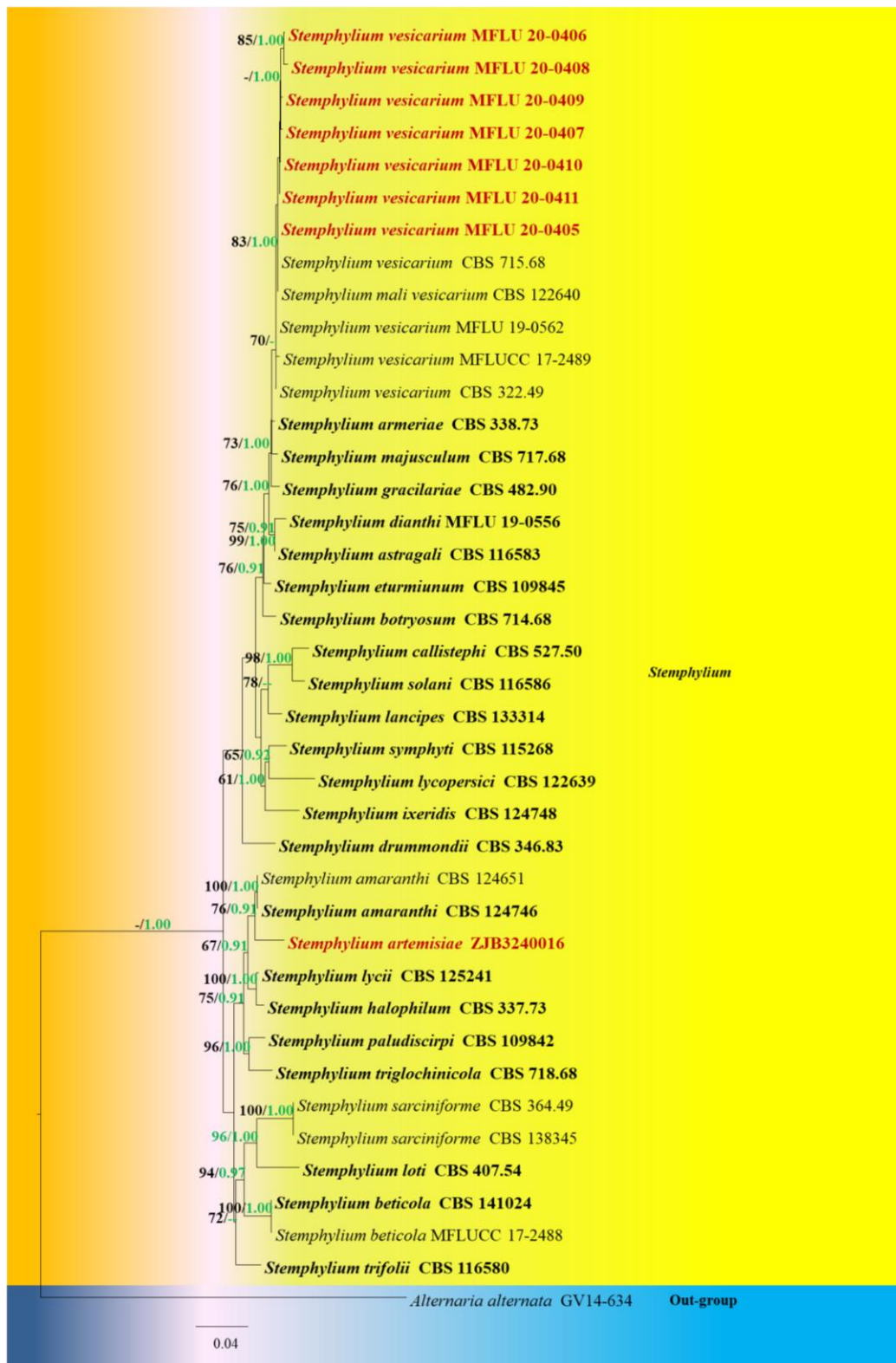
*Stemphylium vesicarium* (Wallr.) E.G. Simmons, Mycologia 61(1): 9 (1969)

Fig. 28

Index Fungorum number: IF339660; Facesoffungi number: FoF04472

*Saprobic* on *Dianthus pseudarmeria*. Sexual morph: *Ascomata* 120–250 × 260–460 µm ( $\bar{x}$  = 200 × 350 µm, n = 5), immersed to semi-immersed, globose to sub-globose, coriaceous, ostiolate. *Ostiole* papillate, ostiolar canal filled with hyaline cells. *Peridium* 35–55 µm, composed with two layers, thick at the sides and thinner at the base, outer layer of heavily pigmented thick-walled cells of *textura angularis*, inner layer composed of hyaline thin-walled cells of *textura angularis*. *Hamathecium* of 2–3 µm wide, cellular, septate, broad, dense pseudoparaphyses. *Asci* 120–215 × 30–40 µm ( $\bar{x}$  = 142 × 35 µm, n = 20), 8-spored, bitunicate, cylindrical to clavate, with a short pedicel and a minute ocular chamber. *Ascospores* 25–40 × 12–18 µm ( $\bar{x}$  = 36 × 14 µm, n = 30), uni- to bi-seriate or partially overlapping, mostly ellipsoidal, muriform, 6 transverse septa and 1–2 longitudinal septa, sectored, with a sheath. Asexual morph: Undetermined.





**Figure 26** – Maximum likelihood analysis with 1000 bootstrap replicates yielded a best tree with the likelihood value of -7963.959646. The combined ITS, CAL and GAPDH sequence dataset comprised 40 strains of *Stemphylium* with *Alternaria alternata* (GV14634) as the outgroup taxon. Tree topology of the ML analysis was similar to the BI analysis. The matrix had 582 distinct alignment patterns, with 9.10% of undetermined characters or gaps. Estimated base frequencies were as follows; A = 0.238736, C = 0.297155, G = 0.232870, T = 0.231239; substitution rates AC = 1.732597, AG = 4.848787, AT = 1.118155, CG = 1.400193, CT = 6.620922, GT = 1.000000; gamma distribution shape parameter  $\alpha$  = 0.162791. Maximum likelihood bootstrap (ML, black)

values equal to or greater than 65% and Bayesian posterior probabilities (PP, green) equal to or greater than 0.95 PP are given above the nodes. The scale bar indicates 0.04 changes. The ex-type strains are black bold and new isolates are in red bold.

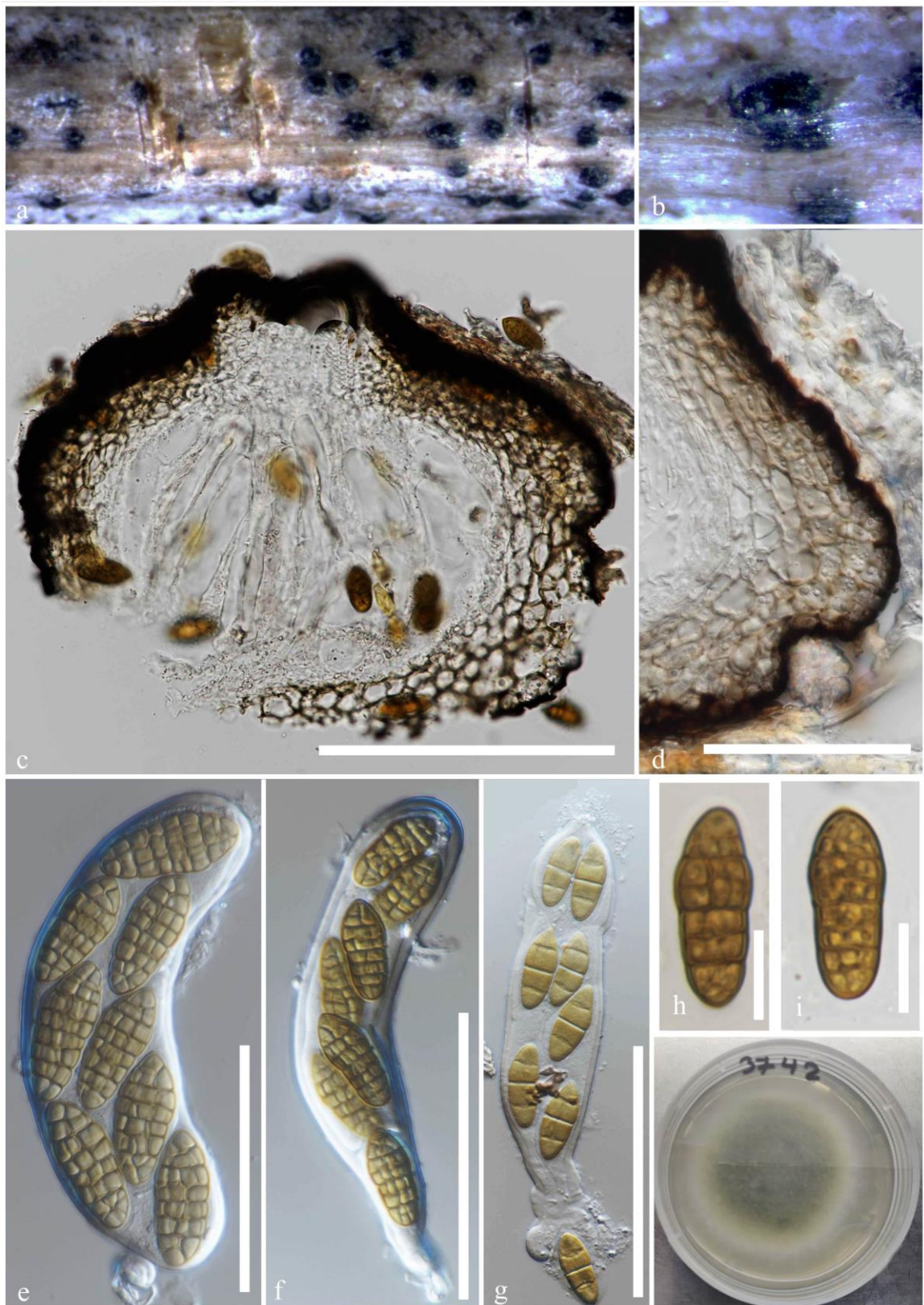


**Figure 27** – *Stemphylium artemisiae* (MFLU 20-0404, holotype). a, b Ascomata on host surface. c Vertical section through an ascoma. d Peridium. e–g Asci. h, i Ascospores. j Culture on PDA. Scale bars: a = 500  $\mu$ m, h, i = 50  $\mu$ m, g–i = 10  $\mu$ m.



**Figure 28** – *Stemphylium vesicarium* (MFLU 20-0405). a, b Ascomata on host surface. c Vertical section through an ascoma. d Peridium. e Pseudoparaphyses. f, g Asci. h, i Ascospores. j, k Culture on PDA (j upper, k lower). Scale bars: a = 500  $\mu$ m, c-f = 50  $\mu$ m, g-i = 20  $\mu$ m.

Culture characteristics – Colonies on PDA reaching 6 cm diam. after 1 weeks at 24°C, later with dense mycelium, circular, smooth margin, grey from upper, reverse brownish yellow.

Material examined – ITALY, Province of Forlì-Cesena, Isola Santa Sofia, on a dead aerial stem of *Dianthus* sp. (Caryophyllaceae), 2 April 2018, E. Camporesi, IT 2461 (MFLU 20-0405; JZBH3240017), living culture JZB3240017; *ibids.*, Cusercoli-Civitella di Romagna, on dead aerial stem of *Tragopogon* sp. (Asteraceae), 14 April 2018, E. Camporesi, IT 3833 (MFLU 20-0406; JZBH3240018); Cusercoli-Civitella di Romagna, dead aerial stem of *Scrophularia canina* (Scrophulariaceae), 8 May 2018, E. Camporesi, IT 1433 (MFLU 20-0407; JZBH3240019); on dead aerial stem of *Onobrychis viciifolia* (Fabaceae), 21 April 2018, E. Camporesi, IT 3835 (MFLU 20-0408; JZBH3240020); Via Cerchia-Forlì, on dead aerial stem of *Torilis arvensis* (Apiaceae), 1 March 2018, E. Camporesi, 3748 (MFLU 20-0409); Castiglione-Forlì, on dead aerial stem of *Vincetoxicum hirundinaria* (Apocynaceae), 12 July 2018, E. Camporesi, IT 3972 (MFLU 20-0410; JZBH3240022); Ridracoli – Bagno di Romagna on dead aerial stem of *Helleborus* sp. (Ranunculaceae), 5 April 2018, E. Camporesi, IT 3819 (MFLU 20-0411; JZBH3240023).

GenBank Accessions – (MFLU 20-0405) ITS: MT370403; CAL: MT729657; GAPDH: MT729659, (MFLU 20-0406) ITS: MT370406; CAL: MT729655; GAPDH: MT729662, (MFLU 20-0407) ITS: MT370402; GAPDH: MT729658, (MFLU 20-0408) ITS: MT370407; GAPDH: MT729660, (MFLU 20-0409) ITS: MT370404; CAL: MT729653; (MFLU 20-0410) ITS: MT370408; CAL: MT729656; GAPDH: MT729663, (MFLU 20-0411) ITS: MT370405; CAL: MT729654; GAPDH: MT729661

Notes – *Stemphylium vesicarium* is widely known as a plant pathogenic fungus and causes leaf spots on a wide range of plant species mostly on *Allium* spp. (Woudenberg et al. 2017). This study reports new host records on *Helleborus* sp., *Onobrychis viciifolia*, *Scabiosa* sp., *Scrophularia canina*, *Torilis arvensis*, *Tragopogon* sp. and *Vincetoxicum hirundinaria* from Italy. According to Farr & Rossman (2020), this species is associated with more than 20 plant species worldwide.

## Acknowledgments

We would like to thank Thailand Research grants entitled Impact of climate change on fungal diversity and biogeography in the Greater Mekong Subregion (grant no: RDG6130001) and (grant no: TRG5880152). We are grateful to the Mushroom Research Foundation for supporting this research. D.N. Wanasinghe would like to thank the National Science Foundation of China and the Chinese Academy of Sciences for financial support under the following grants: 41761144055, 41771063 and Y4ZK111B01. We also acknowledge the Mushroom Research Foundation for partially supporting this research. Rashika Brahmanage offers his deepest gratitude to Dr. Ruvishika Jayawardena, L. Mei and Zhang Wei for their helpful comments and advices.

## References

- Al Ghafri AB, Maharachchikumbura SS, Hyde KD, Al-Saady NA, Al-Sadi AM. 2019 – A new section and a new species of *Alternaria* encountered from Oman. *Phytotaxa* 405, 279–89.
- Al-Nadabi HH, Maharachchikumbura SS, Agrama H, Al-Azri M et al. 2018 – Molecular characterization and pathogenicity of *Alternaria* species on wheat and date palms in Oman. *European journal of plant pathology* 152, 577–88.
- Andersen B, Hollensted M. 2008 – Metabolite production by different *Ulocladium* species. *International journal of food microbiology*. 126, 172–9.
- Ariyawansa HA, Hyde KD, Jayasiri SC, Buyck B et al. 2015a – Fungal diversity notes 111–252 taxonomic and phylogenetic contributions to fungal taxa. *Fungal Diversity* 75, 27–274.
- Ariyawansa HA, Phookamsak R, Tibpromma S, Kang JC, Hyde KD. 2014 – A molecular and morphological reassessment of *Diademaceae*. *The Scientific World Journal*.  
Doi: 10.1155/2014/675348
- Ariyawansa HA, Phukhamsakda C, Thambugala KM, Bulgakov TS et al. 2015b – Revision and phylogeny of *Leptosphaeriaceae*. *Fungal Diversity* 74(1), 19–51.
- Ariyawansa HA, Thambugala KM, Manamgoda DS, Jayawardena R et al. 2015c – Towards a natural classification and backbone tree for *Pleosporaceae*. *Fungal Diversity* 71(1), 85–139.

- Arx JA von, Müller E. 1975 – A re-evaluation of the bitunicate ascomycetes with keys to families and genera. *Studies in Mycology* 9, 1–159.
- Aveling TAS, Snyman HG. 1993 – Infection studies of *Stemphylium vesicarium* on onion leaves. *Mycological Research* 97, 984–988.
- Aveskamp MM, De Gruyter J, Crous PW. 2008 – Biology and recent developments in the systematics of *Phoma*, a complex genus of major quarantine significance. *Fungal Diversity* 31, 1–18.
- Bakhshi M, Arzanlou M, Zare R, Groenewald JZ, Crous PW. 2019 – New species of *Septoria* associated with leaf spot diseases in Iran. *Mycologia* 1116, 1056–1071.
- Barr ME. 1987a – *Prodomus* to class Loculoascomycetes. Published by the author, Amherst, MA. 168 pp. 1991. Notes on and additions to North American members of the Herpotrichiellaceae. *Mycotaxon* 41, 419–436.
- Barr ME. 1987b – *Prodomus* to class Loculoascomycetes. Newell, Amherst
- Barr ME. 1979 – A classification of Loculoascomycetes. *Mycologia* 71, 935–957.
- Barr ME. 1990 – Melanommatales (Loculoascomycetes). *N Am Flora Ser II* 13, 1–129.
- Bennett S. 1983 – Log-logistic regression models for survival data. *Journal of the Royal Statistical Society: Series C (Applied Statistics)* 32, 165–71.
- Berbee ML, Pirseyedi M, Hubbard S. 1999 – *Cochliobolus* phylogenetics and the origin of known, highly virulent pathogens, inferred from ITS and glyceraldehyde-3-phosphate dehydrogenase gene sequences. *Mycologia* 91, 964–977.
- Boehm EW, Schoch CL, Spatafora JW. 2009a – On the evolution of the Hysteriaceae and Mytiliniaceae (Pleosporomycetidae, Dothideomycetes, Ascomycota) using four nuclear genes. *Mycological Research* 113, 461–479.
- Boehm EWA, Mugambi G, Miller AN, Huhndorf S et al. 2009b – A molecular phylogenetic reappraisal of the Hysteriaceae, (Pleosporomycetidae, Dothideomycetes) with key to world Mytiliniaceae and Gloniaceae species. *Studies of Mycology* 64, 49–83.
- Boerema GH. 2004 – *Phoma* identification manual: differentiation of specific and infra-specific taxa in culture. CABI
- Boerema GH, Van Kesteren HA. 1964 – The nomenclature of two fungi parasitizing *Brassica*. *Persoonia* 3, 17–28.
- Brahmanage RS, Lu YZ, Bhat DJ, Wanasinghe DN et al. 2017 – Phylogenetic investigations on freshwater fungi in Tubeufiaceae (Tubeufiales) reveals the new genus *Dictyospora* and new species *Chlamydotubeufia aquatica* and *Helicosporium flavum* *Mycosphere* 8, 917–933.
- Brahmanage RS, Hyde KD, Li XH, Jayawardena RS et al. 2018 – Are pathogenic isolates of *Stemphylium* host specific and cosmopolitan? *Plant Pathology & Quarantine* 8, 153–164.
- Brahmanage RS, Wanasinghe DN, Dayarathne MC, Jeewon R et al. 2019 – Morphology and phylogeny reveal *Stemphylium dianthi* sp. nov. and new host records for the sexual morphs of *S. beticola*, *S. gracilariae*, *S. simmonsii* and *S. vesicarium* from Italy and Russia. *Phytotaxa* 411, 243–263.
- Cai L, Tsui CK, Zhang KQ, Hyde KD. 2002 – Aquatic fungi from Lake Fuxian, Yunnan, China. *Fungal Diversity* 9, 57–70.
- Cai L, Zhang K, McKenzie EHC, Hyde KD. 2003 – Freshwater fungi from bamboo and wood submerged in the Liput River in the Philippines. *Fungal Diversity* 13, 1–12.
- Câmara MPS, O'Neill NR, van Berkum P. 2002 – Phylogeny of *Stemphylium* spp. based on ITS and glyceraldehyde-3-phosphate dehydrogenase gene sequences. *Mycologia* 94, 660–672.
- Cannon PF, Kirk PM. 2007 – *Fungal families of the world*, 7<sup>th</sup> edn. CAB International, Wallingford
- Carbone I, Kohn LM. 1999 – A method for designing primer sets for speciation studies in filamentous ascomycetes. *Mycologia* 91, 553–556.
- Carson ML. 2005 – Yield loss potential of *Phaeosphaeria* leaf spot of maize caused by *Phaeosphaeria maydis* in the United States. *Plant Disease* 89, 986–988.
- Chen Q, Zhang KE, Zhang GU, Cai L. 2015 – A polyphasic approach to characterize two novel species of *Phoma* (Didymellaceae) from China. *Phytotaxa* 197, 267–81.

- Chomnunti P, Hongsanan S, Aguirre-Hudson B, Tian Q, Peršoh D et al. 2014 – The sooty moulds. *Fungal Diversity* 66, 1–36.
- Costa EO, Gandra CR, Pires MF, Couthino SD et al. 1993 – Survey of bovine mycotic mastitis in dairy herds in the State of São Paulo, Brazil. *Mycopathologia* 124, 13–17.
- Dai DQ, Bahkali AH, Li WJ, Bhat DJ et al. 2015 – *Bambusicola loculata* sp. nov. (Bambusicolaceae) from bamboo. *Phytotaxa* 213(2), 122–130.
- Dai D, Bhat DJ, Liu J, Chukeatirote E et al. 2012 – *Bambusicola*, a new genus from bamboo with asexual and sexual morphs. *Cryptogamie Mycologie* 33(3), 363–79.
- Dayarathne MC, Boonmee S, Braun U, Crous PW et al. 2016 – Taxonomic utility of old names in current fungal classification and nomenclature: Conflicts, confusion & clarifications. *Mycosphere* 7, 1622–1648.
- Dayarathne MC, Phookamsak R, Ariyawansa HA, Jones EBG et al. 2015 – Phylogenetic and morphological appraisal of *Leptosphaeria italica* sp. nov. (Leptosphaeriaceae, Pleosporales) from Italy. *Mycosphere* 6, 634–642.
- Dayarathne MC, Jones EBG, Maharachchikumbura SSN, Devadatha B et al. 2020 – Morpho-molecular characterization of microfungi associated with marine based habitats. *Mycosphere* 11, 1–188.
- De Gruyter J, Woudenberg JH, Aveskamp MM, Verkley GJ et al. 2013 – Redisposition of Phoma-like anamorphs in Pleosporales. *Studies in Mycology* 75, 1–36.
- De Hoog GS, Guarro J, Gené J, Figueras MJ. 2000 – Atlas of clinical fungi. Centraalbureau voor Schimmelcultures (CBS).
- Devadatha B, Sarma VV, Jeewon R, Hyde KD, Jones EBG. 2018 – *Morosphaeria muthupetensis* sp. nov. (Morosphaeriaceae) from India: Morphological characterisation and multigene phylogenetic inference. *Botanica Marina* 61, 395–405.
- Ellis MB. 1971 – Dematiaceous hyphomycetes. *Dematiaceous hyphomycetes*. Commonwealth Mycological Institute, Commonwealth Mycological Institute, UK, pp. 608.
- Ellis MB, Gibson IA. 1975 – *Stemphylium lycopersici*. [Descriptions of Fungi and Bacteria]. *IMI Descriptions of Fungi and Bacteria* 127, 1261–1270.
- Ellis MA, Sinclair JB. 1976 – Effect of benomyl field sprays on internally-borne fungi, germination, and emergence of late-harvested soybean seeds. *Phytopathology* 66, 680–2.
- Enjoji S. 1931 – Two diseases of tomato (2) (in Japanese). *Journal of Plant Protection Research* 18, 48–53.
- Eriksson OE, Hawksworth DL. 2003 – *Saccharicola*, a new genus for two *Leptosphaeria* species on sugar cane. *Mycologia* 95, 426–33.
- Faisal M, Elsayed E, Fitzgerald SD, Silva V, Mendoza L. 2007 – Outbreaks of phaeohyphomycosis in the chinook salmon (*Oncorhynchus tshawytscha*) caused by *Phoma herbarum*. *Mycopathologia* 163, 41.
- Falloon PG, Falloon LM, Grogan RG. 1987 – Etiology and epidemiology of *Stemphylium* leaf spot and purple spot of asparagus in California. *Phytopathology* 77, 407–413
- Farr DF, Rossman AY. 2020 – Fungal databases, systematic mycology and microbiology laboratory, ARS, USDA. Retrieved January 6, 2020, from <http://nt.arsgrin.gov/fungaldatabases>.
- Gálvez L, Gil-Serna J, García M, Iglesias C, Palmero D. 2016 – *Stemphylium* leaf blight of garlic (*Allium sativum*) in Spain: taxonomy and in vitro fungicide response. *The Plant Pathology Journal* 32, 388–395.
- Glass NL, Donaldson GC. 1995 – Development of primer sets designed for use with the PCR to amplify conserved genes from filamentous ascomycetes. *Applied and Environmental Microbiology* 61, 1323–1330.
- Ghaderi F, Razavi M. 2018 – Identification of the species *Parastagonospora dactylidis* on poaceous plants in Iran. *Mycologia Iranica* 35–41.
- Hall TA. 1999 – BioEdit: a user-friendly biological sequence alignment editor and analysis program for Windows 95/98/NT. *Nucleic Acids Symposium Series* 41, 95–98.

- Han JH, Shin JH, Fu T, Kim KS. 2019 – A new record and characterization of asparagus purple spot caused by *Stemphylium vesicarium* in Korea. *Mycobiology* 2, 120–5.
- Hanse B. 2013 – Research on *Stemphylium* spp. the causal agent of the yellow leaf spot disease in sugar beet in 2012. IRS, Bergen op Zoom, The Netherlands.
- Hashimoto A, Hirayama K, Takahashi H, Matsumura M et al. 2018 – Resolving the *Lophiostoma bipolare* complex: Generic delimitations within Lophiostomataceae. *Studies in Mycology* 90, 161–189.
- Hawksworth DL. 2004 – *Lichenocodium christiansenii* sp. nov. from *Nodobryoria abbreviata* (Parmeliaceae) in the Pacific Northwest, with a key to the known lichenicolous species. *The Lichenologist* 36, 1–6.
- Heidari K, Mehrabi-Koushki M, Farokhinejad R. 2018 – *Curvularia mosaddeghii* sp. nov., a novel species from the family Pleosporaceae. *Mycosphere* 9, 635–46.
- Höhnelt FV. 1919 – Fragmente zur Mykologie XXIII. *Sitzungsber Akad Wiss Wien, Math-Naturwiss Kl, Abt. 1*, 535–625.
- Hongsanan S, Hyde KD, Phookamsak R, Boonmee S et al. 2020 – Refined families of Dothideomycetes. *Fungal diversity* (in press)
- Huelsenbeck JP, Ronquist F. 2001 – MRBAYES: Bayesian inference of phylogenetic trees. *Bioinformatics* 17, 754–755.
- Hyde KD. 1991 – A new amphispheeriacous fungus from intertidal fronds of *Nypa fruticans*. *Transactions of the Mycological Society of Japan* 32, 265–271.
- Hyde KD, Chaiwan N, Norphanphoun C, Boonmee S et al. 2018 – *Mycosphere notes* 169–224. *Mycosphere* 9, 271–430
- Hyde KD, Dong Y, Phookamsak R, Jeewon R et al. 2020 – Fungal diversity notes 1151–1276: taxonomic and phylogenetic contributions on genera and species of fungal taxa. *Fungal Diversity* 1–273.
- Hyde KD, Fröhlich J, Taylor JE. 1998 – Fungi from palms. XXXVI. Reflections on unitunicate ascomycetes with apiospores. *Sydowia* 50, 21–80.
- Hyde KD, Hongsanan S, Jeewon R, Bhat DJ et al. 2016 – Fungal diversity notes 367–490: taxonomic and phylogenetic contributions to fungal taxa. *Fungal Diversity* 80, 1–270.
- Hyde KD, Jones EBG, Liu JK, Ariyawansa HA et al. 2013 – Families of Dothideomycetes. *Fungal Diversity* 63, 1–313.
- Hyde KD, Norphanphoun C, Bazzicalupo A, Karunarathna A et al. 2017 – Fungal diversity notes 603 – 708: Taxonomic and phylogenetic notes on genera and species. *Fungal Diversity* 87, 1–235.
- Hyde KD, Norphanphoun C, Chen J, Dissanayake AJ et al. 2018 – Thailand’s amazing diversity: up to 96% of fungi in northern Thailand may be novel. *Fungal Diversity* 93, 215–239.
- Ichikawa K, Sato T. 1994 – Leaf and stem spot of aster caused by *Stemphylium vesicarium* (in Japanese with English summary). *Annals of the Phytopathological Society of Japan* 60, 523.
- Irwin JAG. 1984 – Etiology of a new *Stemphylium*-incited leaf disease of alfalfa in Australia. *Plant Disease* 68, 531–532.
- Jaklitsch WM, Checa J, Blanco MN, Olariaga I et al. 2018 – A preliminary account of the Cucurbitariaceae. *Studies in mycology*. 90, 71–118.
- Jaklitsch WM, Voglmayr H. 2016 – Hidden diversity in *Thyridaria* and a new circumscription of the Thyridariaceae. *Studies in Mycology* 85, 35–64.
- Jayasiri SC, Hyde KD, Ariyawansa HA, Bhat J et al. 2015 – The Faces of Fungi database: fungal names linked with morphology, phylogeny and human impacts. *Fungal Diversity* 74, 3–18.
- Jayasiri SC, Hyde KD, Jones EBG, McKenzie EHC et al. 2019 – Diversity, morphology and molecular phylogeny of Dothideomycetes on decaying wild seed pods and fruits. *Mycosphere* 10, 1–186.
- Jayawardena RS, Hyde KD, McKenzie EHC, Jeewon R et al. 2019a – One stop shop III: taxonomic update with molecular phylogeny for important phytopathogenic genera: 51-75. *Fungal Diversity* 98, 77–160.

- Jayawardena RS, Hyde KD, Jeewon R, Ghobad-Nejhad M et al 2019b – One stop shop II: taxonomic update with molecular phylogeny for important phytopathogenic genera: 26–50. *Fungal Diversity* 94, 41–129.
- Jeewon R, Hyde KD. 2016 – Establishing species boundaries and new taxa among fungi: recommendations to resolve taxonomic ambiguities. *Mycosphere* 7, 1669–1677.
- Jeewon R, Ittoo J, Mahadeb D, Jaufeerally-Fakim Y et al. 2013 – DNA based identification and phylogenetic characterisation of endophytic and saprobic fungi from *Antidesma madagascariense*, a medicinal plant in Mauritius. *Journal of Mycology*. Doi: 10.1155/2013/781914
- Jeewon R, Wanasinghe DN, Rampadaruth S, Puchooa D et al. 2017 – Nomenclatural and identification pitfalls of endophytic mycota based on DNA sequence analyses of ribosomal and protein genes phylogenetic markers: A taxonomic dead end? *Mycosphere* 8, 1802–1817
- Johnson DA, Lunden JD. 1986 – Effects of wounding and wetting duration on infection of asparagus by *Stemphylium vesicarium*. *Plant Disease* 70, 419–420.
- Jones EBG, Suetrong S, Sakayaroj J, Bahkali AH et al. 2015 – Classification of marine Ascomycota, Basidiomycota, Blastocladiomycota and Chytridiomycota. *Fungal Diversity* 73, 1–72.
- Jones EBG, Pang KL, Abdel-Wahab MA, Scholz B et al. 2019 – An online resource for marine fungi. *Fungal Diversity* 96, 347–433.
- Katoh K, Rozewicki J, Yamada KD. 2019 – MAFFT online service: multiple sequence alignment, interactive sequence choice and visualization. *Briefings in bioinformatics* 20, 1160–1166.
- Kodsueb R, Dhanasekaran V, Aptroot A, Lumyong S et al. 2006 – The family Pleosporaceae: intergeneric relationships and phylogenetic perspectives based on sequence analyses of partial 28S rDNA. *Mycologia* 98, 571–583.
- Köhl J, Groenenboom-de Haas B, Goossen-van de Geijn H, Speksnijder A et al. 2009 – Pathogenicity of *Stemphylium vesicarium* from different hosts causing brown spot in pear. *European Journal of Plant Pathology* 124, 151
- Kohlmeyer J, Volkmann-Kohlmeyer B. 1991 – Illustrated key to the filamentous higher marine fungi. *Botanica Marina* 34, 1–61.
- Kohlmeyer J. 1969 – Marine fungi of Hawaii including the new genus *Helicascus*. *Canadian Journal of Botany* 9, 1469–87.
- Kruys Å, Eriksson OE, Wedin M. 2006 – Phylogenetic relationships of coprophilous Pleosporales (Dothideomycetes, Ascomycota), and the classification of some bitunicate taxa of unknown position. *Mycological research* 110, 527–536.
- Kurose D, Kanegae Y, Misawa T, Ebihara Y. 2015 – Yellow spot of white lace flower caused by *Pleospora herbarum* in Japan. *Japanese Journal of Phytopathology* 81, 169–172.
- Lamprecht SC, Baxter A, Thompson AH. 1984 – *Stemphylium vesicarium* on *Medicago* spp. In South Africa. *Phytophylactica* 16, 73–75.
- Lawrence DP, Rotondo F, Gannibal PB. 2016 – Biodiversity and taxonomy of the pleomorphic genus *Alternaria*. *Mycological progress* 15, 1–22.
- Li JF, Phookamsak R, Jeewon R, Darbhe J et al. 2017 – Molecular taxonomy and morphological characterization reveal new species and new host records of *Torula* species (Torulaceae, Pleosporales). *Mycological progress* 16, 447–461.
- Li WJ, Bhat DJ, Camporesi E, Tian Q et al. 2015a – New asexual morph taxa in Phaeosphaeriaceae. *Mycosphere* 6, 681–708.
- Li WJ, McKenzie EHC, Liu JK, Bhat J et al. 2020 – Taxonomy and phylogeny of hyaline-spored coelomycetes. *Fungal Diversity* 100, 1–523.
- Liew ECY, Aptroot A, Hyde KD. 2000 – Phylogenetic significance of the pseudoparaphyses in Loculoascomycete taxonomy. *Molecular Phylogeny & Evolution* 16: 392–402.
- Liu JK, Hyde KD, Jeewon R, Phillips AJ et al. 2017 – Ranking higher taxa using divergence times: a case study in Dothideomycetes. *Fungal Diversity* 84, 75–99.



- Liu JK, Hyde KD, Jones EBG, Ariyawansa HA et al. 2015 – Fungal diversity notes 1–110: taxonomic and phylogenetic contributions to fungal species. *Fungal diversity* 72, 1–197.
- Liu YJ, Whelen S, Hall BD. 1999 – Phylogenetic relationships among ascomycetes: evidence from an RNA polymerase II subunit. *Molecular Biology and Evolution* 16, 1799–1808.
- Llorente I, Montesinos E. 2006 – Brown spot of pear: an emerging disease of economic importance in Europe. *Plant Disease* 90, 1368–1375.
- Lugauskas A, Levinskait L, Pečiulytė D. 2003 – *Micromycetes* as deterioration agents of polymeric materials. *International biodeterioration & biodegradation* 52, 233–42.
- Lumbsch HT, Huhndorf SM. 2007 – Outline of Ascomycota. *Myconet* 13, 1–99.
- Luo ZL, Bao DF, Bhat JD, Yang J et al. 2016 – *Sporoschisma* from submerged wood in Yunnan, China. *Mycological progress* 15, 1145–1155.
- Luo ZL, Bhat DJ, Jeewon R, Boonmee S, Bao DF et al. 2017 – Molecular phylogeny and morphological characterization of asexual fungi (Tubeufiaceae) from freshwater habitats in Yunnan, China. *Cryptogamie, Mycologie* 38, 27–53.
- Luo ZL, Hyde KD, Liu JK, Bhat DJ et al. 2018 – Lignicolous freshwater fungi from China II: Novel *Distoseptispora* (Distoseptisporaceae) species from northwestern Yunnan Province and a suggested unified method for studying lignicolous freshwater fungi. *Mycosphere* 9, 444–461.
- Luttrell ES. 1955 – A taxonomic revision of *Helminthosporium sativum* and related species. *American Journal of Botany* 42(1), 57–68.
- Maharachchikumbura SS, Ariyawansa HA, Wanasinghe DN, Dayarathne MC et al. 2019 – Phylogenetic classification and generic delineation of *Hydeomyces desertipleosporoides* gen. et sp. nov., (Phaeosphaeriaceae) from Jebel Akhdar Mountain in Oman. *Phytotaxa*, 391, 28–38.
- Marin-Felix Y, Margarita HR, Michael J, Wingfield A et al. 2019 – Genera of phytopathogenic fungi GOPHY 2. *Studies in mycology* 92, 47–133.
- Miller ME, Taber RA, Amador JM. 1978 – *Stemphylium* blight of onion in South Texas. *Plant Disease Reporter* 62, 851–853.
- Misawa T. 2009 – Brown leaf blight of Chinese chive caused by *Stemphylium botryosum* Wallroth. (Abstract in Japanese). *Japanese Journal of Phytopathology* 75–87.
- Mugambi GK, Huhndorf SM. 2009 – Molecular phylogenetics of Pleosporales: Melanommataceae and Lophiostomataceae recircumscribed (Pleosporomycetidae, Dothideomycetes, Ascomycota). *Studies in Mycology* 64, 103–121.
- Munk A. 1953 – The system of the Pyrenomycetes. A contribution to a natural classification of the group Sphaeriales sensu Lindau. *Dansk Botanisk Arkiv* 15, 1–163.
- Munk A. 1956 – On *Metasphaeria coccodes* (Karst.) Sacc. and other fungi probably related to *Massarina* Sacc. *Massarinaceae* n. fam. *Friesia* 5, 303–308.
- Munk A. 1957 – Danish Pyrenomycetes. *Dan Bot Ark* 17, 1–491.
- Nasehi A, Kadir JB, Esfahani MN, Mahmodi F. 2013 – An outbreak of leaf spot caused by *Stemphylium solani* on eggplant in Malaysia. *Plant Disease* 97, 689.
- Nees von Esenbeck CG. 1816 – *Das system der pilze und schwämme*. Würzburg: Stahelsche Buchhandlung 17.
- Nitschke TR. 1869 – Pleosporaceae. *Verh. Naturhist. Ver Preuss Rheinl.* 26, 74.
- Nylander JA, Ronquist F, Huelsenbeck JP, Nieves-Aldrey J. 2004 – Bayesian phylogenetic analysis of combined data. *Systematic biology* 53, 47–67.
- O'Donnell K, Cigelnik E. 1997 – Two divergent intragenomic rDNA ITS2 types within a monophyletic lineage of the fungus *Fusarium* are non orthologous. *Molecular phylogenetics and evolution* 7(1), 103–116.
- Osterhage C, Schwibbe M, König GM, Wright AD. 2000 – Differences between marine and terrestrial *Phoma* species as determined by HPLC-DAD and HPLC-MS. *Phytochemical analysis* 11, 288–294.

- Pedras MSC, Biesenthal CJ. 2000 – HPLC – analyses of cultures of *Phoma* species: differentiation among groups and species through secondary metabolite profiles. *Canadian Journal of Microbiology* 46, 685–691.
- Pem D, Hongsanan S, Doilom M, Tibpromma S et al. 2019 – <https://www.dothideomycetes.org>: An online taxonomic resource for the classification, identification, and nomenclature of Dothideomycetes. *Asian Journal of Mycology* 2, 287–297
- Phookamsak R, Hyde KD, Jeewon R, Bhat DJ et al. 2019 – Fungal diversity notes 929–1035: taxonomic and phylogenetic contributions on genera and species of fungi. *Fungal Divers* 95, 1–273.
- Phookamsak R, Liu JK, McKenzie EH, Manamgoda DS et al. 2014 – Revision of Phaeosphaeriaceae. *Fungal Diversity* 68, 159–238.
- Phookamsak R, Manamgoda DS, Li WJ. 2015 – *Poaceascoma helicoides* gen et sp. nov., a new genus with scolecospores in *Lentitheciaceae*. *Cryptogamie Mycologie* 36, 225–236.
- Phookamsak R, Wanasinghe DN, Hongsanan S, Phukhamsakda C. 2017 – Towards a natural classification of *Ophiobolus* and ophiobolus-like taxa; introducing three novel genera *Ophiobolopsis*, *Paraophiobolus* and *Pseudoophiobolus* in *Phaeosphaeriaceae* (Pleosporales). *Fungal Diversity* 87, 299–339.
- Pinnoi A, Jeewon R, Sakayaroj J, Hyde KD, Jones EBG. 2007 – *Berkleasmiium crunisia* sp. nov. and its teleomorphic affinities to the Pleosporales based on 18S, 28S and ITS-5.8S rDNA sequence analyses. *Mycologia* 99, 378–384.
- Pitt JI, Hocking AD. 1997 – Fungi and food spoilage (vol. II). Eds. Pitt, JI. and Hocking, AD. Blackie Academic and Professional, London.
- Poursafar A, Ghosta Y, Orina AS, Gannibal PB. 2018 – Taxonomic study on *Alternaria* sections *Infectoriae* and *Pseudoalternaria* associated with black (sooty) head mold of wheat and barley in Iran. *Mycological Progress* 17, 343– 56.
- Preedanon S, Klaysuban A, Suetrong S, Promchoo W. 2017 – *Helicascus mangrovei* sp. nov., a new intertidal mangrove fungus from Thailand. *Mycoscience* 58,174–80.
- Preuss CGT. 1851 – Übersicht untersuchter Pilze, besonders aus der Umgegend von Hoyerswerda. *Linnaea* 24, 99–153.
- Promptutha I, Lumyong S, Vijaykrishna D, McKenzie EHC et al. 2007 – A phylogenetic evaluation of whether endophytes become saprotrophs at host senescence. *Microbial Ecology* 53, 579–590.
- Quaedvlieg W, Verkley GJM, Shin HD, Barretto RW. 2013 – Sizing up *Septoria*. *Studies in Mycology* 75, 307–390.
- Rabie CJ, Rensburg SJV, Watt JJV, Lubben A. 1975 – Onyalai the possible involvement of a mycotoxin produced by *Phoma sorghina* in the aetiology. *South African Medical Journal* 57, 1647–1650.
- Rai M, Deshmukh P, Gade A, Ingle A et al. 2009 – *Phoma* Saccardo: Distribution, secondary metabolite production and biotechnological applications *Critical Reviews in Microbiology* 35, 182–196.
- Rambaut A. 2012 – Fig.Tree. Tree Fig. Drawing Tool, v. 1.4.0
- Ramesh LC, Rao GP, Manoharachari C, Bhat DJ. 2003 – International Book Distributing Company, Lucknow, *Frontiers of Fungal Diversity* 457–479.
- Rannala B, Yang Z. 1996 – Probability distribution of molecular evolutionary trees: a new method of phylogenetic inference. *Journal of Molecular Evolution* 43, 304–311.
- Rehner S, Samuels GJ. 1994 – Taxonomy and phylogeny of *Gliocladium* analyzed from nuclear large subunits ribosomal DNA sequences. *Mycological Research* 98, 625–634.
- Reis A, Boiteux LS, Fonseca MN. 2011 – Identification of solanaceous and nonsolanaceous species as hosts of *Stemphylium solani* isolates in Brazil. *Phytopathology* 101–152.
- Reiss MLC. 1854 – Neue Kernpilze. *Hedwigia* 1, 23–28.
- Ronquist F, Huelsenbeck JP. 2003 – MrBayes 3: Bayesian phylogenetic inference under mixed models. *Bioinformatics* 19, 1572–1574.

- Roberts RG. 2007 – Two new species of *Alternaria* from pear fruit. *Mycotaxon* 100, 159–67.
- Runa F, Park MS, Pryor BM. 2009 – *Ulocladium* systematics revisited: phylogeny and taxonomic status. *Mycological progress* 1, 8–35.
- Saccardo PA. 1883 – Pyrenomyceteae. *Sylloge Fungorum Omnium Hucusque Cognitorum* 2, 1–813.
- Schoch CL, Crous PW, Groenewald JZ, Boehm EWA et al. 2009 – A class-wide phylogenetic assessment of Dothideomycetes. *Studies in Mycology* 64, 1–15.
- Seaney RR. 1973 – Birdsfoot trefoil. In: Heath ME, Metcalfe DS, Barnes RF (eds). *Forages the science of grassland agriculture*. Ames, Iowa, The Iowa State University Press. 177–188.
- Shearer CA, Raja HA, Miller AN, Nelson P et al. 2009 – The molecular phylogeny of freshwater Dothideomycetes. *Studies of Mycology* 64, 145–153.
- Sheridan JE, Soteros JJ. 1974 – A survey of fungi in jet aircraft fuel systems in New Zealand. *International biodeterioration bulletin* 10, 105–107.
- Shibata S, Horiuchi S, Satou M, Yamauchi N. 2000 – *Stemphylium vesicarium*, another causal agent of leaf blight of welsh onion in Japan (in Japanese with English summary). *Annual Report of the Society of Plant Protection of North Japan* 51, 62–65.
- Shoemaker RA, Babcock CE. 1989 – *Phaeosphaeria*. *Canadian Journal of Botany* 67, 1500–1599.
- Shoemaker RA, Babcock CE. 1992 – Planodictyosporous Pleosporales: *Clathrospora*, *Comoclathris*, *Graphyllum*, *Macrospora*, and *Platysporoides*. *Canadian Journal of Botany* 70, 1617–1658.
- Silvestro D, Michalak I. 2012 – raxmlGUI: a graphical front-end for RAxML. *Organisms Diversity & Evolution*. 12, 335–7.
- Simmons EG. 1967 – Typification of *Alternaria*, *Stemphylium*, and *Ulocladium*. *Mycologia*, 59(1), 67–92.
- Simmons EG, Stuteville DL, Erwin DC. 1990 – *Stemphylium* leaf spot. Causal organisms. *Compendium of alfalfa diseases*, 2nd ed. St. Paul, Minnesota: APS Press. 84.
- Sivanesan A. 1984 – *Acantharia*, *Gibbera* and their anamorphs. *Transactions of the British Mycological Society* 82, 507–29.
- Sørensen Annette, Peter SL, Mette L, Kristian FN et al. 2011 – Frisvad. *Aspergillus saccharolyticus* sp. nov., a black Aspergillus species isolated in Denmark. *International journal of systematic and evolutionary microbiology* 61, 3077–3083.
- Stukenbrock EH, Banke S, McDonald BA. 2006 – Global migration patterns in the fungal wheat pathogen *Phaeosphaeria nodorum*. *Molecular Ecology* 15, 2895–2904.
- Subedi S, Shrestha SM, Bahadur G, Thapa RB et al. 2014 – Integrated Approach for the Management of New Threat *Stemphylium botryosum* walr Causing Blight of Lentil (*Lens culinaris* Medik). *Türk Tarım ve Doğa Bilimleri* 6, 1209–1220.
- Suetrong S, Schoch CL, Spatafora JW, Kohlmeyer J et al. 2009 – Molecular systematics of the marine Dothideomycetes. *Studies in Mycology* 64, 155–173.
- Sun JZ, Liu XZ, McKenzie EHC, Jeewon R et al. 2019 – Fungicolous fungi: terminology, diversity, distribution, evolution, and species checklist. *Fungal Diversity* 95, 337–430.
- Suzui T. 1973 – *Stemphylium* leaf spot (*Stemphylium botryosum* Wallr.) on asparagus plants (in Japanese with English summary). *Annals of the Phytopathological Society of Japan* 39, 364–366.
- Tamura K, Stecher G, Peterson D, Filipski A, Kumar S. 2013 – MEGA6: Molecular Evolutionary Genetics Analysis version 6.0. *Molecular Biology and Evolution* 30, 2725–2729
- Tennakoon DS, Phookamsak R, Wanasinghe DN, Yang JB et al. 2017 – Morphological and phylogenetic insights resolve *Plenodomus sinensis* (Leptosphaeriaceae) as a new species. *Phytotaxa* 324(1), 73–82.
- Tanaka K, Hirayama K, Yonezawa H, Hatakeyama S et al. 2009 – Molecular taxonomy of bambusicolous fungi: Tetraplosphaeriaceae, a new pleosporalean family with Tetraploa-like anamorphs. *Studies in mycology* 64, 175–209.

- Tanaka K, Hirayama K, Yonezawa H, Sato G et al. 2015 – Revision of the Massariaceae (Pleosporales, Dothideomycetes). *Studies in Mycology* 82, 75–136.
- Thambugala KM, Daranagama DA, Phillips AJ, Bulgakov TS et al. 2017 – Microfungi on *Tamarix*. *Fungal Diversity* 82, 239–306.
- Thambugala KM, Hyde KD, Tanaka K, Tian Q et al. 2015 – Towards a natural classification and backbone tree for Lophiostomataceae, Floricolaceae, and Amorosiaceae fam. nov. *Fungal Diversity* 74, 199–266.
- Tibpromma S, Hyde KD, Jeewon R, Maharachchikumbura SSN et al. 2017 – Fungal diversity notes 491–602: taxonomic and phylogenetic contributions to fungal taxa. *Fungal Diversity* 83, 1–261.
- Tomioka K, Sato T, Sasaya T, Koganezawa H. 1997 – Leaf spot of kalanchoe caused by *Stemphylium lycopersici*. *Annals of the Phytopathological Society of Japan* 63, 337–340.
- Tomioka K, Sato T. 2011 – Fruit rot of sweet pepper caused by *Stemphylium lycopersici* in Japan. *Journal of General Plant Pathology* 77, 342–344.
- Torres MS, White JF, Cazares G, Bergen M et al. 2005 – A new species and its phylogenetic placement in the *Didymella/Phoma* complex (Phaeosphaeriaceae, Pleosporales). *Mycotaxon* 93, 297–308.
- Vakalounakis DJ, Markakis EA. 2013 – First report of *Stemphylium solani* as the causal agent of a leaf spot on greenhouse cucumber. *Plant Diversity* 97, 287–288.
- Vilgalys R, Hester M. 1990 – Rapid genetic identification and mapping of enzymatically amplified ribosomal DNA from several *Cryptococcus* species. *Journal of Bacteriology* 172, 4238–4243.
- Voronin LV. 1989 – *Phoma* Sacc. species from the water and fish of freshwater reservoirs. *Mikologia i Fitopatologia* 23, 19–27.
- Wanasinghe DN, Jeewon R, EBG Jones, S Boonmee et al. 2018a – Novel palmicolous taxa within Pleosporales: Multigene phylogeny and taxonomic circumscription. *Mycological Progress* 17, 571–590.
- Wanasinghe DN, Camporesi E, Hu DM. 2016 – *Neoleptosphaeria jonesii* sp. nov., a novel saprobic sexual species, in Leptosphaeriaceae. *Mycosphere* 7, 1368–1377.
- Wanasinghe DN, Hyde KD, Jeewon R, Crous PW et al. 2017a – Phylogenetic revision of *Camarosporium* (Pleosporineae, Dothideomycetes) and allied genera. *Studies in Mycology* 87, 207–256.
- Wanasinghe DN, Jeewon R, Jones EBG, Tibpromma S Hyde KD. 2017b – Saprobiic Dothideomycetes in Thailand: *Muritestudina* gen. et sp. nov. (*Testudinaceae*) a new terrestrial pleosporalean ascomycete, with hyaline and muriform ascospores. *Studies in Fungi* 2, 219–234.
- Wanasinghe DN, Jones EBG, Camporesi E, Boonmee S et al. 2014 – An exciting novel member of Lentitheciaceae in Italy from *Clematis vitalba*. *Cryptogamie, Mycologie* 35, 323–337.
- Wanasinghe DN, Phukhamsakda C, Hyde KD, Jeewon R et al. 2018b – Fungal diversity notes 709–839: taxonomic and phylogenetic contributions to fungal taxa with an emphasis on fungi on Rosaceae. *Fungal Diversity* 89, 1–236.
- Wang HK, Aprot A, Crous PW, Hyde KD, Jeewon R. 2007 – The polyphyletic nature of Pleosporales: An example from *Massariosphaeria* based on ribosomal DNA and RBP2 gene phylogenies. *Fungal Biology* 111, 1268–1276.
- White TJ, Bruns T, Lee S, Taylor J. 1990 – Amplification and direct sequencing of fungal ribosomal RNA genes for phylogenetics. In: Innis MA, Gelfand DH, Sninsky JJ, White TJ (eds) *PCR protocols: a guide to methods and applications*. Academic Press, San Diego 315–322.
- Wijayawardene NN, Crous PW, Kirk PM, Hawksworth DL et al. 2014 – Naming and outline of Dothideomycetes - including proposals for the protection or suppression of generic names. *Fungal Diversity* 69, 1–55.
- Wijayawardene NN, Hyde KD, Al-Ani LKT, Tedersoo L et al. 2020 – Outline of Fungi and fungi-like taxa. *Mycosphere* 11, 1060–1456.

- Wijayawardene NN, Hyde KD, Rajeshkumar KC, Hawksworth DL et al. 2017 – Notes for genera - Ascomycota. *Fungal Diversity* 86, 1–594.
- Wijayawardene NN, Hyde KD, Lumbsch HT, Jian KL et al. 2018 – Outline of ascomycota: 2017. *Fungal Diversity* 88, 167–263.
- Wijayawardene NN, Hyde KD, Wanasinghe DN, Papizadeh M et al. 2016 – Taxonomy and phylogeny of dematiaceous coelomycetes. *Fungal diversity* 77, 1–316.
- Woudenberg JHC, Groenewald JZ, Binder M, Crous PW. 2013 – *Alternaria* redefined. *Studies in Mycology* 75, 171–212.
- Woudenberg JH, Seidl MF, Groenewald JZ, De Vries M et al. 2015 – *Alternaria* section *Alternaria*: Species, formae speciales or pathotypes?. *Studies in Mycology* 82, 1–21.
- Woudenberg JHC, Hanse B, Van Leeuwen GCM, Groenewald JZ, Crous PW. 2017 – *Stemphylium* revisited. *Studies in Mycology* 87, 77–103.
- Xianshu Y, Strobel G, Stierle A, Hess WM et al. 1994 – A fungal endophyte-tree relationship: *Phoma* sp. in *Taxus wallachiana*. *Plant Science* 102, 1–9.
- Yang Q, Chen WY, Jiang N, Tian CM. 2019 – Nectria-related fungi causing dieback and canker diseases in China with *Neothyronectria citri* sp. nov. described. *Mycology* 56, 49–66.
- Yarden O, Ainsworth TD, Roff G, Leggat W et al. 2007 – Increased prevalence of ubiquitous ascomycetes in an acropoid coral (*Acropora formosa*) exhibiting symptoms of brown band syndrome and skeletal eroding band. *Applied & Environmental Microbiology* 73, 2755–2757.
- Zeng XY, Jeewon R, Wen TC, Hongsanan S et al. 2018 – Simplified and efficient DNA extraction protocol for Meliolaceae specimens. *Mycological Progress* 17, 403–415.
- Zhang KK, Hongsanan S, Tennakoon DS, Tian SL, Xie N. 2019 – *Phaeosphaeria chinensis* sp. nov. (*Phaeosphaeriaceae*) with an asexual/sexual morph connection from Guangdong Province, China. *Phytotaxa* 419, 28–38.
- Zhang Y, Crous PW, Schoch CL, Hyde KD. 2012 – Pleosporales. *Fungal Diversity* 53, 1–221.
- Zhang Y, Fournier J, Phookamsak R, Bakhali AH, Hyde KD. 2013 – *Halotthiaceae* fam. nov. (*Pleosporales*) accommodates the new genus *Phaeoseptum* and several other aquatic genera. *Mycologia* 40, 107–110.
- Zhang Y, Zhang J, Wang Z, Fournier J et al. 2014 – Neotypification and phylogeny of *Kalmusia*. *Phytotaxa* 176, 64–173.
- Zhang Y, Jeewon R, Fournier J, Hyde KD. 2008 – Multi-gene phylogeny and morphotaxonomy of *Amniculicola lignicola*: novel freshwater fungus from France and its relationships to the Pleosporales. *Fungal Biology* 112, 1186–1194.
- Zhang Y, Schoch CL, Fournier J, Crous PW et al. 2009 – Multi-locus phylogeny of the Pleosporales: a taxonomic, ecological and evolutionary reevaluation. *Studies in Mycology* 64, 85–102.
- Zhaxybayeva O, Gogarten JP. 2002 – Bootstrap, Bayesian probability and maximum likelihood mapping: exploring new tools for comparative genome analyses. *BMC genomics* 3, 4.